

**EXAMINATION OF METHODS TO REDUCE MEMBRANE FOULING DURING
DAIRY MICROFILTRATION AND ULTRAFILTRATION**

A Thesis

Presented to the Faculty of the Graduate School

of Cornell University

in Partial Fulfillment of the Requirements for the Degree of

Master of Science

by

Michael Corey Adams

January 2012

© 2012 Michael Corey Adams

ABSTRACT

Pressure-driven membrane filtration processes such as microfiltration (MF), ultrafiltration (UF), nanofiltration (NF), and reverse osmosis (RO) provide opportunities for the dairy industry to better utilize milk by separating its components based on size. However, widespread adoption of some of these processes has yet to be realized due to membrane fouling. Membrane fouling is the accumulation of soil, or foulant, on the surface or within the pores of a membrane. Fouling prolongs processing times, increases energy and cleaning costs, decreases separation efficiency, and, in severe cases, may lead to irreversible clogging of the membrane.

Microfiltration can be used to remove serum proteins (SP) from skim milk. The process' SP removal efficiency directly influences the technology's financial feasibility. Our first objective was to quantify the capacity of 0.14 μm ceramic Isoflux MF membranes to remove SP from skim milk. The Isoflux membranes' manufacturer claims that using these membranes will reduce localized membrane fouling at the inlet end of the membrane that results from using high cross-flow velocities (5 – 7 m/s) to mitigate overall membrane fouling. Contrary to theoretical cumulative SP removal percentages of 68%, 90%, and 97% after 1, 2, and 3 stages of 3X MF processing, respectively, the 3X Isoflux process removed only 39.5%, 58.4%, and 70.2% after 1, 2, and 3 stages, respectively. Several design aspects of the membrane are thought to have resulted in this inefficiency.

Ultrafiltration can be used to concentrate SP and reduce the lactose content of cheese whey or MF permeate of skim milk to produce 80% whey protein concentrates (WPC80) or 80% serum protein concentrates (SPC80), respectively. The objectives of our second study were to determine if adding annatto color to milk or bleaching whey or MF permeate of skim milk with hydrogen peroxide (H_2O_2) or benzoyl peroxide (BPO) influenced UF flux, diafiltration flux, or

membrane fouling during production of WPC80 or SPC80. Addition of annatto color to milk had no effect on flux or fouling. Bleaching with or without added color increased flux during processing. Bleaching with H_2O_2 produced higher flux than bleaching with BPO. While bleaching with BPO reduced membrane fouling during WPC80 production, it did not impact membrane fouling during SPC80 production. Bleaching with H_2O_2 led to the largest reduction in fouling for both production processes.

BIOGRAPHICAL SKETCH

Michael Adams was born on October 2, 1982 in Nashville, TN. After graduating with honors from Hume-Fogg Academic Magnet High School in 2001, Michael left Nashville for Charleston, SC to attend culinary school at Johnson & Wales University. It was here that Michael was introduced to food science during a baking technology course. He was so taken with this new field that after earning his A.S. in baking and pastry arts, Michael returned to his home state and began his B.S. studies in food science at the University of Tennessee, Knoxville. At Tennessee, Michael worked in the sensory lab, performed undergraduate dairy science research, placed first in the nation in ice cream judging at the IDFA collegiate dairy products judging competition, and served as vice-president of the food science club. During the summer and fall of 2005, he completed an internship at Bush Brothers & Company in their R&D department. In 2006, Michael graduated with high honors and eagerly accepted a research scientist position at Daisy Brand's burgeoning R&D department in Dallas, TX. In 2007, Michael married Shan, his girlfriend of 7 years.

During his time at Daisy Brand, Michael learned about the production of sour cream and cottage cheese and gained an appreciation for the importance of making pure and natural dairy products. Although he enjoyed his time in industry, he wanted to gain a deeper understanding of dairy science. In 2009, Michael and Shan moved from Dallas to Ithaca, NY for what was expected to be a two year commitment to the M.S. program in food science at Cornell University. However, because he enjoyed what he was studying (and his wife's patience matched his love for food science), Michael decided to continue on toward his doctoral training.

I dedicate this work to my mom, Mary Wigger,
who has always encouraged me to follow my passion.

ACKNOWLEDGMENTS

First and foremost I want to extend my deepest gratitude to my advisor, Professor Dave Barbano, for his hours of advice in teaching me to be a more responsible scientist and a more effective presenter.

I also want to express my sincere appreciation to Professor Giles Hooker of the Department of Biological Statistics and Computational Biology for taking the time to guide me in my minor studies.

I am obliged to the New York State Milk Promotion Board, the Northeast Dairy Foods Research Center, and the Cornell University Department of Food Science for their generous funding.

I am grateful for the technical assistance and entertaining pilot plant conversation given graciously by Tim Barnard, Michelle Bilotta, Sara Bova, Tom Burke, Maureen Chapman, Chassidy Coon, Jessica Mallozzi, Mark Newbold, Karen Wojciechowski, and Justyna Zulewska.

It always helps to be in the same boat with outstanding colleagues. I want to thank my fellow graduate lab mates Irma Amelia, Steve Beckman, and Emily Hurt for helping me navigate my way through these last two years.

I would like to give special thanks to Dr. Brandon Nelson for pushing me to pursue my graduate studies and showing me that dairy science is about far more than just manufacturing sour cream and cottage cheese.

Finally, I want to thank my family: my mom, Chris, Stephanie, and especially my intelligent, beautiful, and above all... patient wife, Shan. Your love and support have provided me with more than enough reason and strength to succeed when times have been the most trying.

TABLE OF CONTENTS

Biographical sketch.....	iii
Dedication.....	iv
Acknowledgements.....	v
Table of contents.....	vi
List of figures.....	ix
List of tables.....	xi
List of abbreviations.....	xiii
 Chapter 1: Membrane fouling and flux decline in dairy processing.....	 1
Introduction.....	1
Membrane processes.....	4
Microfiltration.....	4
Ultrafiltration.....	5
Nanofiltration.....	6
Reverse osmosis.....	6
Fouling mechanisms and progression.....	7
Concentration polarization.....	7
Fouling mechanisms.....	8
Stages of fouling.....	10
Effect of feed material.....	12
Foulant material present in dairy fluids.....	12
Feed concentration.....	15
Feed chemistry.....	16
Effect of membrane type.....	18
Membrane material.....	18
Membrane design.....	21
Effect of processing conditions.....	23
Membrane flux and cross-flow velocity.....	23
Transmembrane pressure.....	24
Temperature.....	25
Fouling reduction.....	26
Ceramic microfiltration.....	26
Polymeric spiral wound ultrafiltration.....	29
Cleaning.....	29
Fouling quantification.....	31
Fouling coefficient.....	31
Hydraulic resistance.....	31
Membrane imaging.....	32
Conclusions.....	33
References.....	34

Chapter 2: Serum protein removal from skim milk with a 3-stage, 3X ceramic Isoflux membrane process at 50 °C.....	40
Abstract.....	40
Introduction.....	41
Materials and methods.....	44
Experimental design and statistical analysis.....	44
Microfiltration operation.....	45
Cleaning prior to processing.....	46
Processing.....	47
Cleaning after processing.....	49
Chemical analyses.....	50
SP removal estimation using Kjeldahl analysis of permeates.....	50
Color analysis of skim milk and retentates.....	51
SDS-PAGE electrophoresis.....	51
Relative percentage of β -LG to β -LG plus α -LA in skim milk, permeate and retentate samples.....	53
CN passage through the membrane.....	53
Comparison of membranes for 95% SP removal.....	53
Stage number calculation.....	53
Membrane surface area calculation.....	54
Results.....	54
MF processing parameters.....	54
Composition and color.....	61
Skim milk composition.....	61
Permeate composition.....	61
Retentate composition.....	62
Stage feed, retentate, and permeate pH.....	63
Skim milk and retentate color.....	64
SP removal and CN passage.....	64
SP removal.....	64
β -LG and α -LA partitioning.....	65
CN passage into permeate.....	68
Discussion.....	68
SP removal comparison.....	68
Possible reasons for differences in SP removal with various ceramic membranes.....	72
Conclusions.....	78
Acknowledgments.....	78
References.....	79

Chapter 3: Effect of annatto addition and bleaching on ultrafiltration flux during production of 80% whey protein concentrate and 80% serum protein concentrate....	82
Abstract.....	82
Introduction.....	83
Materials and methods.....	85
Experimental design.....	85
Whey protein concentrate production.....	86
Cheddar cheese whey manufacture.....	86
Bleaching of whey.....	86
Ultrafiltration of whey.....	87
Serum protein concentrate production.....	89
Pre-microfiltration processing.....	89
Microfiltration.....	89
Bleaching of MF permeate.....	92
Ultrafiltration of MF permeate.....	92
Fouling coefficient calculations.....	93
Chemical analyses.....	93
Statistical analysis.....	94
Results and discussion.....	99
UF stage feed compositions.....	99
Flux during 80% protein concentrate production.....	101
80% whey protein concentrate.....	101
80% serum protein concentrate.....	104
80% whey protein concentrate, 80% serum protein concentrate comparison.....	107
Membrane fouling during 80% protein concentrate production.....	108
80% whey protein concentrate.....	108
80% serum protein concentrate.....	108
Possible reasons for observed effects of bleaching.....	112
Conclusions.....	115
Acknowledgments.....	116
References.....	116
Chapter 4: Conclusions and future work.....	120

LIST OF FIGURES

Figure 1.1. Passed and rejected dairy components based on membrane pore size.....	2
Figure 1.2. Flux decline during dead end and cross-flow filtration processes.....	3
Figure 1.3. Common forms of membrane fouling.....	9
Figure 1.4. The three stages of flux decline during cross-flow filtration.....	11
Figure 1.5. Illustration of differences in ceramic membrane flow channel design.....	23
Figure 1.6. Pressure profiles across the length of the membrane during low and high cross-flow velocity filtration.....	27
Figure 2.1. Mean flux and permeate inlet pressures while flushing the microfiltration system with skim milk at 50°C during startup using 0.14 µm Isoflux membranes.....	55
Figure 2.2. Mean inlet transmembrane pressures during processing for stage 1, stage 2, and stage 3 when microfiltering skim milk at 50°C with 0.14 µm Isoflux membranes using two diafiltration stages.....	57
Figure 2.3. Mean outlet transmembrane pressures during processing for stage 1, stage 2, and stage 3 when microfiltering skim milk at 50°C with 0.14 µm Isoflux membranes using two diafiltration stages.....	58
Figure 2.4. Mean flux during processing for stage 1, stage 2, and stage 3 when microfiltering skim milk at 50°C with 0.14 µm Isoflux membranes using two diafiltration stages.....	59
Figure 2.5. Mean permeate inlet pressures during processing for stage 1, stage 2, and stage 3 when microfiltering skim milk at 50°C with 0.14 µm Isoflux membranes using two diafiltration stages.....	60
Figure 2.6. Proteins in skim milk and the microfiltration retentates produced in each stage as determined by SDS-PAGE.....	66
Figure 2.7. Proteins in skim milk and the microfiltration permeates produced in each stage as determined by SDS-PAGE.....	67
Figure 2.8. TAMI Isoflux (left) and Membralox GP (right) membrane cross sections.....	75
Figure 2.9. Mean fouling coefficients for ceramic 0.1 µm uniform transmembrane pressure, 0.1 µm graded permeability, and 0.14 µm Isoflux membrane systems after 3X skim milk microfiltration.	77

Figure 3.1. Mean flux at 50°C during the ultrafiltration of separated Cheddar cheese whey treated with no annatto and no bleach, annatto and no bleach, no annatto and 50 ppm benzoyl peroxide, annatto and 50 ppm benzoyl peroxide, no annatto and 500 ppm hydrogen peroxide, and annatto and 500 ppm hydrogen peroxide before processing.....	102
Figure 3.2. Mean flux at 50°C during the diafiltration of separated Cheddar cheese whey treated with no annatto and no bleach, annatto and no bleach, no annatto and 50 ppm benzoyl peroxide, annatto and 50 ppm benzoyl peroxide, no annatto and 500 ppm hydrogen peroxide, and annatto and 500 ppm hydrogen peroxide before processing.....	103
Figure 3.3. Mean flux at 50°C during the ultrafiltration of 0.1 µm microfiltration permeate of skim milk treated with no annatto and no bleach, annatto and no bleach, no annatto and 50 ppm benzoyl peroxide, annatto and 50 ppm benzoyl peroxide, no annatto and 500 ppm hydrogen peroxide, and annatto and 500 ppm hydrogen peroxide before processing.....	105
Figure 3.4. Mean flux at 50°C during the diafiltration of 0.1 µm microfiltration permeate of skim milk treated with no annatto and no bleach, annatto and no bleach, no annatto and 50 ppm benzoyl peroxide, annatto and 50 ppm benzoyl peroxide, no annatto and 500 ppm hydrogen peroxide, and annatto and 500 ppm hydrogen peroxide before processing.....	106
Figure 3.5. Effect of annatto colorant and bleaching treatments of separated Cheddar cheese whey on fouling coefficients of polyethersulfone membranes after the production of 80% whey protein concentrate.....	109
Figure 3.6. Linear correlations between average of ultrafiltration and diafiltration flux values and fouling coefficients from treatments within 80% whey protein concentrate and 80% serum protein concentrate ultrafiltration production processes.....	110
Figure 3.7. Effect of annatto colorant and bleaching treatments of 0.1 µm microfiltration permeate of skim milk on fouling coefficients of polyethersulfone membranes after the production of 80% serum protein concentrate.....	111

LIST OF TABLES

Table 2.1. Mean transmembrane pressures at the membrane inlet and outlet, differences in transmembrane pressure over the length of the membrane, permeate inlet pressure, flux, and concentration factors for each stage of the 0.14 μm Isoflux ceramic microfiltration process.....	56
Table 2.2. Mean composition of pasteurized skim milk.....	61
Table 2.3. Mean composition of permeate from each stage of the 0.14 μm Isoflux ceramic microfiltration process.....	62
Table 2.4. Mean composition of the retentate from each stage of the 0.14 μm Isoflux ceramic microfiltration process.....	63
Table 2.5. Mean pH values (50°C) of the feed material, final retentate, and final permeate from each stage of the 0.14 μm Isoflux ceramic microfiltration process.....	63
Table 2.6. Mean Hunter L, a, b color values of the initial skim milk and the retentates from each stage of the 0.14 μm Isoflux ceramic microfiltration process.....	64
Table 2.7. Mean cumulative serum protein removal percentages and serum protein removal rates after each stage of the 0.14 μm Isoflux ceramic microfiltration process as determined by Kjeldahl analysis of the permeates.....	65
Table 2.8. Mean relative percentages of β -LG to β -LG plus α -LA in skim milk, permeate and retentate samples from each stage of the 0.14 μm Isoflux ceramic microfiltration process as determined by densitometry analysis of SDS-PAGE gels.....	68
Table 2.9. Mean rate of serum protein removal by each stage of the 0.14 μm Isoflux ceramic, 0.10 μm graded permeability ceramic, 0.10 μm uniform transmembrane pressure ceramic, and 0.30 μm polyvinylidene fluoride spiral-wound microfiltration processes as determined by Kjeldahl analysis of the permeates.....	69
Table 2.10. Mean cumulative serum protein removal percentage after each stage of the 0.14 μm Isoflux ceramic, 0.10 μm graded permeability ceramic, 0.10 μm uniform transmembrane pressure ceramic, and 0.30 μm polyvinylidene fluoride spiral-wound microfiltration processes as determined by Kjeldahl analysis of the permeates.....	70
Table 2.11. Number of stages and membrane surface area theoretically required to remove 95% of the serum proteins from 1000 kg of skim milk in 12 h using 0.14 μm Isoflux ceramic, 0.10 μm graded permeability ceramic, 0.10 μm uniform transmembrane pressure ceramic, and 0.30 μm polyvinylidene fluoride spiral-wound microfiltration processes.....	71

Table 3.1. ANOVA split-plot design with df, type III SS, and <i>P</i> values for predictive variables of ultrafiltration (after first 15 min of processing) and diafiltration (prior to last 15 min of processing) flux during the production of 80% whey protein concentrate.....	97
Table 3.2. ANOVA split-plot design with df, type III SS, and <i>P</i> values for predictive variables of ultrafiltration (after first 15 min of processing) and diafiltration (prior to last 15 min of processing) flux during the production of 80% serum protein concentrate.....	98
Table 3.3. Mean compositional and pH data for separated Cheddar cheese whey and 0.1 µm microfiltration permeate of skim milk used to feed the ultrafiltration unit during production of 80% whey protein concentrate and 80% serum protein concentrate, respectively.....	100
Table 3.4. Mean ultrafiltration and diafiltration flux at 50°C during the production of 80% whey protein concentrate from separated Cheddar cheese whey treated with no annatto and no bleach, annatto and no bleach, no annatto and 50 ppm benzoyl peroxide, annatto and 50 ppm benzoyl peroxide, no annatto and 500 ppm hydrogen peroxide, and annatto and 500 ppm hydrogen peroxide before processing.....	101
Table 3.5. Mean ultrafiltration and diafiltration flux at 50°C during the production of 80% serum protein concentrate from 0.1 µm microfiltration permeate of skim milk treated with no annatto and no bleach, annatto and no bleach, no annatto and 50 ppm benzoyl peroxide, annatto and 50 ppm benzoyl peroxide, no annatto and 500 ppm hydrogen peroxide, and annatto and 500 ppm hydrogen peroxide before processing.....	104
Table 3.6. Mean ultrafiltration and diafiltration flux at 50°C during the production of 80% whey protein concentrates and 80% serum protein concentrates made from separated Cheddar cheese whey or 0.1 µm microfiltration permeate of skim milk, respectively, treated with no bleach, 50 ppm benzoyl peroxide, or 500 ppm hydrogen peroxide before processing.....	108

LIST OF ABBREVIATIONS

α -LA.....	Alpha lactalbumin
ANOVA.....	Analysis of variance
β -LG.....	Beta lactoglobulin
BPO.....	Benzoyl peroxide
BSA.....	Bovine serum albumin
CF.....	Concentration factor
CN.....	Casein
CN%TP.....	Casein as a percentage of true protein
CP.....	Crude protein
df.....	Degrees of freedom
DF.....	Diafiltration factor
FC.....	Fouling coefficient
GP.....	Graded permeability
H ₂ O ₂	Hydrogen peroxide
MF.....	Microfiltration
NCN.....	Noncasein nitrogen
NF.....	Nanofiltration
NPN.....	Nonprotein nitrogen
<i>P</i>	Level of significance
PVDF SW.....	Polyvinylidene fluoride spiral wound
RO.....	Reverse osmosis
SAS.....	Statistical analysis system
SDS-PAGE.....	Sodium dodecyl sulfate polyacrylamide gel electrophoresis
SP.....	Serum protein
SPC.....	Serum protein concentrate
SPC80.....	80% Serum protein concentrate
SS.....	Sum of squares
TAMI.....	Technologies Avancees & Membrane Industrielles
TMP.....	Transmembrane pressure
TN.....	Total nitrogen
TP.....	True protein
TS.....	Total solids
UF.....	Ultrafiltration
UTP.....	Uniform transmembrane pressure
WPC.....	Whey protein concentrate
WPC80.....	80% Whey protein concentrate

CHAPTER ONE

Membrane Fouling and Flux Decline in Dairy Processing

Introduction

Bovine milk is a complex biological fluid that contains proteins, lipids, lactose (a carbohydrate), minerals, bacteria, and various micronutrients. As such, there has always been great interest in separating milk to better utilize its components. The earliest of these separation techniques was cheese making, which, at its heart, is simply a separation of casein (CN) and fat from the majority of water and lactose. Centrifugal separation processes for removing cream or particulate matter from various dairy fluids revolutionized the industry in the late 19th century. Since the early 1970's, more sophisticated separation processes involving filtration membranes have been adapted for use in the dairy industry that can separate milk components at the molecular level (Pouliot, 2008).

There are 4 pressure-driven membrane filtration processes used in the dairy industry today: microfiltration (MF), ultrafiltration (UF), nanofiltration (NF), and reverse osmosis (RO). Each filtration process produces retentate and permeate streams which represent the rejected and passed feed material, respectively. Though each process fractionates dairy components differently (Figure 1.1), all of their efficiencies are primarily hindered by fouling of the filter. Fouling is the general term applied to the accumulation of soil, or foulant, on the surface or within the pores of a membrane. Fouling prolongs processing times, increases energy and cleaning costs, decreases separation efficiency, and, in severe cases, may lead to irreversible clogging of the membrane (Brans et al., 2004).

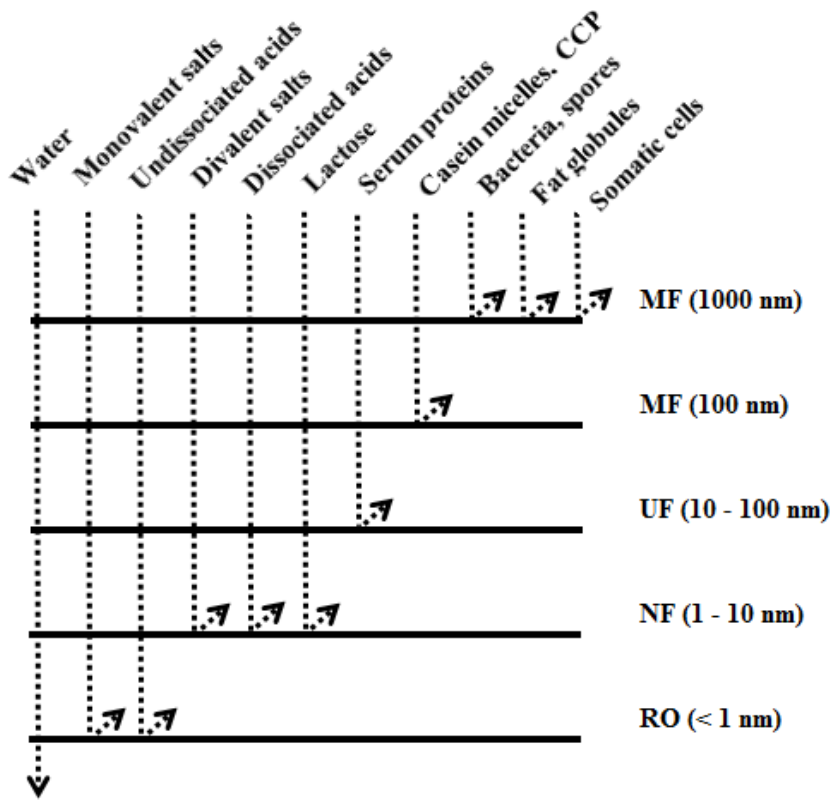


Figure 1.1. Passed and rejected dairy components based on membrane pore size. CCP = colloidal calcium phosphate associated with the casein micelle, MF = microfiltration, UF = ultrafiltration, NF = nanofiltration, RO = reverse osmosis.

Flux is the amount of permeate (a volume or mass) removed from the feed stream of a membrane process per unit of membrane surface area per unit of time. Achieving higher process flux permits a manufacturer to increase throughput. As indicated by Equation 1, flux (J) is equal to the difference between transmembrane pressure (TMP) (i.e., the difference in pressure between the retentate and permeate sides of the membrane) and osmotic pressure at the membrane surface (π) divided by the product of the permeate viscosity (η) and the total resistance to permeate passage. Total resistance is a series summation of the resistances due to the membrane (R_M), the foulant layer (R_F), and the gel layer caused by concentration polarization (R_G) (Cheryan, 1998).

$$J = \frac{TMP - \pi}{\eta(R_M + R_F + R_G)} \quad \text{Equation (1)}$$

Clearly, flux is inversely related to the amount of foulant present on the membrane. It should be noted that during MF and UF, the effects of osmotic pressure can generally be assumed to be negligible due to the large size of the retained material (Cheryan, 1998).

Though there are many filtration system designs available, no process is exempt from fouling. Membrane systems can be configured for either “dead end” or “cross-flow” filtration. In the former, the fluid is fed perpendicular to the surface of the membrane. In the latter, the fluid is pumped tangentially over the surface of the membrane. The general form of flux decline is different in each configuration (Figure 1.2).

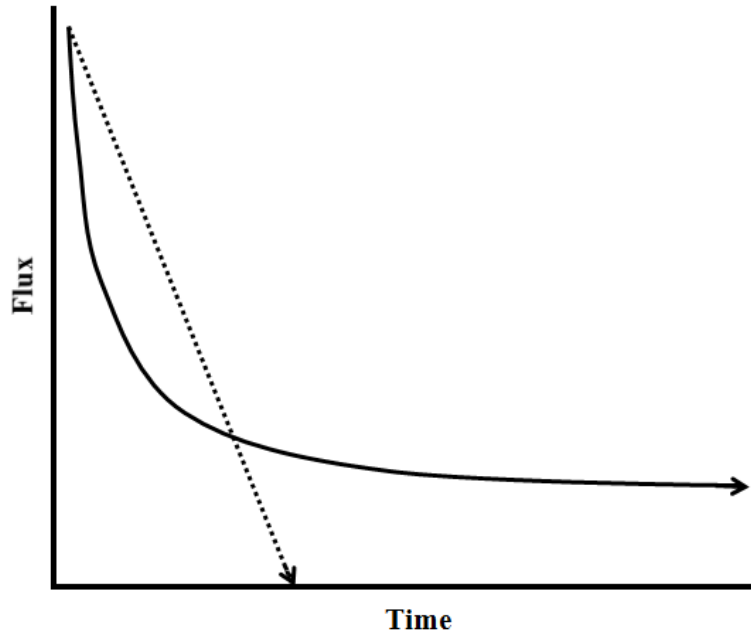


Figure 1.2. Flux decline during dead end (· ·) and cross-flow (—) filtration processes.

Cross-flow filtration is commonly used in industrial applications because it permits longer run times between cleaning cycles. Because of its industrial ubiquity, only cross-flow filtration will be examined in this review. Once a steady state has been reached, cross-flow filtration processes

may be operated in either constant flux or constant pressure mode. The former indicates that permeate flux is held constant by increasing TMP as foulant accumulates on the membrane. The latter indicates that a constant TMP is maintained while permeate flux is allowed to decline as fouling limits membrane permeability. Feed characteristics, membrane type, and processing conditions each impact the level of foulant buildup. The 2 objectives of this review are to familiarize the reader with the phenomena of membrane fouling and flux decline (assuming a constant pressure operation) during processing of dairy fluids with pressure-driven filtration systems and to provide an updated description of means to reduce fouling.

Membrane Processes

The filtration process (i.e., MF, UF, NF, or RO) and fluid being processed will impact the fouling characteristics of a system. Before much discussion on fouling can begin, it is important to understand each of these processes and how they are used in the dairy industry.

Microfiltration. Microfiltration is designed to remove particulate matter in the range of 0.1 μm to 10 μm from a fluid medium. Due to this wide size range, MF processes have informally been described in the dairy industry as either large pore or small pore MF. Large pore MF describes the use of membranes with an approximate pore diameter of 1 to 2 μm . This process has been used to remove bacteria and somatic cells from skim milk and cheese brine (Rosenberg, 1995) and to separate large fat globules from small fat globules (Gouderanche et al., 2000). By removing bacteria and spores from milk's skim fraction prior to pasteurization, fluid milk with an extended shelf life can be produced (Elwell and Barbano, 2006). By fractionating milk fat globules based on size (above and below 2 μm), Gouderanche et al. (2000) were able to prepare a wide variety of dairy products with differing sensory properties attributed to the difference in the starting cream's fat globule size distribution.

Small pore MF uses 0.1 to 0.3 μm membranes to separate CN micelles from serum proteins (SP), remove fat from whey, or separate alpha lactalbumin (α -LA) polymers from beta lactoglobulin (β -LG) (Rosenberg, 1995; Gesan-Guizieu et al., 1999). Fractionation of CN and SP is made possible because the CN micelles are, on average, $> 0.1 \mu\text{m}$ in diameter while SP exist in solution and are roughly 100 times smaller (Walstra et al., 2006). This separation allows processors to better utilize the proteins in milk. Examples of such applications include the standardization of a cheese milk's CN-to-fat ratio, fortification of retorted beverages with CN-rich MF retentates, and fortification of clear, acidic beverages with SP-rich MF permeate concentrates (Nelson and Barbano, 2005b; Evans et al., 2010; Hurt et al., 2010). Microfiltration processes have proven useful in defatting whey after thermocalcic lipoprotein aggregation (Rosenberg, 1995). In addition to improving the functional properties of the subsequent whey protein concentrates, this defatting process offers the additional benefits of microbial reduction and reduced fouling during subsequent UF.

Ultrafiltration. Unlike MF, UF is usually used to concentrate all of the proteins in a dairy fluid. The pore size range for UF processes is often quoted by molecular weight cut-off instead of a nominal pore size. This range extends from 1,000 to 200,000 Da and corresponds to a nominal pore diameter of 10 to 100 nm. Ultrafiltration is the most widely used membrane process in the dairy industry today because of its industrial familiarity, ease of scale-up, and variety of applications. On-farm UF is a particularly useful application in which the raw milk is fractionated by the farm operation prior to shipping (Zall, 1987). This reduces refrigeration, storage, and transportation costs and can reduce the costs of cheese production (Renner and El-Salam, 1991). Additionally, the UF permeate can be used by the farmer as a source for cattle feed (Renner and El-Salam, 1991). Whey protein concentrates are made by ultrafiltering whey

from cheese processes (often Cheddar or mozzarella in the United States) to remove lactose and concentrate SP. Nelson and Barbano (2005a) determined that a similar ingredient, serum protein concentrate, could be made without the fat and glycomacropeptide content of whey by applying the same UF process to a 0.1 μm MF permeate of skim milk. Because CN is also concentrated during UF, this separation can be used to create milk protein concentrates and fluid milks with increased protein or reduced lactose contents (Tossavainen and Sahlstein, 2010). This concept can be extended to the production of cheese milks or protein concentrates which can be used to achieve a given protein-to-fat ratio that improves the consistency of a cheese making process (Rosenberg, 1995) without increasing the lactose concentration.

Nanofiltration. As with UF, the pore sizes of NF membranes are often quoted on a molecular weight cut-off basis. The range for NF membranes falls between 300 and 1,000 Da. This corresponds to a nominal pore diameter between 1 and 10 nm. These small pore sizes make NF desirable for capturing lactose from the permeates of UF operations or fat, protein, and lactose removal from recycled cheese brine solutions. In addition, NF membranes are often electrically charged to various degrees to aid in reclamation of ionic species. This characteristic, paired with its small pore size, makes NF a useful tool for partial demineralization of sweet whey and UF permeate, partial desalting of salt whey, and partial acid removal from acid whey (Rice et al., 2009). If concentrated by RO, the NF permeate produced from milk UF permeate may also be used as a salt source to balance the flavor of reduced lactose milks (Tossavainen and Sahlstein, 2010).

Reverse Osmosis. Reverse osmosis processes are strictly used to remove water from a fluid. The permeate that passes through the < 100 Da molecular weight cut-off membranes is virtually free of solids. On-farm RO operations may be used to the same ends as on-farm UF

operations. However, because dairy minerals and lactose are retained at RO membrane surfaces, higher osmotic pressures (2700 – 3500 kPa at 25% solids) must be overcome using high TMP for permeate to flow (Marshall and Daufin, 1995). This increases the energy costs associated with raw milk concentration by RO when compared to those of on-farm UF. Processed milk and whey may also be concentrated using RO processes before transportation to reduce shipping costs or before spray drying to alleviate the high energy costs associated with evaporators (Hiddink et al., 1980). When water is RO filtered, the permeate (henceforth described as RO water) may be used during diafiltration or for membrane cleaning because it lacks the mineral content of tap water that would contribute to fouling.

Fouling Mechanisms and Progression

Membrane fouling is a dynamic process that is heavily influenced by the fluid mechanics of the filtration system, the feed material properties, and the membrane itself. As such, this phenomenon's complexity cannot be overstated. That being said, the following section describes the current understanding of the development of membrane fouling as it pertains to the dairy industry.

Concentration Polarization. When a liquid is separated by a membrane that can retain any of its solids, the flux will always be lower than that of its pure solvent because of concentration polarization. Concentration polarization is the dynamic accumulation of retained feed solids at the surface of a membrane due to the balance of convective transport toward the membrane and the rate of back diffusion away from the membrane (Cheryan, 1998). The result of this accumulation is a boundary layer near the membrane surface that is commonly referred to as the “gel layer,” as it is thought that supersaturation of rejected species may result in localized gelation near the membrane surface. Increases in viscosity due to filtration and declines in fluid

velocity due to friction result in laminar flow in this gel layer (Cheryan, 1998). While it is not fouling in the strictest sense of the word, concentration polarization leads to an observable flux decline. Two mechanisms may cause this decrease (Marshall and Daufin, 1995; Cheryan, 1998). The first is that the gel layer simply impedes the passage of permeating species. The second is that the large osmotic pressure formed at the membrane surface acts against the process' driving force, TMP. As previously noted, the second mechanism will be less important in dairy UF and MF processes due to the larger size of the retained solids. Concentration polarization leads to fouling by increasing the proportion of foulant material available to interact with the surface of the membrane. Concentration polarization is inevitable in filtration processes; without it, the separation would be different. It is a function of the hydrodynamic conditions of the system and is not influenced by the membrane itself (Marshall et al., 1993). Concentration polarization, unlike fouling, is reversible if either the TMP or feed concentration is decreased or cross-flow velocity is increased (Cheryan, 1998). Each of these actions results in fewer solids being present in the gel layer, causing the flux lost to concentration polarization to be partially restored.

Fouling Mechanisms. Once concentration polarization is in effect, fouling can proceed by several means. Brans et al. (2004) mention 4 mechanisms: adsorption, pore blocking, cake layer formation, and depth fouling (Figure 1.3). It should be noted that while foulant adsorption is certainly promoted by concentration polarization, studies by Tong et al. (1988) and Rudan (1990) have proven that milk proteins adsorb to polymeric, non-cellulosic, membrane surfaces under static conditions (i.e., with no concentration polarization caused by an applied TMP). Therefore, adsorption may very well suppress flux ahead of the effect of concentration polarization.

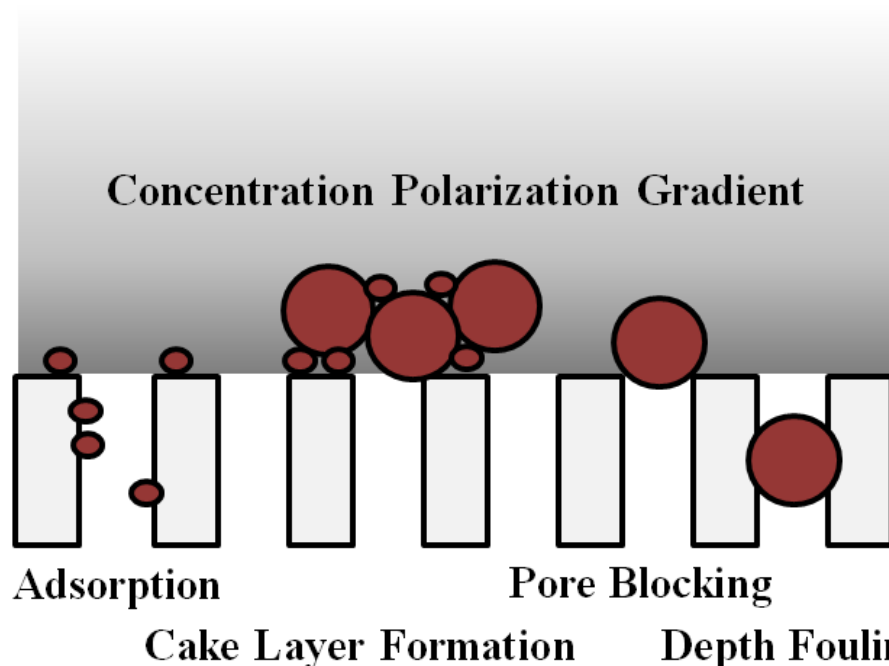


Figure 1.3. Common forms of membrane fouling: (left to right) adsorption, cake layer formation, pore blocking, and depth fouling.

The common thread among all forms of fouling is that they describe an interaction between the foulant and the membrane that is only reversible with cleaning. Adsorption occurs when foulant adheres to the surface of the membrane. This may take place on top of the membrane or within the membrane's pores. Adsorption within the pores reduces flux by narrowing the channels for permeate passage. Adsorption at the membrane surface can lead to the formation of so-called cake layers. Cake layers are created when particles aggregate to form bridges and piles that cover sections of the membrane. These aggregates are made up of large particles that would typically be concentrated and smaller ones that could potentially be separated. In the case of 0.1 μm skim milk MF, CN micelles would represent the larger particles that form the bulk of the foulant matrix and SP would represent the smaller particles which could act as fillers (Marshall et al., 1993). Because of the wide range of particle size within this matrix, the layer can be firmly compressed if allowed to remain on the membrane's surface, thus adding an additional layer of resistance to permeate flow. Pore blocking involves the superficial plugging of a pore. This form

of fouling takes place when a particle that is slightly larger than the pore becomes lodged at the pore's entrance. Depth fouling occurs when a large particle, such as one involved in a pore blocking scenario, is forced deep into a pore through which it would not normally pass. This is often due to the application of excessive TMP. As with pore blocking, depth fouling acts to reduce flux by decreasing the number of available pores through which permeate can pass. While the forms of fouling that take place on the membrane surface can often be removed with proper cleaning techniques, foulant within the pores is much more difficult to get at, and may remain bound to the membrane (Renner and El-Salam, 1991). Irreversibly bound foulant such as this limits the membrane's usable lifespan (Renner and El-Salam, 1991).

Stages of Fouling. After concentration polarization and fouling have been initiated, the membrane is not the only resistance which dictates the process separation. In fact, once the foulant layer has been laid down, it contributes a much larger resistance than the membrane itself (Fritsch and Moraru, 2008). Hanemaaijer et al. (1989) noted that the resistance due to the foulant layer and concentration polarization can be between 10 to 50 times that of the resistance contributed by the membrane itself in the case of UF. During skim milk MF, Gesan-Guizieu et al. (2000) found the ratio of total resistance to initial membrane resistance was 7.5 below a critical flux to shear ratio of $0.95 \text{ L/m}^2 \text{ h Pa}$ (i.e., when fouling was limited). When this critical flux to shear ratio was exceeded, the ratio of total resistance to initial membrane resistance increased rapidly to above 70.

A generalized trend of flux decline in cross-flow membrane processes is depicted in Figure 1.4.

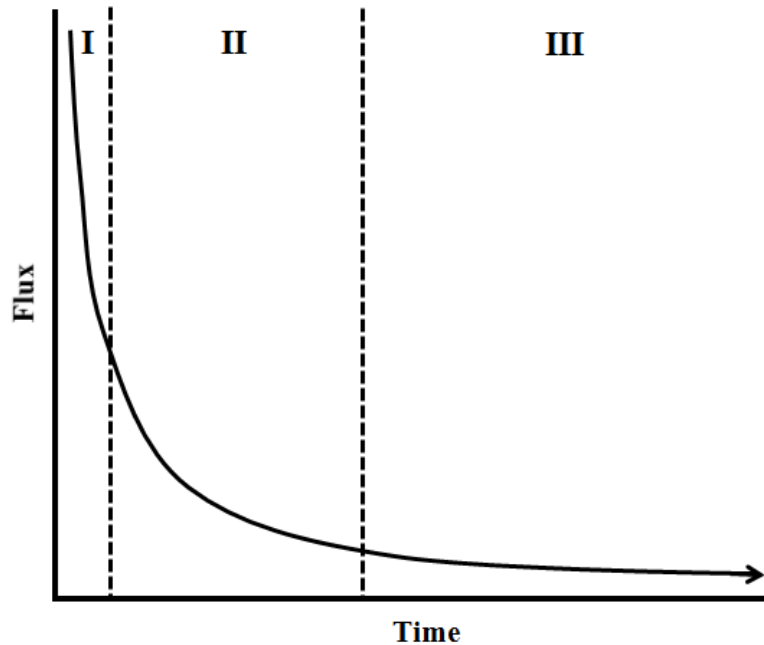


Figure 1.4. The three stages of flux decline during cross-flow filtration. Adapted from Marshall and Daufin (1995).

Because concentration polarization promotes fouling, it is often associated with stage I of flux decline (Marshall et al., 1993; Marshall and Daufin, 1995). This phase occurs early in the process (within seconds or minutes) and is characterized by a rapid drop in membrane flux. However, immediate foulant adsorption also contributes to this initial flux decrease, as rapid (within 5 min) adsorption of protein to the membrane surface has been noted to occur even without the effects of concentration polarization (Tong et al., 1988; Rudan, 1990). If the membrane being used is easily deformable, as many polymeric varieties are, membrane compaction may also be responsible for suppressing the flux during this initial stage (Marshall et al., 1993).

According to Marshall and Daufin (1995), stages II and III of UF flux decline are due to fouling. The initial deposition of foulant onto the membrane is responsible for the drop during stage II (Marshall and Daufin, 1995). This decrease is less dramatic than the decline due to concentration polarization. Stage III shows an asymptotic decline and is due to additional

deposition and compaction of the foulant layer (Marshall and Daufin, 1995). Belfort et al. (2004) offered a similar progression for MF fouling with colloidal solutions (i.e., skim milk): after solutes and colloidal particles adsorb to the surface of the membrane, monolayers (cake layers) are formed, these monolayers overlap to form multilayers, then the multilayers are compacted under the system's TMP.

Effect of Feed Material

Foulant Material Present in Dairy Fluids. Dairy fluids contain a variety of solids including proteins, minerals, lactose, and fat. These components have been noted to foul membranes to varying degrees. The chemical nature of the solid and the solution in which it is present dictate its fouling capacity. It is generally accepted that proteins and minerals account for the majority of foulant in dairy membrane operations (Marshall and Daufin, 1995). Lactose is not considered to be an important foulant, but could become trapped in the foulant matrix during NF (Rice et al., 2008) and RO processes. Furthermore, due to its effect on osmotic pressure, the role of lactose in contributing to concentration polarization during NF and RO should not be overlooked (Cheryan, 1998). The presence of fat has been shown to influence flux depending on the feed material (Marshall and Daufin, 1995).

Proteins constitute a large proportion of the foulant layer in most dairy membrane processes because the charged and hydrophobic regions within their structures are able to interact with other feed components and the membrane itself (Marshall et al., 1993; Cheryan, 1998). More specifically, the negatively charged milk proteins may engage in either electrostatic attractions with positively charged membranes or cation-mediated electrostatic attractions to negatively charged membranes (Marshall et al., 1993). The hydrophobic regions within these proteins may also be forced to interact with similarly hydrophobic membranes or proteins to

produce a more energetically favorable system (Marshall et al., 1993). Proteins with free sulfhydryl groups have also been shown to form intermolecular disulfide bonds which promote flux decline (Kelly and Zydney, 1997). Several authors have noted that thick (i.e., 5 to 30 μm) layers of protein have been observed on the surfaces of fouled membranes and that cross-flow operations result in thinner layers than dead-end operations (Marshall and Daufin, 1995). While protein has often been found within the pores of MF membranes after dairy processing, this is less often the case with UF, NF, and RO membranes due to their smaller pore sizes. When such entry does occur in UF membranes, the protein likely only goes into pores which are on the larger end of the membrane's pore size distribution (i.e., those which are closer to MF size range) (Marshall and Daufin, 1995). Tong et al. (1988) characterized the makeup of the monomeric proteinaceous foulant after whole milk UF with polysulfone membranes and determined that α -LA and β -LG were adsorbed preferentially (the former to a greater extent), not CN. A similar study was conducted to characterize the protein foulant after sweet whey UF, wherein CN proteolysis products and α -LA were determined to be the primary protein monomers responsible for fouling (Tong et al., 1989). Because α -LA contains sites which strongly bind divalent calcium ions, the authors attributed the ubiquity of α -LA foulant to calcium-mediated salt bridging between the negatively charged membrane and the negatively charged α -LA (Tong et al., 1989). Casein appears to play a large role in the fouling of polymeric MF membranes. Zulewska et al. (unpublished) compared the flux and SP passage during polyvinylidene spiral-wound (PVDF SW) MF of skim milk and CN-free skim milk (MF permeate from a uniform transmembrane pressure (UTP) ceramic MF system). They found higher flux and SP passage during the processing of CN-free skim milk, indicating that CN is a major foulant during PVDF

SW MF. Daufin and Merin (1995) cite several studies which have attributed ceramic MF fouling to CN micelles.

Much work has been done to quantify the degree of protein fouling associated with single protein systems such as α -LA, bovine serum albumin (BSA), and β -LG (Kelly and Zydney, 1997; Vyas et al., 2000). Though these studies have contributed to the fundamental knowledge of the filtration field, the experiments are often conducted in model solutions that fail to mimic the complex chemistries of milk and whey. Therefore, the findings from these experiments should be interpreted with caution (Marshall and Daufin, 1995).

Mineral fouling is considered to be one of the leading causes of membrane flux decline in dairy processes. These mineral deposits are usually devoid of magnesium, sodium, potassium, sulfur, or chlorine; however, calcium phosphate is always present (Hanemaaijer et al., 1989). Not only can calcium phosphate precipitate and form scale deposits on and within the membrane, but divalent cations such as Ca^{2+} can facilitate protein-protein and protein-membrane interactions (Rice et al., 2009). The fact that calcium phosphate solubility decreases with increasing temperature (i.e., reverse solubility which causes scale buildup) only complicates the matter, as decreasing temperature in membrane processes leads to flux decline due to increased permeate viscosity per Equation (1). With respect to calcium equilibrium, too low of a temperature causes calcium to be removed from the CN micelle (yielding more fouling substrate) and too high of a temperature causes existing free calcium to precipitate. Extremes of both instances will increase fouling, so a balance must be reached.

It is known that skim milk will foul a typical UF membrane to a lesser degree than cheese whey. Cheryan (1998) attributes this both to the scouring effect of CN micelles in skim milk and the presence of additional free calcium (calcium not bound within the CN micelle) in whey. It

should also be remembered that proteins (CN in particular) stabilize calcium phosphate in solution (Marshall and Daufin, 1995; Fox, 1997). For this reason, in systems in which CN is mostly absent, like whey or MF permeate, mineral fouling may proceed more rapidly than it would when processing skim milk. This problem would be magnified further when concentrating UF permeate by NF or RO due to the lack of SP as well.

Whole milk contains about 3.4% fat, on average. However, despite constituting 28% of the total solids and imparting a much greater viscosity to the fluid, fat does not appear to play as critical a role in whole milk fouling as do proteins and minerals. This is evidenced by the fact that whole milk flux during UF is typically only 20% lower than that observed with skim milk (Marshall and Daufin, 1995). However, the small amounts of fat present in whey, which exist mostly as milk fat globule membrane fragments and free fat as opposed to the intact milk fat globules in milk, are known to promote UF fouling (Marshall and Daufin, 1995). Thermocalcic aggregation is a whey preprocessing procedure that causes the trace amounts of phospholipids from the milk fat globule membrane to aggregate into larger particles through calcium bridging. When performed upstream of a MF operation, this pretreatment is currently used as an efficient alternative to centrifugation to remove fat from whey prior to UF (Rosenberg, 1995). Though the fat removal and calcium aggregation processes have not been decoupled to conclude that the fat reduction is what solely drives the flux increase, unpublished, practical experience has demonstrated the fat plays a critical role in whey fouling (Marshall and Daufin, 1995).

Feed Concentration. According to film theory, an engineering model that predicts flux decline according to mass transfer effects, flux decreases exponentially with increasing concentration of the feed fluid (Cheryan, 1998). While film theory addresses concentration polarization specifically, it impacts fouling as described above. Generally speaking, increasing

the concentration of a feed stream increases the level of reversible foulant (that which can be removed by cleaning). This amounts to an increase in observed cake layer formation and a decline in flux. (Marshall et al., 1993).

Increasing the concentration factor (CF) (Equation 2) during a membrane process has the same effect on fouling as increasing the feed concentration because the feed solids build up to a greater extent on the retentate side of the membrane.

$$CF = \frac{\text{Retentate Mass} + \text{Permeate Mass}}{\text{Retentate Mass}} \quad \text{Equation (2)}$$

Therefore, a manufacturer operating in a batch process mode (i.e., the retentate being returned to the feed vat) should expect there to be a critical concentration, above which the system will begin to rapidly foul. At this point, production must cease and the system should be cleaned to prevent damage to the membrane. It is equally important to consider one's CF when operating in a continuous feed-and-bleed process mode (i.e., retentate and permeate removed continuously), as too high of a CF can lead to high solids concentrations in the retentate recirculation loop. To maximize productivity, the appropriate CF should be chosen so as to achieve the desired level of separation, but allow the system to operate for a long period of time before cleaning is necessary.

Feed Chemistry. The chemistry of a dairy feed stream will also impact its fouling potential. The physical conformations of proteins and calcium phosphate have been observed to be the causes of this effect (Marshall and Daufin, 1995). Previous research has determined that BSA, like other proteins, exhibits maximum membrane deposition to membranes at its isoelectric point (de la Casa et al., 2007). Consequently, flux minima during the filtration of protein solutions are also observed at the isoelectric point(s) of the protein(s), as this is the pH at which a protein is least soluble (Cheryan, 1998; de la Casa et al., 2007). This finding is at odds with the

fact that the nature of the electrostatic relationship between the protein and membrane is also important. If the degree of electrostatic repulsion or attraction were the only important factor, one might expect the maximum flux to occur at the highest protein charge obtainable that is opposite to that of the membrane. In practice, however, 2 local flux maxima exist, one at the lowest pH that can reasonably be processed (i.e., when the protein is most positively charged) and one at the highest pH that can reasonably be processed (i.e., when the protein is most negatively charged) (Cheryan, 1998). This infers that protein solubility plays a more important role in fouling than charge repulsion or attraction.

Above or below the isoelectric point, it has been shown that increased ionic strength reduces flux because the ionic species shields protein charges, which leads to protein contraction and greater adsorption (Marshall and Daufin, 1995). By increasing the feed's NaCl concentration to a point below its saturation level, protein adsorption and flux loss have been noted to increase in protein solutions (Cheryan, 1998) due to "salting out" of the proteins. This trend does not hold true at a protein's isoelectric point (Marshall and Daufin, 1995), probably because protein solubility is already at its minimum.

Because protein and calcium conformations are influenced by pH, the acidity of the feed stream also has a profound effect on membrane fouling. The effect of pH in relation to the isoelectric point of a protein has already been addressed above. If dairy fluids only contained proteins and no coagulation were observed, altering the pH either above or below that of these proteins' isoelectric points would result in reduced fouling. However, the other principal membrane foulant, calcium, is less soluble at higher pH. Increasing pH from 5 to 7.5 has been shown to decrease the amount of soluble calcium present in UF permeate of whey, thus indicating that calcium is precipitating and being rejected at higher pH values (Hanemaaijer et

al., 1989). Above pH 6.5, mineral fouling in whey will proceed rapidly (Marshall and Daufin, 1995). Decreasing the pH of whey will generally improve flux because precipitation onto the membrane is reduced (Cheryan, 1998). Care should be taken when acidifying feed streams which contain CN, as cheese fines resulting from the acid coagulation of CN micelles (or movement of bound calcium within the micelles into solution) can also contribute to flux decline (Marshall and Daufin, 1995; Cheryan, 1998).

Effect of Membrane Type

Membrane Material. Membranes can be manufactured from a variety of materials into a myriad of shapes to fit a given application. The two main classes of materials with which membranes are manufactured today for the dairy industry are ceramics and polymers. Within each class, there is a diverse range of products, but there are several key facts which distinguish ceramic and polymeric membranes. First, ceramic membranes exist almost exclusively in tubular conformations. On the other hand, polymeric membranes come in a range of shapes; the most popular in the dairy industry being the spiral-wound design (Schwinge et al., 2004). Polymeric membranes are relatively inexpensive to manufacture, but are damaged by chemical agents and high temperatures. Consequently, they are difficult to clean and exhibit short lifetimes (approximately 1 year in an industrial setting) (Cheryan, 1998). Ceramic membranes, on the other hand, can be cleaned with a wide variety of chemical agents, heat-sanitized with temperatures in excess of 100°C, and may last up to 10 years without replacement. (Cheryan, 1998). In addition, ceramic membranes exhibit narrower pore size distributions (de la Casa et al., 2007), which provide cleaner separations of retained and passed components. Saboya and Maubois (2000) even went so far as to assert that, “ceramic membranes are the only ones that satisfy all of the requirements of the applications in the dairy industry.” However, 2 factors make

ceramic membranes undesirable from a processor's point of view: there is a risk of cracking the membrane if it is not handled gently or is subjected to a rapid temperature change (i.e., $>10^{\circ}\text{C}/\text{min}$) and the initial investment is quite high compared to that of non-ceramic membranes. While the former concern can be alleviated using carefully programmed process logic controls, the latter is inevitable. Polymeric membranes cost approximately \$50 to \$100 per m^2 of membrane surface area, but ceramic membranes are more on the order of \$500 to \$3000 per m^2 (Cheryan, 1998).

Because the physico-chemical relationship between the feed material and the membrane has a profound effect on fouling, it can be correctly surmised that ceramic and polymeric membranes will exhibit different fouling characteristics. As previously mentioned, proteins have an affinity for binding to membrane surfaces, particularly hydrophobic ones. Tong et al. (1988) illustrated the magnitude of this phenomenon by decoupling the effects of adsorption and concentration polarization-driven fouling during whole milk UF. The polymeric polysulfone plate-and-frame membranes used in the study were either soaked in whole milk for 5 min without any applied pressure or subjected to 120 min of UF processing. After each treatment, the fouled water flux was determined and compared to the clean water flux. The plates that were simply soaked in whole milk exhibited a 68% decrease from the clean water flux. This was only slightly lower than the 76% decline noted after whole milk UF processing, indicating that rapid adsorption plays a large role in flux decline for polysulfone membranes. Because much of the fouling during dairy filtration is due to the protein foulant's hydrophobic interaction with the membrane, making the membrane as hydrophilic as possible reduces the likelihood of protein adsorption. Rudan (1990) performed similar adsorption studies by soaking polyethersulfone (hydrophobic) and cellulosic (hydrophilic) membranes in whole milk. While the

polyethersulfone membranes exhibited 38 to 60% losses in water permeability after soaking in milk and rinsing with water, the cellulosic membranes exhibited no loss in water permeability. It should be noted that the importance of the membrane's hydrophobicity diminishes as concentration polarization increases and the foulant layer covers the surface of the membrane (Marshall and Daufin, 1995). Though successful efforts have been made to create polymeric membranes that are more hydrophilic (Marshall and Daufin, 1995), ceramic materials will always be more hydrophilic than polymeric ones. Consequently, ceramic membranes generally adsorb protein to a much lesser extent than polymeric membranes (Zulewska et al., 2009).

Caric et al. (2000) demonstrated that the ceramic membrane material may also play an integral role in the degree of protein adsorption. They found that alumina membranes adsorbed more whey protein during quiescent submersion in whey protein solutions and exhibited lower flux values during cross-flow filtration of whey protein solutions than membranes made of zirconia. The caveat to this study was that the two membranes had different pores sizes (zirconia = 50 nm, alumina = 200 nm). They attributed the increased fouling of the alumina membrane both to its composition and its larger pore size; the latter of which would permit additional protein adsorption. Unfortunately, these effects were not tested independently.

Another difference between polymeric and ceramic membranes that will affect membrane flux, but is unrelated to fouling, involves membrane compaction. Because polymeric membranes (especially spiral-wound) are easily deformed under pressure, flow channels may be constricted with increased TMP (above 300 kPa) and processing time, causing additional membrane resistance and reduced flux (Renner and El-Salam, 1991). In extreme cases the compaction of a polymeric membrane is not reversible. Daufin and Merin (1995) indicate that due to their increased rigidity, ceramic membranes do not exhibit membrane compaction.

Membrane Design. Cheryan (1998) explains that the following membrane characteristics should be considered when trying to predict the extent of fouling: membrane hydrophilicity, pore size, surface roughness, and membrane charge. The impact of membrane hydrophilicity on fouling has already been addressed. The pore size, or more accurately, the ratio of the pore size to the rejected species is also important. In the case of small pore MF of skim milk, the pore must be large enough to pass SP, but small enough not to cradle CN micelles; the latter of which could result in pore blockage and depth fouling. Therefore, a narrower membrane pore will adsorb less foulant when compared to a more open pore. Caric et al. (2000) indicated that adsorption of whey protein to ceramic membranes was greater when pore sizes were larger (200 nm vs. 50 nm) because proteins could enter the pores and cover additional surface area. Despite the enhanced adsorption capacity of relatively large pores, flux will be reduced to a greater degree if a narrower pore becomes fouled to the same extent as a larger pore, simply because there is less open space to be lost (van der Horst, 1995). Minimizing surface roughness reduces the risk of fouling simply by taking away points at which foulant can easily attach to the membrane. Membrane charge is yet another consideration. Given that biological proteins (including CN micelles and SP) are negatively charged at near-neutral pH, positively charged membranes or even neutral membranes would foul to a lesser extent than a positively charged membrane when filtering dairy fluids, assuming minimal cation salt bridging. This assumption, however, is unlikely as Ca^{2+} is prevalent in almost all dairy fluids and will link the negatively charged proteins to one another or a negatively charged membrane through via electrostatic interactions.

Ho and Zydney (1999) determined that a MF membrane's pore structure plays a large role in the initial rate of flux decline during protein (BSA) fouling. Membranes with highly

interconnected pore systems exhibited slower rates of initial flux decline (i.e., slower fouling) than membranes with straight-through pores (i.e., no interconnectivity) because permeate was able to maneuver around foulant deposited on and just below the surface of the interconnected-pore membrane. In addition, membrane porosity was found to be inversely proportional to the initial rate of flux decline, at least at relatively low porosities. In this low porosity region, an increased number of pores allowed more foulant to be applied without diminishing flux. However, porosity was eventually increased to a point at which flux decline was no longer mitigated because localized areas of foulant buildup obstructed more than one pore, offsetting the benefit of additional pores. Bacchin et al. (2006) indicate that by increasing the membrane's porosity further still, pores could eventually become so close to one another that foulant deposition would be limited by particle-particle steric repulsions. When interconnected pore structures are not present, the pore's shape has been shown to impact a membrane's critical flux (the maximum flux prior to rapid fouling). Microsieves are membranes, usually made from metals, that have a well defined pore structure which is created by precision etching. Bacchin et al. (2006) indicated that microsieves with slotted pores have been shown to exhibit higher critical flux values when compared to those with circular pores.

The channel shape within a membrane through which the product flows may also be of importance in regard to fouling. When working with membranes containing star-shaped channels at cross-flow velocities between 0.6 and 2 m/s, Chiu et al. (2005) noted that a higher critical flux could be expected using this design than might be observed with traditional circular channels. This observation was attributed to the star-shaped channel's ability to promote turbulent flow at the membrane surface. In 1999, Technologies Avancees & Membrane Industrielles (TAMI) produced a patent regarding the creation of non-circular membrane channels which were

triangular in nature (Grangeon and Lescoche, 1999). Aside from increasing the amount of surface area in a given element volume, this design is purported to confer the following advantages over circular designs: reduced headloss within the support structure and increased flow speed of the permeate through the channels. These claims are based on the fact that the majority of the channel's surface area (the triangle side opposite of the minimum angle) is oriented toward the element's periphery (Figure 1.5).

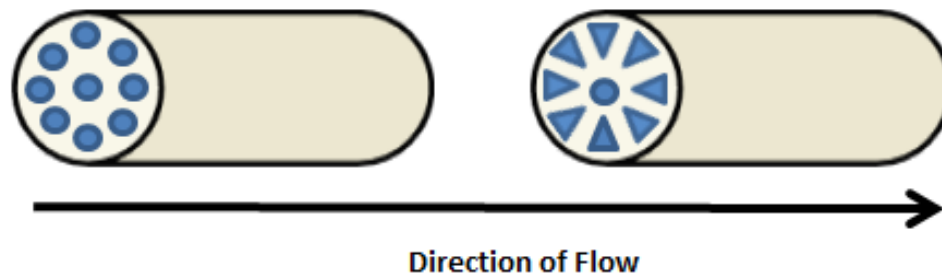


Figure 1.5. Illustration of differences in ceramic membrane flow channel design. Left: traditional circular channels, right: triangular channels as proposed by Grangeon and Lescoche.

Effect of Processing Conditions

Each of the following processing parameters impacts the degree of fouling in a membrane operation. Often, flux maxima or fouling minima cannot be attained by simply pushing these processing values to one extreme or another, but rather, there is a careful balance to be made. The fact that most of the processing parameters that influence fouling are tied to one another further complicates the matter.

Membrane Flux and Cross-flow Velocity. The effects of membrane flux and cross-flow velocity on membrane fouling depend heavily on one another. In general, increasing the cross-flow velocity increases the limiting flux (Marshall and Daufin, 1995). When operating in constant flux mode, flux is maintained and pressure on the retentate side of the membrane is allowed to increase until the system flux is too low and the system must be cleaned or the process is completed. The chosen flux in this operating scheme impacts fouling in the system

because an increased flux at a constant pressure increases convection toward the membrane surface which fouls the membrane to a greater extent.

Shear stress at the membrane wall can be increased by increasing the cross-flow velocity on the retentate side of the membrane. In doing so, turbulent flow is promoted. This turbulence scours the surface of the membrane to break up the reversible foulant layer and provides inertial lift from the membrane surface which mitigates concentration polarization, thus reducing the potential for fouling (Belfort et al., 1994). Le Berre and Daufin (1996) considered various flux values (30 to 109 L/m² h) along with various shear stresses (23 – 97 Pa) at the surface of a ceramic membrane during skim milk 0.1 µm MF and concluded that there exists a critical flux to shear ratio of 1.0 L/m² h Pa. Below this ratio, the MF membranes did not foul appreciably and the process exhibited longevity. Above this ratio, rapid fouling was noted because convective forces toward the membrane exceeded erosion of the foulant layer. Similarly, Grandison et al. (2000) determined that increasing shear stress at the membrane wall (at constant TMP) and decreasing TMP decreased the resistances due to reversible and irreversible fouling during skim milk UF. It should be noted that in tubular ceramic membrane systems, cross-flow velocities are typically in the range of 5 to 7 m/s. Polymeric flat sheet membrane systems are also capable of being operated at high cross-flow velocities (Belfort et al., 1994). However, polymeric spiral-wound membrane systems are generally limited to about 1 m/s to prevent delamination of the spiral polymeric membrane structure. Therefore, limiting foulant buildup on a polymeric spiral-wound membrane is more difficult than doing so in a tubular ceramic or flat sheet polymeric membrane system.

Transmembrane Pressure. Transmembrane pressure, or the pressure on the retentate side of the membrane minus the pressure on the permeate side of the membrane, is the driving force

behind pressure-driven membrane technologies. When operating in constant pressure mode, TMP is maintained and flux is allowed to decrease until the system must be cleaned or the process is completed. The effect of TMP on membrane fouling and flux varies depending on magnitude of the pressure. The TMP-dependant nature of flux can be explained by the critical flux theory (Brans et al., 2004). Briefly, 3 regimes exist; wherein the TMP is below, slightly above, and well above a critical pressure, respectively. In the first regime, flux is linearly dependent on TMP according to Darcy's law (Saboya and Maubois, 2000). In this state, no cake layer will be formed. As the TMP increases, however, the second regime is initiated in which a cake layer is being deposited and flux is almost independent of TMP. If the TMP is forced too much higher, flux begins to decline rapidly, as depth fouling and cake layer compaction predominates. Processors should strive to maintain their operations within the second stage to maximize flux efficiency (Brans et al., 2004). It follows that maintaining a uniformly low TMP across the length of the membrane would be desirable in attaining this goal, as was first proposed by Sandblom (1978).

Temperature. As stated above, the processing temperature can affect fouling characteristics in a dairy filtration process by influencing the chemical makeup of the feed stream. However, it can also impact membrane flux and fouling strictly from a physical point of view. Equation 1 indicates that the membrane flux is inversely proportional to the permeate viscosity. The viscosity of a fluid will invariably decrease with increasing temperature (unless a chemical change occurs) due to increased molecular diffusivity. It follows that a processor would wish to operate at as high a temperature as possible to maximize processing efficiency (provided that no protein denaturation or mineral precipitation occurs and the system is not damaged). In the dairy industry, this maximum temperature is generally accepted to be 50 to 55°C. Though no

SP denature at temperatures below 62°C (deWit and Klarenbeek, 1984), calcium phosphate is less soluble at higher temperatures. Conventionally, this 50 to 55°C range was adopted due to the temperature limitations of polymeric membranes. Additional work is lacking in the literature which addresses whether or not this temperature range could be extended using ceramic membranes without severe mineral fouling.

Even though flux can be maximized at higher temperatures, there are incentives to operating at temperatures < 7°C. The primary dairy applications for cold filtration include limiting bacterial growth during processing and isolating β -CN from the CN micelle. Both uses involve MF and have been studied (van Hekken and Holsinger, 2000; Fritsch and Moraru, 2008), but have failed to garner widespread industrial interest due to the low flux associated with the cold processes.

Fouling Reduction

Ceramic Microfiltration. It was previously noted that increasing cross-flow velocity on the retentate side of the membrane can enhance back diffusion from the membrane surface, thus reducing fouling. However, with higher recirculation rates, not only are energy costs increased, but there is also a proportionate increase in the pressure drop from inlet to outlet along the membrane's retentate side. This results in an elevated TMP at the membrane inlet (causing rapid fouling at the inlet) and a low TMP at the outlet, which may result in underutilization of the membrane (Figure 1.6).

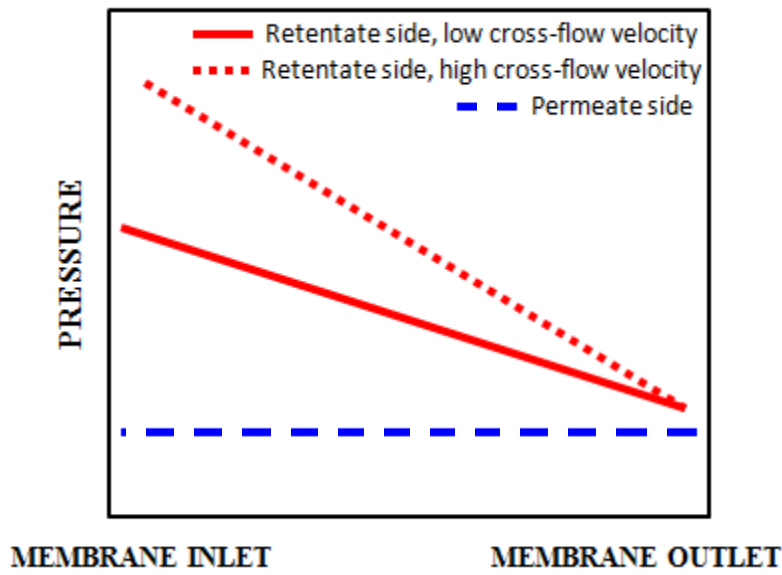


Figure 1.6. Pressure profiles across the length of the membrane during low and high cross-flow velocity filtration. Transmembrane pressure = pressure on the retentate side of the membrane – pressure on the permeate side of the membrane.

To overcome this challenge, uniform permeate flux systems have been developed. The subsequent techniques for achieving such an effect have been well described by Saboya and Maubois (2000), Brans et al. (2004), Pouliot (2008), and Zulewska et al. (2009). Alfa-Laval developed the first method of achieving this goal by placing a pump on the permeate side of the membrane to co-currently match the retentate side's pressure drop on the permeate side of the membrane (Sandblom, 1978). In this so-called uniform transmembrane pressure (UTP) process, TMP at the inlet is almost identical to TMP at the outlet. Furthermore, these identical pressures can be kept lower than traditional MF TMP (< 45 kPa instead of about 250 kPa), providing enough driving force for the separation to take place, but not enough to rapidly foul the membrane (Hurt et al., 2010). In the UTP process, polymeric beads are also placed in the permeate housing to occupy dead volume and enhance the process's stability by reducing pressure fluctuations. While reliable, the process' permeate pump adds to the capital cost of the system and the variable energy costs necessary to operate the system.

To circumvent these additional expenses, yet still provide uniform permeate flux, Societe des Ceramiques Techniques (SCT) and TAMI patented the Membralox Graded Permeability (GP) and Isoflux membranes, respectively, in 2002. (Garcera and Toujas, 2002; Grangeon et al., 2002) Each membrane is designed with a more tortuous path at the membrane's inlet through which the permeate must travel. This effect is gradually reduced along the length of membrane so as to achieve an even permeate flux despite high cross-flow velocities. The GP patent involves incorporating a gradient along the external surface of the membrane support structure that decreases in resistance to permeate flow from inlet to outlet. The Isoflux patent seeks to achieve uniform permeate flux by decreasing the thickness of the selective layer from the inlet to the outlet.

While UTP, GP, and Isoflux membranes are some of the more common means for reducing fouling in industrial ceramic MF systems, several other techniques described by Brans et al. (2004) have been developed, but are not widely commercialized due to scale-up difficulties. Backpulsing is a technique that involves intermittently reversing the membrane TMP (usually with pressurized CO₂) to reincorporate foulant into the bulk retentate flow. This method has been shown to improve average cold MF (6°C) flux during raw skim milk bacteria removal by almost 50% when backpulsing once per min (Fritsch and Moraru, 2008). Vibrating modules and rotating disk units work by increasing the shear stress near the surface of the membrane by vibrating the membrane and sweeping the membrane surface, respectively (Brans et al., 2004). Other methods which act to disturb fluid flow near the membrane surface include pulsating the cross-flow, sending air slugs through the system, and incorporating turbulence promoters within the flow path (Brans et al., 2004).

Polymeric Spiral Wound Ultrafiltration. As noted above, fouling may be reduced in cross-flow filtration processes by increasing the cross-flow velocity. However, this technique cannot be used during polymeric spiral wound processing due to these membranes' propensities to delaminate under the high shear stresses caused by high cross-flow velocities. Additionally, the tendency for polymeric membranes to deform under TMP makes them susceptible to damage by backpulsing techniques or application of back pressure on the permeate side of the membrane. Consequently, other measures must be taken to limit fouling during polymeric spiral wound UF. A popular method for doing so in these instances involves pretreating the feed stream prior to UF to remove foulant material or render potential foulant less likely to accumulate on the membrane (Hiddink et al., 1981). These goals may be reached by imparting a chemical pretreatment on the feed material, utilizing separations (centrifugal, sedimentation, or larger pore size membrane processes) upstream of the process in question, or a combination of both. The polymeric membrane may also be chemically rendered more hydrophilic to reduce the likelihood of initial deposition due to hydrophobic interactions between the membrane and the foulant. Of course, membrane modifications such as these are no longer effective once the membrane has been concealed with foulant monolayers.

Cleaning. The importance of proper cleaning after membrane processes cannot be overemphasized. The cleaning regimen must be such that it returns the system's flux capacity to what it was prior to processing and removes any bacteriological contamination without damaging the membranes or other heat and chemical-sensitive parts (i.e., gaskets) of the system (Krack, 1995). Assuming no damage to the membrane or system, the factors which positively influence the efficacy of a cleaning process include: temperature, concentration of the cleaning chemicals, system flow dynamics (i.e., pressure and flow rate), and residence time (Krack, 1995). If any one

of these factors is decreased, another one must be increased to compensate for the loss of cleaning ability (Krack, 1995; Bird and Bartlett, 2002).

Increased temperature reduces the viscosity of the cleaning solution, thereby increasing fluid turbulence, and increases the rate of the cleaning agents' reactions with foulant material (i.e., protein hydrolysis) (Bird and Bartlett, 2002). When cleaning ceramic and stainless steel flat sheet membranes after WPC MF, Bartlett et al. (1995) found that increasing the temperature of the cleaning process from 30 to 70°C decreased the cleaning time at which maximum flux recovery (the ratio of the flux during cleaning to that of pure water under the same conditions) was attained. However, while heating from 30 to 50°C increased maximum flux recovery, increasing the temperature from 50 to 70°C decreased maximum flux recovery. The latter decrease in flux recovery was attributed to protein denaturation or calcium precipitation during the cleaning process. However, this finding was based on cleaning with sodium hydroxide alone, not a formulated alkaline cleaning agent (which would aid in protein solubilization) or an acid (which would remove mineral deposits). Both of these chemicals would be used sequentially in an industrial practice, and would act synergistically to alleviate protein and mineral fouling.

From the information above, it can be inferred that the type of cleaning chemicals, their concentrations, and the order in which they are used largely determine the quality of a membrane cleaning treatment. During the same WPC study, Bartlett et al., (1995) determined that using 0.3% nitric acid recovered roughly 25% of the initial clean water flux, 0.4% sodium hydroxide about 70%, and 0.5% Ultrasil 11 (a formulated alkaline membrane cleanser containing surfactants) about 80%. Additionally, Bartlett et al. (1995) found that cleaning with nitric acid after sodium hydroxide produced a higher flux recovery than the opposite sequence, presumably because the sodium hydroxide treatment removed proteinaceous foulant that encased mineral

deposits which could only be removed with nitric acid. Cleaning a membrane system with acid after an alkaline wash is a common dairy industry practice, as the reverse sequence would lead to protein aggregation when CN is present.

To maximize foulant removal during cleaning of RO, NF, and UF membranes, processors should operate the membrane system under low TMP and as high of a cross-flow velocity as the system will permit to limit additional cake layer formation during the cleaning process (Bartlett et al., 1995; Krack, 1995; Bird and Bartlett, 2002). Because foulant in dairy fluids is more likely to penetrate the membrane larger pores of MF, it is advised that TMP be held low initially and gradually increased during MF cleaning (Krack, 1995).

Fouling Quantification

Fouling Coefficient. One way to determine the extent of fouling after a membrane process is to calculate a fouling coefficient based on the pure water flux of the system before and after processing under standard conditions. By maintaining a consistent applied pressure on the retentate side of the membrane at a given temperature, a processor can determine how much of the initial membrane permeability is lost due to the addition of firmly deposited foulant material on the membrane. To calculate a fouling coefficient, the “fouled water” flux (which is determined after the membrane is rinsed with RO water, but not cleaned with chemical agents) is divided by the initial “clean water” flux and the quotient is subtracted from 1 (Rao, 2002). A higher fouling coefficient indicates a greater degree of membrane fouling, with a value of 1 corresponding to complete membrane blockage.

Hydraulic Resistance. Another method to estimate fouling that relies on membrane permeability involves calculating the resistances contributed by various flux reduction phenomena. This is done by first calculating the resistance due to the clean membrane using

Equation (1) under standard conditions with pure water. Once the membrane resistance is established, additional sources of resistance may be estimated as described in Caric et al., (2000) and Fritsch and Moraru (2008). By soaking the membrane in the feed material then conducting a fouled water flux measurement, a rough estimation of the resistance due to general adsorption may be quantified after subtracting out the membrane's resistance. An overall gauge of the resistance due to the final foulant layer may be established after processing as in the description for the fouling coefficient above. The concentration polarization component of flux reduction may then be accounted for by deducting the adsorption and membrane resistances from the overall resistance during steady state process flux. Of course, these measurements would all need to be conducted under the same thermal and hydrodynamic conditions to maintain relative precision.

Membrane Imaging. If there is no need to determine the flux reduction caused by fouling, imaging techniques may be used to examine the membranes before and after processing to elucidate the distribution of foulant material. Most commonly, scanning electron microscopy, atomic force microscopy, and X-ray photoelectron spectroscopy have been used in the past (James et al., 2003; Fritsch and Moraru, 2008). Scanning electron microscopy can be used to image cross sections of membranes to examine internal fouling structures. By using this technique, Fritsch and Moraru (2008) determined that multichannel ceramic MF membranes foul to a greater extent within channels at the periphery of the membrane when compared to more interior channels. This finding was attributed to the existence of a velocity gradient within the diameter of the membrane element. Atomic force microscopy is better suited to visualizing surface fouling or characterizing clean membrane surface roughness, as cross sections usually prove to be too irregularly shaped for this method. While not a form of microscopy, X-ray

photoelectron spectroscopy has the benefit of being able to detect the chemical makeup of the membranes. James et al. (2003) were able to identify localized areas of nitrogen buildup in skim milk-fouled membranes (thus, indicating the presence of protein foulant), whereas no nitrogen was detected in clean membranes. It should be considered, that each of the above techniques are highly invasive and would require the destruction of the membrane for analysis. Furthermore, because these methods require extensive preparation of the membrane before imaging, the original form of the foulant may be altered prior to analysis (Chan and Chen, 2004).

Conclusions

Fouling limits the productivity of membrane processes by reducing the flux. Flux reduction is the result of concentration polarization, adsorption of foulant to the membrane's surface, and in some cases, membrane compaction. When processing dairy fluids, this problem is particularly acute due to the ubiquity of two known foulants among milk and whey: proteins and calcium mineral complexes. While fouling cannot be eliminated completely, processors may limit its progression by choosing membrane materials which adsorb less foulant, optimizing processing conditions such as cross-flow velocity, temperature, and TMP, pretreating system feeds to reduce their propensities to foul, or adopting novel technologies which seek to limit fouling. A proper cleaning regimen will also reduce the amount of irreversible foulant buildup over the lifetime of the membrane. The extent of fouling may be quantified in several ways, the most common of which include: visual observation of the foulant layer through microscopy, calculation of the resistances contributed by different fouling-related phenomena, and comparison of the membrane's clean and fouled water flux values.

REFERENCES

- Association of Official Analytical Chemists. 2000. Official Methods of Analysis. 17th ed. AOAC, Gaithersburg, MD.
- Bacchin, P., P. Aimar, and R. W. Field. 2006. Critical and sustainable fluxes: theory, experiments, and applications. *J. Membr. Sci.* 281:42-69.
- Bird, M.R. and M. Bartlett. 2002. Measuring and modeling flux recovery during the chemical cleaning of MF membranes for the processing of whey protein concentrate. *J. Food Eng.* 53:143-152.
- Bartlett, M., M.R. Bird, and J.A. Howell. 1995. An experimental study for the development of a qualitative membrane cleaning model. *J. Membr. Sci.* 105:147-157.
- Beckman, S. L., J. Zulewska, M. Newbold, and D. M. Barbano. 2010. Production efficiency of micellar casein concentrate using polymeric spiral-wound microfiltration membranes. *J. Dairy Sci.* 93:4506-4517.
- Belfort, G., Davis, R. H. and A. L. Zydney. 1994. The behavior of suspensions and macromolecular solutions in crossflow microfiltration. *J. Membr. Sci.* 96:1-58.
- Brans G., C. G. P. H. Schroen, R. G. M. van der Sman, R. M. Boom. 2004. Membrane fractionation of milk: state of the art and challenges. *J. Membr. Sci.* 243:263–72.
- Caric, M. D., S. D. Milanovic, D. M. Krstic, and M. N. Tekic. 2000. Fouling of inorganic membranes by adsorption of whey proteins. *J. Membr. Sci.* 165:83-88.
- Chan, R. and V. Chen. 2004. Characterization of the protein fouling on membranes: opportunities and challenges. *J. Membr. Sci.* 242:169-188.
- Cheryan M. 1998. Ultrafiltration and microfiltration handbook. Technomic Publishing Company, Inc., Lancaster, PA, USA.

- Chiu, T. Y., M. V. Lara Dominguez, and A. E. James. 2005. Non-circular ceramic membranes for use in wastewater treatment. *Environ. Prot. Eng.* 31:53-60.
- Daufin, G. and U. Merin. 1995. Fouling of inorganic membranes in filtration processes of dairy products. *Fouling and Cleaning in Pressure Driven Membrane Processes*. International Dairy Federation Bulletin.
- de la Casa, E. J., A. Guadix, R. Ibanez, and E. M. Guadix. 2007. Influence of pH and salt concentration on the cross-flow microfiltration of BSA through a ceramic membrane. *Biochem. Eng. J.* 33:110-115.
- deWit, J. N. and G. Klarenbeek. 1984. Effects of various heat treatments on structure and solubility of whey proteins. *J. Dairy Sci.* 67:2701-2710
- Elwell, M. W. and D. M. Barbano. 2006. Use of microfiltration to improve fluid milk quality. *J. Dairy Sci.* 89:E10-E30.
- Evans, J., J. Zulewska, M. Newbold, M. A., Drake, D. M. Barbano. 2010. Comparison of composition and sensory properties of 80% whey protein and milk serum protein concentrates. *J. Dairy Sci.* 93:1824-1843.
- Fox, P. F. 1997. *Advanced Dairy Chemistry Volume 3: Lactose, Water, Salts, and Vitamins*, Second Edition. Chapman & Hall. London, UK.
- Fritsch, J. and C. I. Moraru. 2008. Development and optimization of a carbon dioxide-aided cold microfiltration process for the physical removal of microorganisms and somatic cells from skim milk. *J. Dairy Sci.* 91:3744-3760.
- Garcera, R. M. and E. Toujas, inventors. 2002. Graded permeability macroporous support for crossflow filtration. Societe de Ceramiques Techniques, assignee. US Pat. No. 6,375,014 B1.

- Gesan-Guiziou, G., G. Daufin, and E. Boyaval. 2000. Critical stability conditions in skimmed milk crossflow microfiltration: impact on operating modes. *Lait*. 80:129-140.
- Gesan-Guiziou, G., G. Daufin, M. Timmer, D. Allersma, and C. van der Horst. 1999. Process steps for the preparation of purified fractions of α -lactalbumin and β -lactoglobulin from whey protein concentrates. *J. Dairy Res.* 66:225-236.
- Gouderanche, H., J. Fauquant, and J. L. Maubois. 2000. Fractionation of globular milk fat by membrane microfiltration. *Lait*. 80:93-98.
- Grangeon, A., P. Lescoche, T. Fleischmann, and B. Ruschel, inventors. 2002. Cross-flow filter membrane and method for manufacturing it. *Technologies Avancees & Membranes Industrielles*, assignee. US Pat. No. 6,499,606 B1.
- Grangeon, A. and P. Lescoche, inventors. 1999. Inorganic tubular filter element including channels of non-circular section having optimized profile. *Technologies Avancees & Membranes Industrielles*, assignee. US Pat. No. 5,873,998.
- Hanemaaijer, J. H., T. Robbertsen, T. van den Boomgaard, and J.W. Gunnink. 1989. Fouling of ultrafiltration membranes – the role of protein adsorption and salt precipitation. *J. Membr. Sci.* 40:199-217.
- Hiddink, J., R. De Boer, and P.F.C. Nooy. 1981. Effect of various pretreatments on the ultrafiltration of sweet cheese whey at about 55°C. *Milchwissenschaft*. 36:657-663.
- Ho, C. and A. L. Zydney. 1999. Effect of membrane morphology on the initial rate of protein fouling during microfiltration. *J. Membr. Sci.* 155:261-275.
- Hurt, E. and D. M. Barbano. 2010. Processing factors that influence casein and serum protein separation by microfiltration. *J. Dairy Sci.* 93:4928-4941.
- Hurt, E., J. Zulewska, M. Newbold, and D. M. Barbano. 2010. Micellar casein concentrate

- production with a 3X, 3-stage uniform transmembrane pressure ceramic membrane process at 50°C. *J. Dairy Sci.* 93:1941-1947
- James, B. J., Y. Jing, and X. D. Chen. 2003. Membrane fouling during filtration of milk – a microstructural study. *J. Food Eng.* 60:431-437.
- Krack, R. 1995. Chemical agents and costs in cleaning and disinfection of membrane equipment. *Fouling and Cleaning in Pressure Driven Membrane Processes*. International Dairy Federation Bulletin 9504. Brussels, Belgium.
- Marshall, A. D. and G. Daufin. 1995. Physico-chemical aspects of membrane fouling by dairy fluids. *Fouling and Cleaning in Pressure Driven Membrane Processes*. International Dairy Federation Bulletin 9504. Brussels, Belgium.
- Marshall, A. D., P. A. Munro, and G. Tragardh. 1993. The effect of protein fouling in microfiltration and ultrafiltration on permeate flux, protein retention and selectivity: a literature review. *Desalination*. 91:65-108.
- Nelson, B. K. and D. M. Barbano. 2005. A microfiltration process to maximize removal of serum proteins from skim milk before cheese making. *J. Dairy Sci.* 88: 1891-1900.
- Nelson, B. K. and D. M. Barbano. 2005. Yield and aging of Cheddar cheeses manufactured from milks with different serum protein contents. *J. Dairy Sci.* 88:4183-4194.
- Papadatos, A., M. Neocleous, A. M. Berger, and D. M. Barbano. 2003. Economic feasibility evaluation of microfiltration of milk prior to cheesemaking. *J Dairy Sci.* 86:1564-1577.
- Pouliot, Y. 2008. Membrane processes in dairy technology – from a simple idea to worldwide panacea. *Int. Dairy J.* 18:735-740.
- Rao, H. G. R. 2002. Mechanisms of flux decline during ultrafiltration of dairy products and influence of pH on flux rates of whey and buttermilk. *Desalination* 144:319–324.

- Renner, E. and M. H. Abd El-Salam. 1991. Application of Ultrafiltration in the Dairy Industry. Elsevier Science Publishing Company, Inc. New York, New York.
- Rice, G., A. Barber, A. O'Conner, G. Stevens, and S. Kentish. 2009. Fouling of NF membranes by dairy ultrafiltration permeates. *J. Membr. Sci.* 330:117-126.
- Rosenberg, M. 1995. Current and future applications for membrane processes in the dairy industry. *Trends Food Sci. Technol.* 6:12-19.
- Rudan, M.A. 1990. Membrane fouling during ultrafiltration of milk. MS Thesis. Cornell University, Ithaca, NY.
- Saboya, L. V. and J. L. Maubois. 2000. Current developments of microfiltration technology in the dairy industry. *Lait.* 80:541-553.
- Sandblom, R. M., inventor. 1978. Filtering process. Alfa-Laval AB, assignee. US Pat. No. 4,105,547.
- Schwinge, J., P.R. Neal, D.E. Wiley, D.F. Fletcher, and A.G. Fane. 2004. Spiral wound modules and spacers – review and analysis. *J. Membr. Sci.* 242:129-153.
- Tong, P. S., D. M. Barbano, and M. A. Rudan. 1988. Characterization of proteinaceous membrane foulants and flux decline during the early stages of whole milk ultrafiltration. *J. Dairy Sci.* 71:604-612.
- Tong, P. S., D. M. Barbano, and W. K. Jordan. 1989. Characterization of proteinaceous membrane foulants from whey ultrafiltration. *J. Dairy Sci.* 72:1435-1442.
- Tossavainen, O. and J. Sahlstein. 2010. Process for producing a lactose-free milk product. Valio Ltd., assignee. US Pat. No. 7,829,130 B2.
- van der Horst, H. C. 1995. Fouling of organic membranes during processing of dairy liquids. *Fouling and Cleaning in Pressure Driven Membrane Processes. International Dairy*

- Federation Bulletin 9504. Brussels, Belgium.
- van Hekken, D. L. and V. H. Holsinger. 2000. Use of cold microfiltration to produce unique β -casein enriched milk gels. *Lait*. 80:69-76.
- Vyas, H. K., R. J. Bennett, and A. D. Marshall. 2000. Influence of feed properties on membrane fouling in crossflow microfiltration of particulate suspensions. *Int. Dairy J.* 10:855-861.
- Walstra, P., J. T. M. Wouters, and T. J. Geurts. 2006. *Dairy Science and Technology: Second Edition*. Taylor & Francis Group. Boca Raton, FL.
- Zall, R. R. 1987. Accumulation and quantification of on-farm ultrafiltered milk: the California experience. *Milchwissenschaft* 42:98-100.
- Zulewska, J., M. Newbold, and D. M. Barbano. 2009. Efficiency of serum protein removal from skim milk with ceramic and polymeric membranes at 50°C.

CHAPTER TWO

Serum Protein Removal from Skim Milk

with a 3-Stage, 3X Ceramic Isoflux Membrane Process at 50 °C

ABSTRACT

Small pore microfiltration (MF) can be used to remove serum proteins (SP) from skim milk. The process' SP removal efficiency directly influences the technology's economic feasibility. Our objective was to quantify the capacity of 0.14 μm ceramic Isoflux MF membranes to remove SP from skim milk. A 3-stage, 3X, feed-and-bleed MF study with diafiltration in the latter 2 stages was conducted at 50°C using Isoflux membranes to determine cumulative SP removal percentages and SP removal rates at each processing stage. The experiment was replicated 3 times starting with different batches of raw milk.

In contrast to 3X MF theoretical cumulative SP removal percentages of 68%, 90%, and 97% after 1, 2, and 3 stages, respectively, the 3X Isoflux MF process removed only 39.5%, 58.4%, and 70.2% of SP after 1, 2, and 3 stages, respectively. Previous research has been published that provides the skim milk SP removal capacities of 3-stage, 3X 0.1 μm ceramic Membralox uniform transmembrane pressure (UTP), 0.1 μm ceramic Membralox graded permeability (GP), and 0.3 μm polymeric polyvinylidene fluoride spiral-wound (PVDF SW) MF systems at 50°C. No difference in cumulative SP removal percentage after 3 stages was detected between the Isoflux and previously published PVDF SW (70.3%) values, but SP removal was lower than published GP (96.5%) and UTP (98.3%) values. To remove 95% of SP from 1000 kg of skim milk in 12 h it would take 7, 3, 3, and 7 stages with 6.86, 1.91, 2.82, and 14.24 m^2 of membrane surface area for the Isoflux, GP, UTP, and PVDF SW systems, respectively. The MF systems requiring more stages would produce additional permeate at lower protein

concentrations. The ceramic MF systems requiring more surface area would incur higher capital costs.

Possible reasons why SP removal with the Isoflux membranes was lower than theoretical include: a range of membrane pore sizes existed (i.e., some pores were too small to pass SP), the selective layer modification and reverse flow conditions at the membrane outlet combined to reduce the effective membrane surface area, and the geometric shape of the Isoflux flow channels promoted early fouling of the membrane and rejection of SP by the foulant.

INTRODUCTION

Microfiltration (MF) is a membrane process used to remove suspended particles from a fluid medium. Though it lacks the ubiquity afforded to other membrane processes in the dairy industry such as ultrafiltration and reverse osmosis (RO), MF can offer a variety of innovative applications to the dairy industry. One such application is the processing of skim milk to separate serum proteins (SP) from CN. Serum proteins (0.003 to 0.010 μm) exist as soluble proteins in skim milk, but CN is present in colloidal micelles (0.02 to 0.40 μm , mean = 0.10 μm) (Walstra et al., 2006). Consequently, a 0.1 μm MF separation of skim milk results in a CN-rich retentate fraction and a SP-rich permeate fraction.

Like all other membrane processes, MF efficiency is hindered by membrane fouling. Fouling occurs through a variety of mechanisms that ultimately cause the membrane pores to become obstructed by adsorbed material, or foulant. This phenomenon results in decreased flux, shortened processing times, and decreased efficiency of separation of the feed material solutes. Cross-flow filtration, or pumping the fluid tangential to the membrane's surface, is often employed in industrial settings to minimize fouling. The high cross-flow velocities used in ceramic MF systems (typically 5 to 7 m/s) limit the buildup of foulant by mitigating

concentration polarization via fluid turbulence. More specifically, increased shear and enhanced inertial lift at the surface of the membrane due to the high velocity result in a portion of the concentration polarization layer being reincorporated into the bulk flow (Belfort et al., 1994). However, due to the direct relationship between pressure drop and a fluid's velocity through a conduit, increasing cross-flow velocity results in a high transmembrane pressure (TMP) at the membrane's inlet and a low TMP at its outlet. This results in a decreasing flux gradient over the length of the membrane causing rapid fouling at the inlet and underutilization of the membrane at the outlet. Though uniform transmembrane pressure (UTP) processes have been proven to circumvent this drawback, they require an additional pump on the permeate side of the membrane to match the pressure drop on the retentate side of the membrane. This increases both the capital and energy costs.

Two ceramic membrane designs have been introduced that claim to deliver uniform permeate flux along the length of the membrane without the need for a permeate recirculation pump. Traditionally, ceramic membranes are composed of a thin selective layer that is bonded onto a rigid, macroporous support structure. The pore size of the selective layer determines the membrane's selectivity, while the support layer provides the membrane's mechanical strength without contributing to its rejection characteristics. The Membralox graded permeability (GP) membrane, patented by SCT in 2002, is equipped with a permeability gradient along the exterior surface of the macroporous support structure that increases in mean porosity from inlet to outlet. This provides a gradual decrease in hydraulic resistance from inlet to outlet (Garcera and Toujas, 2002).

Technologies Avancees & Membranes Industrielles (TAMI) approached the non-uniform flux problem differently by patenting the Isoflux membrane later that year. The Isoflux

membrane contains a selective layer on the interior surface of the flow channels that tapers in thickness from the inlet end of the membrane to the outlet. It is designed to provide a constant ratio of TMP to selective layer thickness that is purported to deliver equal permeate flux across the entire length of the membrane (Grangeon et al., 2002). The method by which TAMI creates this membrane involves sequentially adding selective layers to the internal surfaces of the flow channels within the support structure (Grangeon et al., 2002). For example, should the manufacturer choose to apply 4 selective layers: the first layer would be applied to the entire length of the membrane, the second layer would be applied to three quarters of the membrane (starting at the inlet end), the third layer would be applied to the first half of the membrane, and the final layer would be applied to the first quarter of the membrane. This process results in a uniformly stepped selective layer gradient.

Hurt et al., (2010) confirmed that an optimized 3X, 3-stage MF UTP process could remove 97% of the SP from pasteurized skim milk, as was proposed in theory (Hurt and Barbano, 2010). However, the actual SP removal efficiency has been shown to vary considerably among different membrane types: 98.3% UTP (Hurt et al., 2010), 96.5% GP (J. Zulewska, unpublished data), and 70.3% polyvinylidene fluoride spiral wound (PVDF SW) (Beckman et al., 2010). There has been no published research to determine the actual amount of SP that can be removed in a MF process utilizing the TAMI Isoflux ceramic membrane technology. Our objectives were to determine the cumulative SP removal percentages and SP removal rates for each stage in a 3-stage, 3X feed-and-bleed MF system equipped with 0.14 μm ceramic Isoflux membranes when processing pasteurized skim milk at 50°C with 2 stages of water diafiltration and to compare these values to those of other membrane systems determined under similar conditions.

MATERIALS AND METHODS

Experimental Design and Statistical Analysis

One lot of bovine milk (about 370 kg) was separated in the Cornell University dairy plant at 4°C using a Model 590 Air Tight Centrifuge, (DeLaval Co., Chicago, IL). Raw skim milk was pasteurized using a plate heat exchanger equipped with 3 sections: regeneration, heating, and cooling (Model 080-S, AGC Engineering, Manassas, VA) at 72°C with a holding time of 16 s. Temperature was kept at minimum for pasteurization to minimize denaturation of SP. The milk was cooled to 4°C and stored at $\leq 4^{\circ}\text{C}$ until MF processing the following day. Just before processing, the pasteurized skim milk was heated to 50°C with a plate heat exchanger (Model A3, DeLaval, Inc., Kansas, MO) and microfiltered using a pilot-scale system equipped with the ceramic Isoflux membranes in a constant flux, feed-and-bleed mode to continuously produce a 3X MF retentate and MF permeate (1 kg of retentate for every 2 kg of permeate) at 50°C. The MF retentate was collected and diluted back to a 1X concentration with pasteurized RO water (2 kg of RO water for every 1 kg of retentate), then diafiltered with the ceramic Isoflux MF system to produce a 3X retentate. This diafiltration step was repeated once more to complete a 3-stage process. This process was replicated 3 times using different batches of raw milk.

Data were analyzed by ANOVA using the Proc GLM procedure of SAS (SAS version 8.02, SAS Institute Inc., Cary, NC). To detect differences ($P < 0.05$) in Isoflux sample composition and color among stages, the general linear model (GLM) was dependent variable = processing stage + replicate + error. To detect differences in SP removal among several different membrane systems (i.e., UTP, GP, and PVDF SW) for each stage, the GLM was dependent variable $_{\text{STAGE}} = \text{system} + \text{replicate} + \text{error}$. For comparisons of least square means among the 3 stages and different systems, a Tukey-Kramer adjustment was made for multiple comparisons.

To determine if flux or permeate inlet pressure (P_{p_i}) changed during startup or transmembrane pressure at the inlet (TMP_i), transmembrane pressure at the outlet (TMP_o), flux, or P_{p_i} changed over time within each processing stage, a model for each processing variable was constructed for each time frame (i.e., during startup or during stages 1, 2, or 3). The GLM for each processing variable was dependent variable $_{TIME\ FRAME} =$ transformed time + replicate + error, where transformed time (a continuous variable) was the mean-centered processing time in minutes. If the model term for transformed time was significant ($P < 0.05$), the processing variable was determined to have changed. A decrease or increase in a processing variable over time was indicated by a negative or positive sign, respectively, for each model's transformed time parameter estimate.

Microfiltration Operation

A pilot-scale MF system (Tetra Alcross M7, TetraPak Filtration Systems, Aarhus, Denmark) equipped with ceramic Isoflux (TAMI, Nyons, France) membranes (sunflower channel design, selective layer: titanium dioxide, support structure: titanium dioxide, nominal pore diameter = $0.14\ \mu\text{m}$; surface area = $1.05\ \text{m}^2$) was used. Three tubular, 23-channel (3.5 mm equivalent diameter) ceramic membranes measuring 1.178 m in length were housed in a tubular stainless steel module. Variable area flow meters from GEMÜ Valves, Inc. (Atlanta, GA) were used to measure the volumetric removal rates of both the retentate (model 55/-/23) and permeate (model 57/-/23) streams. The MF system consisted of a feed pump (type LKH 10/110 SSS 1.75 kW) and a retentate recirculation pump (type LKH 20/125 SSS 6.3 kW), both from Alfa Laval, (Kansas City, MO). The retentate recirculation pump was equipped with a variable frequency drive (MC Series, Model M12100C, Lenze AC Tech, Uxbridge, MA) and a magnetic flow transmitter (I/A Series, IMT25, Foxboro, Foxboro, MA) so that the linear velocity could be

controlled and monitored, respectively. The membranes were mounted vertically in the MF system with retentate flow from the top to the bottom of the module. Because the membranes were mounted vertically, the inlet and outlet gauge pressures had to be corrected for differences due to the weight of the vertical column of liquid. Corrections were determined as follows: with 50°C RO water in the system, only the feed pump turned on, and the retentate and permeate outlet valves closed, the retentate inlet pressure (R_{p_i}), permeate inlet pressure (P_{p_i}), retentate outlet pressure (R_{p_o}), and permeate outlet pressure (P_{p_o}) were measured. Gauge pressure correction factors were calculated as follows: the R_{p_i} gauge pressure correction was P_{p_o} minus R_{p_i} , the R_{p_o} gauge pressure correction was P_{p_o} minus R_{p_o} , the P_{p_i} gauge pressure correction was P_{p_o} minus P_{p_i} , and the P_{p_o} gauge pressure correction was zero. These correction factors were determined at the beginning of each processing run. Next the retentate recirculation pump was turned on, the retentate removal rate was set to 30 L/h, and the permeate removal rate was set to 60 L/h. The elevation corrected inlet and outlet pressures were measured and the TMP from the retentate to the permeate side of the membrane at the inlet (TMP_i) and the outlet (TMP_o) ends of the membrane were calculated. The change in TMP along the length of the membrane (ΔTMP) was calculated as the difference between TMP_i and TMP_o .

Cleaning Prior to Processing. The day prior to processing, the MF system was cleaned. Storage solution (0.55% vol/vol solution nitric acid) was flushed out of the system with room temperature RO water until the pH was neutral. The MF flow system was heated with RO water to 80°C and then Ultrasil 25 (Ecolab Inc., Food and Beverage Division, St Paul, MN) liquid alkaline membrane cleaner (1.95 % vol/vol) was added to the water to reach pH 11. The alkaline solution was recirculated for 25 min at a permeate removal rate of approximately 1000 L/h and a retentate removal rate of approximately 160 L/h with both pumps running. After cleaning, the

membrane system was slowly ($< 10^{\circ}\text{C}$ per min) cooled to 50°C with a tubular heat exchanger in the recirculation loop. The MF system was then flushed with RO water (about 300 kg at 30°C) until neutral pH was reached. At this point, the permeate and retentate outlet valves were closed and the pumps were turned off. The day of processing, the membrane was flushed with 50°C RO water (about 60 kg) until the system temperature was 50°C and the initial clean water flux was determined. The following conditions were applied during the initial clean water flux measurement: the retentate outlet valve was closed, the permeate outlet valve was fully open, and only the feed pump was turned on.

Processing. Pasteurized skim milk (about 340 kg) was processed under constant flux (about $54\text{ kg/m}^2\text{ h}$) to approximately a 3X concentration factor (CF) at 50°C using the pilot-scale MF system described above. The MF system was started on 50°C RO water and there was a transition from water to milk with both pumps running, the retentate recirculation rate was approximately 259 L/min which corresponded to a linear velocity of approximately 6.5 m/s. Approximately 115 kg of the skim milk was used to flush the 50°C water out of the system at the beginning of the process. About 35 kg of retentate and 70 kg of permeate were collected in standard 38 L milk cans, the weights were recorded using a high capacity scale (ChampTM, Ohaus Corporation, Florham Park, NJ), and both were discarded. While flushing the water out of the system, samples of retentate and permeate were collected in 89 mL snap lid vials (Capital Vial, Inc., Fultonville, NY) every 5 to 15 min and analyzed for composition using an infrared spectrophotometer (IR) (Lactoscope FTIR, Delta Instruments, Drachten, The Netherlands) to ensure that all of the water had been removed from the system. After flushing the water from the system, the remaining skim milk (about 225 kg) was added to the system and retentate and permeate were collected continuously. Retentate and permeate removal rates, as measured by the

aforementioned variable area flow meters, were controlled using manual diaphragm valves and maintained at approximately 30 and 60 L/h, respectively. Typical retentate (R_{p_i}) and permeate (P_{p_i}) inlet pressures were 441 and 215 kPa, respectively, and typical retentate (R_{p_o}) and permeate (P_{p_o}) outlet pressures were 232 and 229 kPa, respectively. The flux ($\text{kg/m}^2 \text{ h}$) was measured every 15 min and samples of the permeate and the retentate were taken for composition analysis using IR to monitor the process. The CF was also monitored every 15 min by collecting retentate and permeate from the system in two tared, 19 L buckets over 2 min. The buckets' weights were determined using a balance (SB 32000, Mettler Toledo, Columbus, OH) and the CF was calculated as the sum of the retentate (about 950 g) and permeate (about 1900 g) masses divided by the retentate mass. If the measured CF fell outside of the range of 3.00 ± 0.05 , the removal rates were adjusted and the weighing process was repeated. At the end of each MF stage, the collected retentate and permeate were mixed separately and sampled. The masses of the permeate and retentate collected throughout the MF stage plus their respective losses due to sampling were totaled and used to calculate an overall stage CF. The permeate was subsequently discarded, while the retentate was diluted back to 1X using pasteurized, 50°C RO water. This equated to a diafiltration factor (DF) of 3X. The average total time of processing was about 152 min for the first stage, 147 min for the second stage and 141 min for the third stage. Preliminary work was done to ensure that these processing times would result in data representative of a longer processing run. During a 360 min single stage trial, P_{p_i} did not fall below values reported in each of the 150 min runs at a constant flux (about $54 \text{ kg/m}^2 \text{ h}$). This indicated that there was little additional fouling occurring between 150 and 360 min that might hinder a longer process' SP removal productivity.

Cleaning After Processing. Immediately after processing, 50°C RO water (about 175 L) was flushed through the system with both pumps on. The retentate and permeate removal rates were set at approximately 160 L/h and 60 L/h, respectively. The MF system was flushed until no retentate was visible in the flush water on the retentate side. When the water flush was complete, the fouled membrane water flux was determined with the retentate outlet valve closed, the permeate outlet valve completely open, the feed pump on, and the temperature maintained at 50°C. On average, fouled membrane flux was about 31% of the clean membrane water flux (194 vs. 632 L/m² h). Next, the MF flow system was heated with RO water to 80°C. Ultrasil 25 liquid alkaline membrane cleaner (Ecolab Inc.) was added (1.95% vol/vol) to the water to reach pH 11. With both pumps on, this solution was recirculated for 25 min with the permeate and retentate exit flows at approximately 1000 and 160 L/h, respectively. After cleaning, the membrane system was slowly (< 10°C per min) cooled to 50°C with the heat exchanger on retentate recirculation loop. The membrane was then flushed with 30°C RO water until neutral pH was reached. The MF flow system was then heated to 50°C by flushing with 50°C RO water and the post-run clean water flux was determined. During the flux determination the retentate outlet valve was closed, the permeate outlet valve was fully open, the temperature was maintained at 50°C, and only the feed pump was turned on. The post-run clean water flux values were close to the pre-run clean water flux values (about 628 L/m² h, on average). After determination of the clean water flux, a 0.55% vol/vol solution of nitric acid and water was recirculated through the membrane at 50°C for 10 min. Permeate and retentate outlet flows were approximately 1000 and 160 L/h, respectively. After 10 min of the nitric acid solution recirculation, the permeate and retentate outlet valves were closed and the pumps were turned off. The membrane was stored in 0.55% vol/vol nitric acid solution.

Chemical Analyses

Samples of the feed material, permeate, and retentate from each stage were collected during processing and analyzed using IR for fat, lactose, and true protein content (Kaylegian et al., 2006). This was done to quickly monitor the composition of retentate and permeate to confirm that the system was running normally. The pH of the feed material, final permeate, and final retentate from each stage were measured with a solid polymer electrode (HA405-DXK-S8/120, Mettler-Toledo, Bedford, MA) and an Accumet 915 pH meter (Fisher Scientific, Pittsburgh, PA) that was calibrated at 50°C using standard pH 4 and 7 buffer solutions (Fisher Scientific, Pittsburgh, PA).

The initial skim milk, final permeate, and final retentate from each stage were analyzed for total solids (TS), total nitrogen (TN), nonprotein nitrogen (NPN), and noncasein nitrogen (NCN) content using forced air oven drying (AOAC, 2000; method 990.20; 33.2.44), Kjeldahl (AOAC, 2000; method 991.20; 33.2.11), Kjeldahl (AOAC, 2000; method 991.21; 33.2.12), and Kjeldahl (AOAC, 2000; method 998.05; 33.2.64), respectively. Crude protein (CP) was calculated by multiplying TN by 6.38, true protein (TP) was calculated by subtracting NPN from TN and multiplying by 6.38, casein (CN) was calculated by subtracting NCN from TN and multiplying by 6.38, and SP content was calculated by subtracting NPN from NCN and multiplying by 6.38. In addition, the fat content of the initial skim milk and retentates were determined using ether extraction (AOAC, 2000; method 989.05; 33.2.26).

SP Removal Estimation Using Kjeldahl Analysis of Permeates. The SP removal percentage and removal rate for each stage were estimated using Kjeldahl analysis (CP, NPN, and NCN) of permeates. Serum protein removal equaled the percentage of SP in the original skim milk removed in each stage. It was calculated by dividing the mass of SP (SP concentration

was calculated from CP, NPN, and NCN concentrations obtained by Kjeldahl analysis of the permeates, and mass of SP was calculated by multiplying the concentration of SP by the mass of permeate) in the permeate of each stage by the mass of SP in the starting skim milk, then multiplying by 100. Serum protein removal rate was calculated by dividing the mass of SP removed (kg) in a given stage by the product of the membrane surface area (1.05 m^2) and the processing time (h) of the stage.

Color Analysis of Skim Milk and Retentates

Hunter L, a, b values for the initial skim milk and retentates were determined in duplicate with a Macbeth Color-Eye spectrophotometer (Model 2020; Kollmorgen Instruments, Corp., Newburgh, NY) with ProPalette software (Version 5.0; Kollmorgen Instruments, Corp., Newburgh, NY). A white color tile was used as a reflectance standard and was measured at the beginning of each session to verify instrument performance. Hunter values were computed from the diffuse reflectance of light in the 360 to 750 nm range, at 10 nm intervals, based on illuminant A. The measurements were made at $24 \pm 1^\circ\text{C}$ using a 1 cm path length glass cuvette. Final retentate samples for color analysis were taken at the end of each processing stage.

SDS-PAGE Electrophoresis

A 10 to 20% polyacrylamide gradient was used to determine the relative proportion of protein types in initial skim milks, retentates, and permeates. Skim milk samples (0.1 mL) were diluted with sample buffer (0.9 mL) consisting of 10 mM Tris-HCl pH 6.8, 1.0% SDS, 20% glycerol, 0.02% bromophenol blue tracking dye, and 50 mM dithiothreitol in glass vials (Target DP™ Vials C4000-1W, National Scientific Company, Rockwood, TN) and sealed with DP Blue Caps (C4000-51B, National Scientific Company). Diluted samples were heated to 100°C in a steam chamber, held at 100°C for 3 min, and then cooled to about 25°C . Samples were promptly

stored frozen (-17°C) until use. Retentates and permeates were prepared in the same manner, except that the retentates (0.1 mL) were diluted in 2.9 mL of sample buffer and stage 1, 2, and 3 permeates (0.2, 0.4, and 0.5 mL, respectively) were diluted in 0.8, 0.6, and 0.5 mL, respectively, of sample buffer. Skim milks, retentates, and stage 1, 2, and 3 permeates were loaded 9, 9, 22, 21, and 28 μL , respectively, onto an SDS-PAGE gel to standardize the level of the sample's principal protein (α_{s1} -CN for the skim and retentate samples and β -LG for the permeate samples) loaded across samples to approximately 0.90 μg . Loading of the samples was chosen to achieve an optical density (OD) of the predominant protein in the sample in the range of 1.0 to 1.4 OD. The procedure of Verdi et al. (1987) was used for running, staining, and destaining the gels. Gels were scanned with USB GS 800 Densitometer using Quantity 1 1-D Analysis software (BIO-RAD Laboratories, Inc., Hercules, CA) to obtain a relative protein composition of samples. Two gels were prepared for each replicate, one containing the retentate samples from each stage of processing, the other containing the permeate samples from each stage of processing. This layout was chosen to account for replicate error in the results during statistical analysis. Each sample of retentate or permeate was loaded in triplicate from a common vial. A single skim milk sample from the respective replicate was run on each gel as a reference for proper resolution of milk proteins and a check for consistency of quantitative analysis from gel to gel. The background was adjusted separately for each lane using the rolling disk method of subtraction to obtain a flat base on the pop-up trace. The line that defined each lane was adjusted using the lane tool function (add, adjust anchors) in the software so that the lane line crossed each band at the center. The adjust band function of the software was used with brackets to set the leading and trailing edge for each band as visually observed on the image of the gel, not based on the

beginning and end of the peak in the pop-up trace. The bracket width was set to include the full width of all bands.

Relative Percentage of β -LG to β -LG Plus α -LA in Skim Milk, Permeate and Retentate Samples. To ascertain if β -LG was being rejected by the membrane to a greater extent than α -LA, the relative percentages of β -LG (i.e., β -LG / (β -LG + α -LA)) in the retentate and permeate samples from each stage were compared to those of skim milk.

CN Passage Through the Membrane. To examine the level of CN contamination in the permeates and to confirm that the Kjeldahl NCN permeate analyses were accurate, CN as a percentage of true protein (CN%TP) was determined for each permeate sample by summing the relative densities of all CN bands, dividing by the sum of the relative densities of all bands (SP and CN) and then multiplying by 100.

Comparison of Membranes for 95% SP Removal

Using data from the present and past studies (Beckman et al., 2010; Hurt et al., 2010; J. Zulewska, unpublished data), models were developed using Excel 2007 (Microsoft, Redmond, WA) to calculate the number of stages and the membrane surface area (m^2) required to remove 95% of the SP from 1000 kg of skim milk in 12 h. Assumptions for the models were as follows: CF = 3X for all stages, DF = 3X for all stages, flux values for the first 3 stages were those reported in the literature, flux values for additional processing stages (if necessary) were maintained at the reported third stage's value, and SP accounted for 0.60% (w/w) of the skim milk's mass. All SP removal values in the models were based on Kjeldahl analyses of the permeates and initial skim milk as described above.

Stage Number Calculation. The number of stages necessary to remove 95% of the SP in skim milk was determined 2 ways. The first method involved plotting experimentally-derived

cumulative SP removal (% of original SP) after each of the first 3 stages against stage number, then fitting a logarithmic regression line ($R^2 > 0.99$) to each data set. Each regression equation was used to solve for the number of stages at which 95% of the SP would be removed in each membrane system. The second method involved plotting the experimentally-derived SP removal rates ($\text{kg/m}^2 \text{ h}$) through 3 stages against stage number and fitting a power law regression line ($R^2 > 0.95$) to each data set. These equations were used to predict future stage removal rates for all membranes. The removal rates were then multiplied by their respective stages' processing times and experimental membrane surface areas, divided by the initial skim milk's SP mass, multiplied by 100, and added to the previous stage's value (if applicable) to establish cumulative SP removal values for each stage. These cumulative SP removal values were then subjected to the first method described above ($R^2 > 0.99$) to determine the number of processing stages necessary to remove 95% of the SP. The average of the 2 methods was rounded up to the nearest integer and reported. In all but 1 instance, both methods resulted in the same value when rounded up.

Membrane Surface Area Calculation. The surface area required to remove 95% of the SP from 1000 kg of skim milk in 12 h was determined by allocating a percentage of the 12 h of processing time to each stage according to its flux. The average number of stages from the previous calculation (non-integer) was used to establish how many stages would be involved in this calculation. The mass of permeate in a given stage (667 kg) was then divided by the stage flux and the stage process time to calculate the necessary membrane surface area.

RESULTS

MF Processing Parameters

While flushing the system with skim milk during startup, flux did not change ($P > 0.05$), but Pp_i decreased steadily with time ($P < 0.05$) (Figure 2.1). During processing, mean TMP_i and

TMP_o values decreased ($P < 0.05$) with each successive stage (Table 2.1) because of reductions in feed viscosity due to diafiltration.

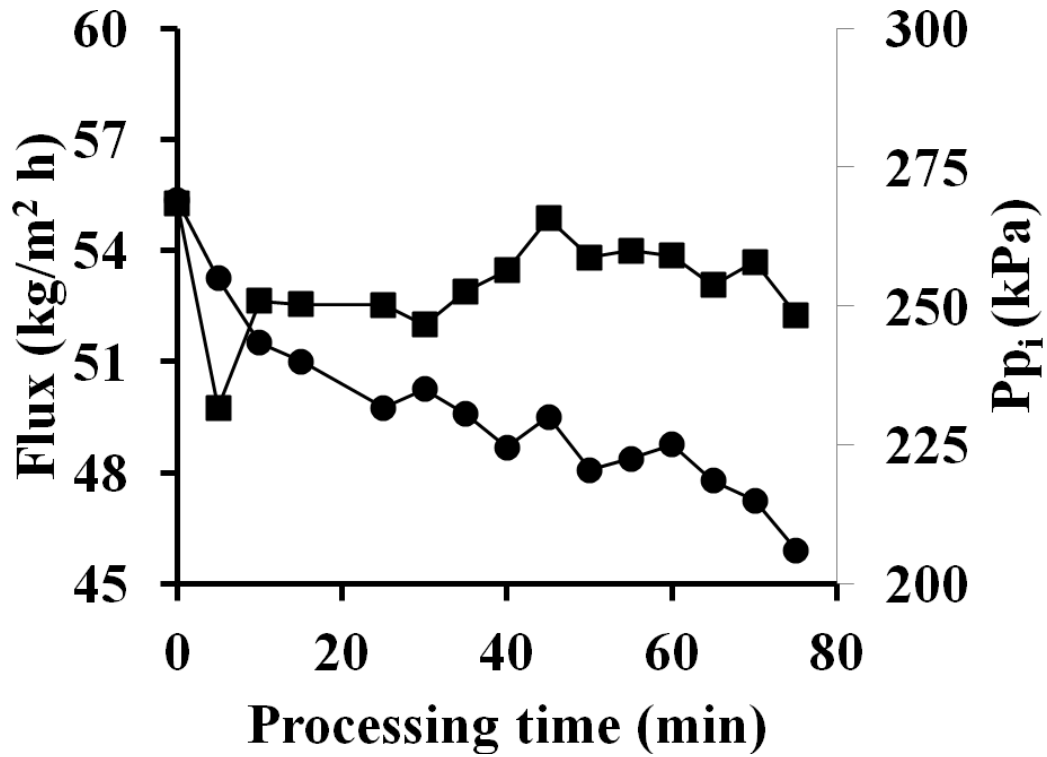


Figure 2.1. Mean ($n = 3$) flux (■) and permeate inlet pressures (Pp_i) (●) while flushing the microfiltration system with skim milk at 50°C during startup using 0.14 μm Isoflux membranes.

Table 2.1. Mean ($n = 3$) transmembrane pressures at the membrane inlet (TMP_i) and outlet (TMP_o), differences in TMP over the length of the membrane (ΔTMP)¹, permeate inlet pressure (P_{pi}), flux, and concentration factors for each stage of the 0.14 μm Isoflux ceramic microfiltration (MF) process

MF stage	TMP_i (kPa)	TMP_o (kPa)	ΔTMP (kPa)	P_{pi} (kPa)	Flux ($kg/m^2 h$)	Concentration factor
1	257 ^a	12 ^a	246 ^a	203 ^c	53.89 ^b	3.03
2	233 ^b	-3 ^b	236 ^b	217 ^b	55.06 ^a	2.97
3	220 ^c	-12 ^c	232 ^b	226 ^a	55.21 ^a	3.02
SEM	3.657	2.377	2.593	1.900	0.351	0.074
R^2	0.98	0.98	0.93	0.98	0.87	0.25

^{a - c} Means in the same column not sharing a common superscript are different ($P < 0.05$).

¹ $\Delta TMP = TMP_i$ minus TMP_o

No change was detected in ($P > 0.05$) TMP_i (Figure 2.2) or TMP_o (Figure 2.3) with time during the first stage of processing. However, TMP_i (Figure 2.2) and TMP_o (Figure 2.3) decreased ($P < 0.05$) during processing in both the second and third stages. The TMP_o values descended below 0 kPa in the second and third stages, indicating reverse flow (Hurt et al., 2010) from the permeate side of the membrane to the retentate side at the outlet end of the membrane. Reverse flow at the membrane outlet was also observed in each stage of 3X MF processing using GP membranes (J. Zulewska, unpublished data). Mean ΔTMP along the length of the membrane decreased ($P < 0.05$) from the first to the second stage, but no change ($P > 0.05$) between the second and third stages was detected (Table 2.1). The average ΔTMP across the three stages was 238 kPa (Table 2.1), over eight times the ΔTMP of 27 kPa achieved by Hurt et al. (2010) when using a ceramic UTP system. Conversely, the Isoflux average ΔTMP across the 3 stages was similar in magnitude to the average ΔTMP of the GP system (250 kPa) described by J. Zulewska (unpublished data).

There was an increase ($P < 0.05$) in mean flux between the first and second stages; though no difference ($P > 0.05$) was detected between the second and third stages (Table 2.1). Flux did not change ($P > 0.05$) with time in stages 1 and 3, but did decrease ($P < 0.05$) during processing in stage 2 (Figure 2.4). Mean Pp_i increased ($P < 0.05$) with each successive stage (Table 2.1). Though Pp_i did not change ($P > 0.05$) with time in stage 1, it increased ($P < 0.05$) with time in stages 2 and 3 (Figure 2.5). No differences ($P > 0.05$) were detected in CF among stages (Table 2.1).

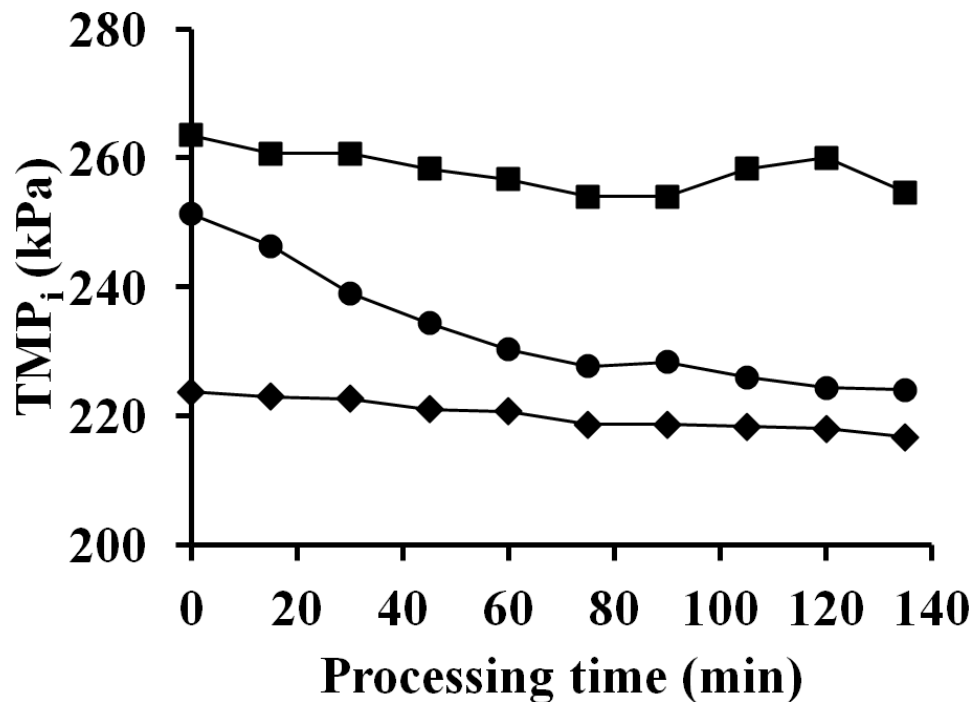


Figure 2.2. Mean ($n = 3$) inlet transmembrane pressures (TMP_i) during processing for stage 1 (■), stage 2 (●), and stage 3 (◆) when microfiltering skim milk at 50°C with 0.14 μm Isoflux membranes using two diafiltration stages.

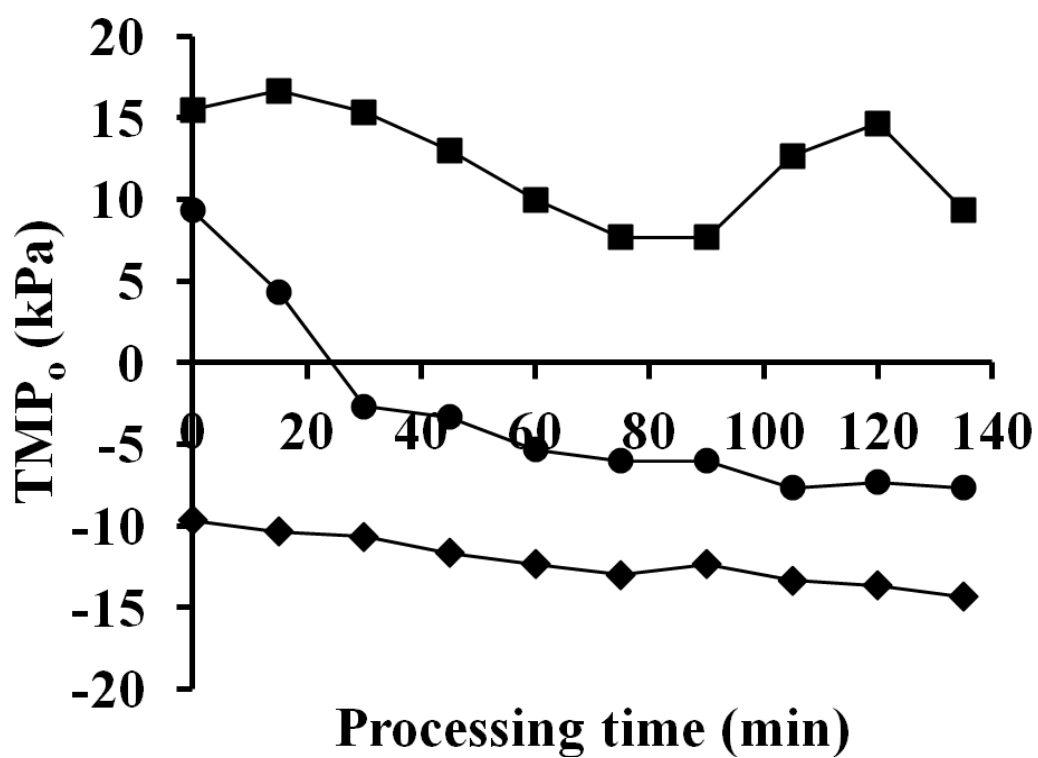


Figure 2.3. Mean ($n = 3$) outlet transmembrane pressures (TMP_o) during processing for stage 1 (■), stage 2 (●), and stage 3 (◆) when microfiltering skim milk at 50°C with 0.14 μm Isoflux membranes using two diafiltration stages.

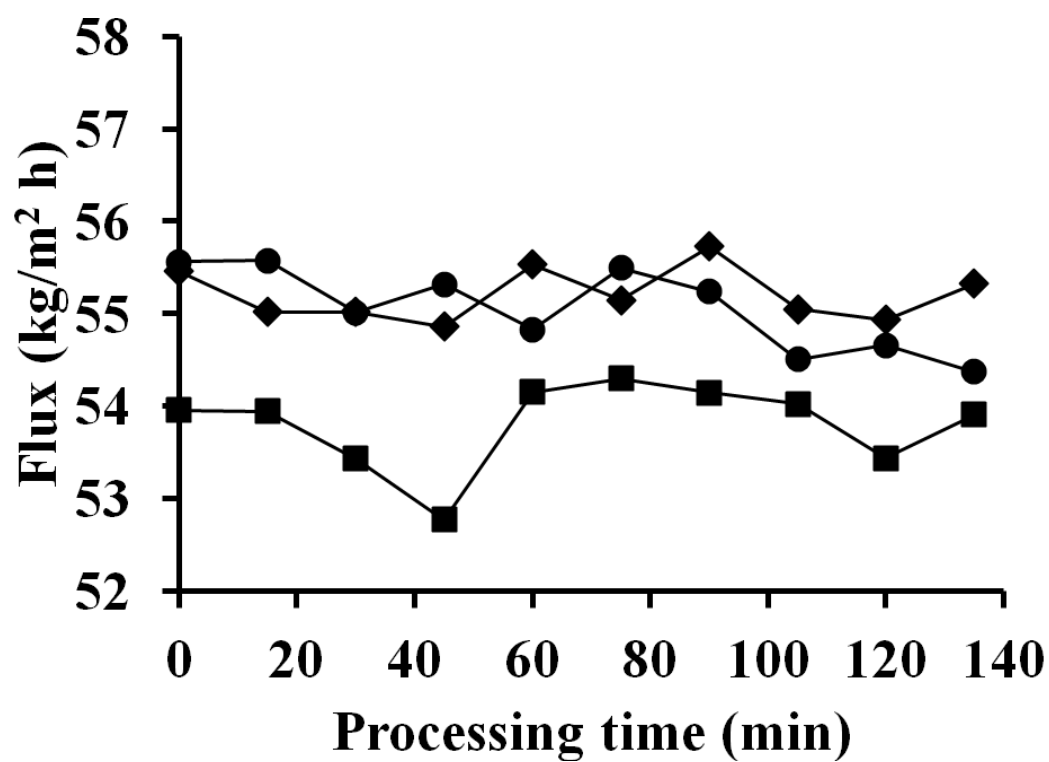


Figure 2.4. Mean ($n = 3$) flux during processing for stage 1 (■), stage 2 (●), and stage 3 (◆) when microfiltering skim milk at 50°C with 0.14 μm Isoflux membranes using two diafiltration stages.

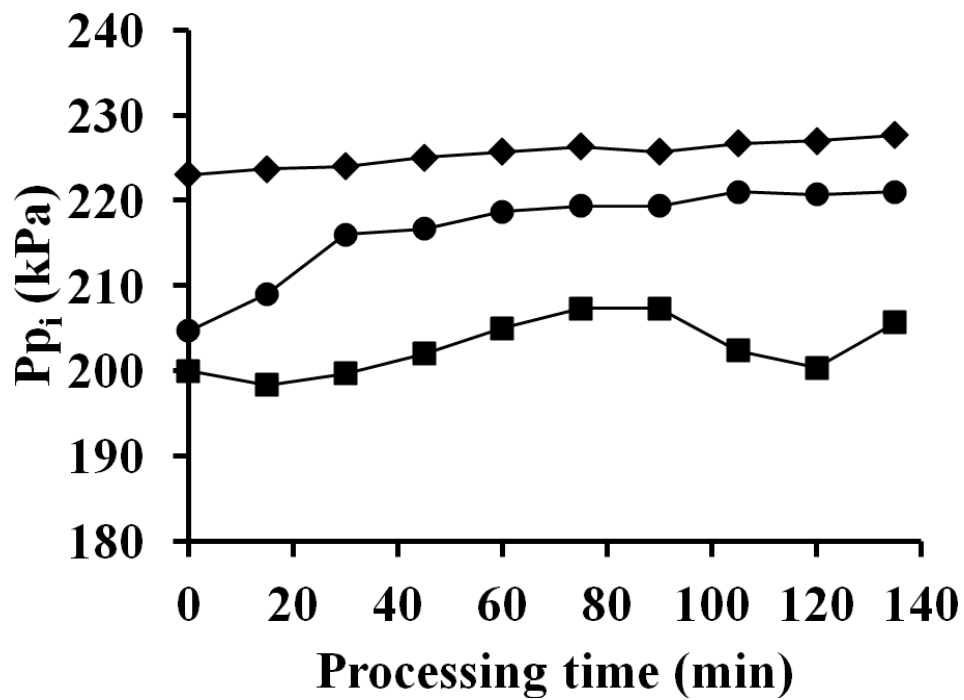


Figure 2.5. Mean ($n = 3$) permeate inlet pressures (P_{p_i}) during processing for stage 1 (■), stage 2 (●), and stage 3 (◆) when microfiltering skim milk at 50°C with 0.14 μm Isoflux membranes using two diafiltration stages.

Composition and Color

Skim Milk Composition. Pasteurized skim milk composition was similar among replicates (Table 2.2).

Table 2.2. Mean (n = 3) composition¹ of pasteurized skim milk (% by weight)

Replicate	TS	Fat	CP	NPN	NCN	TP	CN	SP	CN%TP
1	9.289	0.105	3.439	0.194	0.770	3.246	2.669	0.577	82.228
2	9.313	0.106	3.438	0.198	0.795	3.240	2.643	0.597	81.581
3	9.197	0.109	3.331	0.188	0.764	3.143	2.566	0.577	81.656
Mean	9.266	0.107	3.403	0.193	0.777	3.210	2.626	0.583	81.822
SD	0.061	0.002	0.062	0.005	0.016	0.058	0.053	0.012	0.354

¹TS = total solids; CP = crude protein = total nitrogen x 6.38; NPN = nonprotein nitrogen x 6.38; NCN = noncasein nitrogen x 6.38; TP = true protein = CP minus NPN; CN = casein = CP minus NCN; SP = serum proteins = NCN minus NPN; CN%TP = CN as a percentage of TP = (CN/TP) x 100.

No difference ($P > 0.05$) was detected in mean raw milk (81.32%) and pasteurized milk (81.82%) CN%TP values. Temperatures above 70°C cause SP (β -LG) to denature and fuse to CN (κ -CN) through disulfide bonding (Singh, 1995). Though it is well established that CN makes up approximately 81% of the TP in bovine milk, it has been shown that CN in a given sample can be overestimated due to the coprecipitation of bound SP during indirect NCN analysis if thermal denaturation is extensive (Lynch et al., 1998). However, given the present study's similar raw and pasteurized CN%TP values, the possibility of significant SP denaturation was ruled out.

Permeate Composition. The TS, CP, NPN, NCN, TP, and SP content of permeate decreased ($P < 0.05$) with each successive stage of processing (Table 2.3) due to diafiltration using RO water as a diluent. There was no difference ($P > 0.05$) detected in CN content of permeate among the 3 stages. Permeate CN%TP was lower ($P < 0.05$) in the first stage than in the second and third stages. This was due to the combined effects of a progressively lower

concentration of TP in the diafiltration stages' permeates with a constant background leakage of CN through the membrane.

Table 2.3. Mean (n = 3) composition¹ (% by weight) of permeate from each stage of the 0.14 µm Isoflux ceramic microfiltration (MF) process

MF stage	TS	CP	NPN	NCN	TP	CN	SP	CN%TP
1	6.299 ^a	0.544 ^a	0.189 ^a	0.537 ^a	0.355 ^a	0.007	0.348 ^a	1.980 ^b
2	2.565 ^b	0.268 ^b	0.078 ^b	0.255 ^b	0.190 ^b	0.013	0.177 ^b	6.679 ^a
3	1.089 ^c	0.159 ^c	0.035 ^c	0.148 ^c	0.124 ^c	0.011	0.113 ^c	8.363 ^a
SEM	0.028	0.008	0.001	0.007	0.008	0.002	0.007	0.731
R ²	>0.99	>0.99	>0.99	>0.99	>0.99	0.71	>0.99	0.97

^{a-c} Means in the same column not sharing a common superscript are different ($P < 0.05$).

¹ TS = total solids; CP = crude protein = total nitrogen x 6.38; NPN = nonprotein nitrogen x 6.38; NCN = noncasein nitrogen x 6.38; TP = true protein = CP minus NPN; CN = casein = CP minus NCN; SP = serum proteins = NCN minus NPN; CN%TP = CN as a percentage of TP = (CN/TP) x 100.

Retentate Composition. Retentate TS and NPN values decreased ($P < 0.05$) with each successive processing stage (Table 2.4) due to diafiltration and the passage of lactose, SP, low molecular weight nitrogen compounds, and minerals through the membrane. No differences in fat, CN, CP, or TP ($P > 0.05$) among stages were detected. Though the similarities in fat and CN values among stages were to be expected, the similarities in CP and TP among stages were not. Because SP passes through the membrane, one would expect that both CP and TP would decrease as the stages progressed. These discrepancies were likely consequences of slight variations in CF among replicates. The NCN and SP values were greater ($P < 0.05$) in the first stage than in the second. However, no differences ($P > 0.05$) were detected in NCN and SP between the second and third stages. Correspondingly, CN%TP decreased ($P < 0.05$) from the first to the second stage, but remained the same from the second to the third stage ($P > 0.05$). Unfortunately, the retentate samples' NCN analysis filtrates were noted to be cloudy. This indicated that the buffer volume used in the NCN method for milk was not sufficient to reduce

the pH of a MF retentate to 4.6, the isoelectric point of CN. The cloudiness of the NCN filtrate signified the presence of unprecipitated CN and inflated the reported NCN values. Therefore, we feel that the actual CN and CN%TP values were underestimated and the actual SP values were overestimated. Additional work is being done in our laboratory to develop a more robust NCN method for analysis of milk protein concentrates.

Table 2.4. Mean (n = 3) composition¹ (% by weight) of the retentate from each stage of the 0.14 µm Isoflux ceramic microfiltration (MF) process

MF stage	TS	Fat	CP	NPN	NCN	TP	CN	SP	CN%TP
1	15.299 ^a	0.314	9.045	0.199 ^a	1.502 ^a	8.846	7.544	1.302 ^a	85.279 ^b
2	11.988 ^b	0.320	8.818	0.103 ^b	1.239 ^b	8.715	7.579	1.136 ^b	86.968 ^a
3	10.560 ^c	0.320	8.592	0.070 ^c	1.147 ^b	8.522	7.445	1.077 ^b	87.361 ^a
SEM	0.233	0.010	0.235	0.003	0.036	0.235	0.222	0.035	0.401
R ²	>0.99	0.44	0.69	>0.99	0.98	0.59	0.36	0.95	0.93

^{a-c} Means in the same column not sharing a common superscript are different ($P < 0.05$).

¹ TS = total solids; CP = crude protein = total nitrogen x 6.38; NPN = nonprotein nitrogen x 6.38; NCN = noncasein nitrogen x 6.38; TP = true protein = CP minus NPN; CN = casein = CP minus NCN; SP = serum proteins = NCN minus NPN; CN%TP = CN as a percentage of TP = (CN/TP) x 100.

Stage Feed, Retentate, and Permeate pH. Feed, retentate, and permeate pH (Table 2.5) increased ($P < 0.05$) with each stage due to the dilution of hydrogen ions and milk buffering salts with RO water during diafiltration. Permeate samples were noted to change to the greatest degree between stages, followed by the feed samples, followed by the retentate samples. This trend can be explained by the dilution of soluble salts in the samples' serum phases.

Table 2.5. Mean (n = 3) pH values (50°C) of the feed material, final retentate, and final permeate from each stage of the 0.14 µm Isoflux ceramic microfiltration (MF) process

MF stage	Feed material	Retentate	Permeate
1	6.45 ^c	6.42 ^c	6.51 ^c
2	6.67 ^b	6.66 ^b	6.71 ^b
3	6.85 ^a	6.80 ^a	6.89 ^a
SEM	0.018	0.030	0.013
R ²	>0.99	0.98	>0.99

^{a-c} Means in the same column not sharing a common superscript are different ($P < 0.05$).

Skim Milk and Retentate Color. Casein micelles and fat globules possess refractive indices that are much different than those of the water in which they are suspended. This disparity allows these colloidal particles to reflect all wavelengths of the visible spectrum quite evenly, resulting in milk's white color when it is observed under white light (Quinones et al., 1998). When compared to the initial skim milk, all retentates were whiter and less green, more red ($P < 0.05$) (Table 2.6). These findings can be directly attributed to the elevated levels of CN in the retentate samples relative to that of skim milk. Though retentate from the first stage was more yellow, less blue than skim milk ($P < 0.05$), retentates from subsequent stages were the opposite. Retentate from the third stage of processing was whiter ($P < 0.05$) than retentate from the first stage. Moreover, retentate redness and yellowness increased (greenness and blueness decreased) ($P < 0.05$) with each stage of processing.

Table 2.6. Mean ($n = 3$) Hunter L, a, b color values of the initial skim milk and the retentates from each stage of the 0.14 μm Isoflux ceramic microfiltration (MF) process

Sample	L-value	a-value	b-value
Skim milk	75.39 ^c	-5.88 ^d	1.95 ^b
Stage 1 retentate	78.38 ^b	-4.26 ^c	3.32 ^a
Stage 2 retentate	78.87 ^{ab}	-4.03 ^b	1.34 ^c
Stage 3 retentate	79.23 ^a	-3.80 ^a	0.27 ^d
SEM	0.228	0.038	0.105
R ²	0.99	>0.99	>0.99

^{a-d} Means in the same column not sharing a common superscript are different ($P < 0.05$).

SP Removal and CN Passage

SP Removal. The rate of SP removal for Isoflux membranes ($\text{kg}/\text{m}^2 \text{ h}$) decreased ($P < 0.05$) with each stage of processing (Table 2.7). Given that there was less SP to be removed with each sequential stage, this was to be expected. Cumulative SP removal (% of original SP) increased ($P < 0.05$) with each stage, indicating continued SP passage (Table 2.7).

Table 2.7. Mean (n = 3) cumulative serum protein (SP) removal percentages and SP removal rates after each stage of the 0.14 μm Isoflux ceramic microfiltration (MF) process as determined by Kjeldahl analysis of the permeates

MF stage	Cumulative SP removal percentage (% of original SP)	SP removal rate ($\text{kg}/\text{m}^2 \text{ h}$)
1	39.5 ^c	0.19 ^a
2	58.4 ^b	0.10 ^b
3	70.2 ^a	0.06 ^c
SEM	0.411	0.011
R ²	>0.99	0.98

^{a-c} Means in the same column not sharing a common superscript are different ($P < 0.05$).

β -LG and α -LA Partitioning. Bands used for SDS-PAGE densitometry analyses are identified and labeled in the representative retentate (Figure 2.6) and permeate (Figure 2.7) gels. The relative proportion of β -LG to β -LG plus α -LA varied between the skim milk, retentate, and permeate samples (Table 2.8). In skim milk, β -LG accounted for 79.9% of the 2 major SP. However, retentates from all stages contained larger ($P < 0.05$) relative proportions of β -LG when compared to skim milk, indicating that the membrane was selectively rejecting β -LG, the larger of the 2 SP. Correspondingly, the relative proportion of β -LG in each of the permeates was lower ($P < 0.05$) than that of skim milk. Moreover, a larger ($P < 0.05$) relative proportion of β -LG was present in the stage 3 permeate when compared to the stage 1 permeate. This could be accounted for by the increased passage of α -LA relative to β -LG in stages 1 and 2, which would gradually reduce the amount of α -LA available to be passed by stage 3.

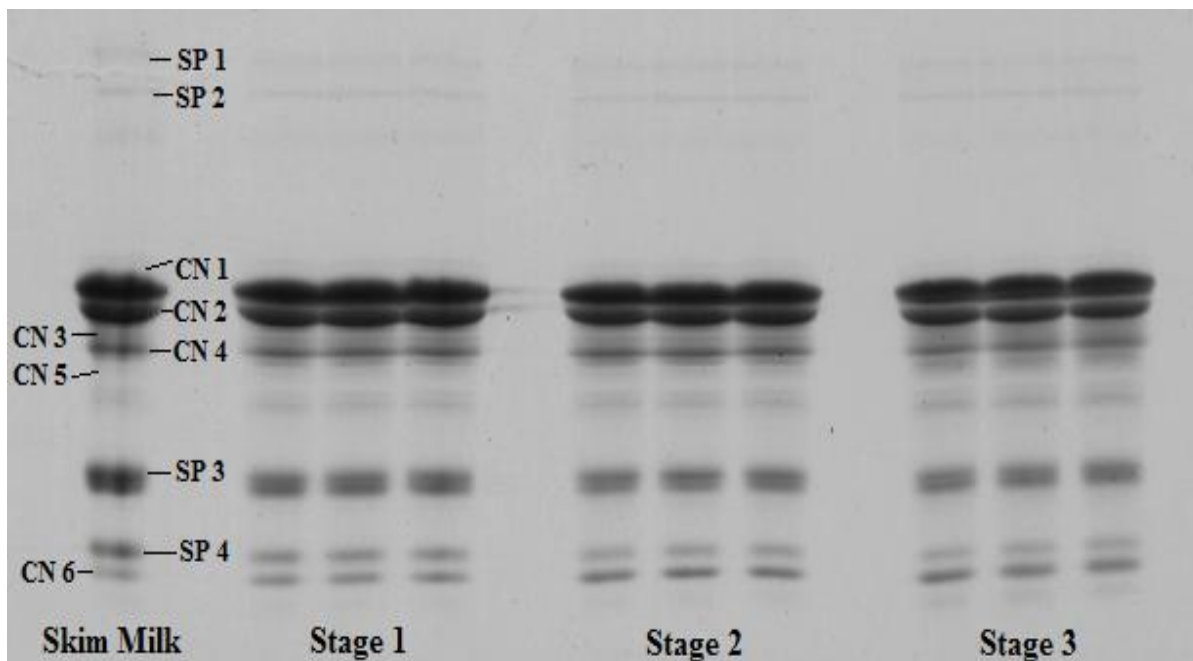


Figure 2.6. Proteins in skim milk and the microfiltration retentates produced in each stage as determined by SDS-PAGE. The three slots within stage 1, 2, and 3 represent the retentate from replicates 1, 2, and 3, respectively. Bands in skim milk are identified on the gel as follows: SP1, SP2 = serum proteins, CN1 = α_s -CN (combination of α_{s1} and α_{s2} -CN), CN2 = β -CN; CN4 = κ -CN; CN3, CN5 and CN6 = proteolysis products of CN; SP3 = β -LG; and SP4 = α -LA.

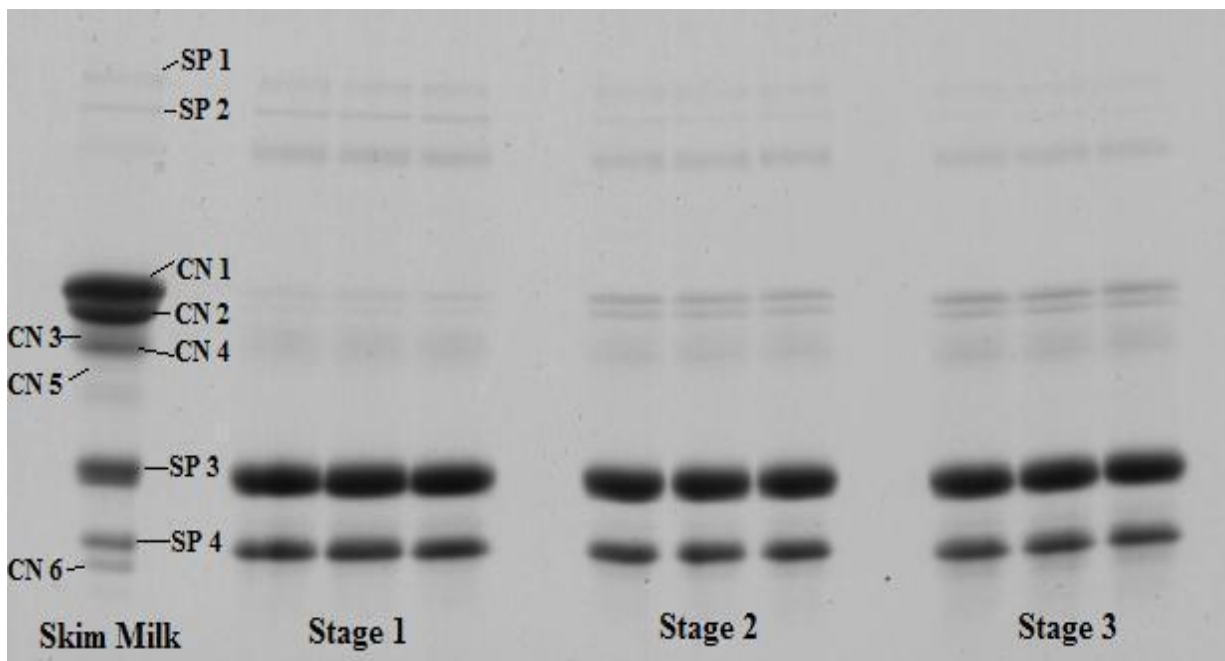


Figure 2.7. Proteins in skim milk and the microfiltration permeates produced in each stage as determined by SDS-PAGE. The three slots within stage 1, 2, and 3 represent the retentate from replicates 1, 2, and 3, respectively. Bands in skim milk are identified on the gel as follows: SP1, SP2 = serum proteins, CN1 = α_s -CN (combination of α_{s1} and α_{s2} -CN), CN2 = β -CN; CN4 = κ -CN; CN3, CN5 and CN6 = proteolysis products of CN; SP3 = β -LG; and SP4 = α -LA.

Table 2.8. Mean (n = 3) relative percentages of β -LG to β -LG plus α -LA in skim milk, permeate and retentate samples from each stage of the 0.14 μ m Isoflux ceramic microfiltration (MF) process as determined by densitometry analysis of SDS-PAGE gels

Skim Milk MF stage	Relative percentage of β -LG	
	79.9 ^b Retentate	79.9 ^a Permeate
1	84.4 ^a	71.5 ^c
2	87.0 ^a	73.0 ^{bc}
3	86.9 ^a	74.6 ^b
SEM	1.235	0.957
R ²	0.91	0.96

^{a-c} Means in the same column not sharing a common superscript are different ($P < 0.05$).

CN Passage into Permeate. The levels of CN contamination in permeate samples as determined by SDS-PAGE densitometry analysis followed a similar trend to those determined by Kjeldahl analysis, but were approximately 50% lower. Using the Kjeldahl TN and NCN methods, CN%TP values for the stage 1, 2, and 3 permeates were 1.98%, 6.68% and 8.36%, respectively. Using the SDS-PAGE method, CN%TP values for the stage 1, 2, and 3 permeates were 1.24%, 2.95% and 3.77%, respectively.

DISCUSSION

SP Removal Comparison

Compared to other ceramic membranes evaluated under similar 3-stage, 3X MF processing conditions (Hurt et al., 2010; J. Zulewska, unpublished data), the Isoflux membranes removed less SP in a given amount of time on the first and second stages of processing ($P < 0.05$) (Table 2.9). The SP removal rates for the GP membranes were determined using higher mean flux values in each stage (72.5, 84.5, and 92.7 kg/m² h for stages 1, 2, and 3, respectively) (J. Zulewska, unpublished data) than those used in the present study. Because near theoretical levels of SP were removed using the GP membranes, it was not surprising that the GP

membranes' SP removal rates would exceed those of the Isoflux membranes at each stage. However, the UTP system examined by Hurt et al. (2010) was operated at flux values similar to those used in the present study (54.0, 54.0, and 54.6 kg/m² h for stages 1, 2, and 3, respectively). Though the Isoflux membranes' first and second stage SP removal rates were lower than those of the UTP system's, the third stage values were similar between the 2 systems. The SP removal rate similarity between the UTP and Isoflux systems' third stages can be attributed to the Isoflux feed having a larger amount of SP remaining in the stage 3 feed. Spiral wound membranes contain far more membrane surface area per unit volume than ceramic membranes. This fact, combined with the poor SP removal capacity of the PVDF SW membranes determined by Beckman et al. (2010), resulted in the PVDF SW system's SP removal rates being lower than any of the ceramic systems examined at each stage of processing ($P < 0.05$).

Table 2.9. Mean ($n = 3$) rate of serum protein (SP) removal (kg/m² h) by each stage of the 0.14 μ m Isoflux ceramic, 0.10 μ m graded permeability (GP) ceramic, 0.10 μ m uniform transmembrane pressure (UTP) ceramic, and 0.30 μ m polyvinylidene fluoride spiral-wound (PVDF SW) microfiltration (MF) processes as determined by Kjeldahl analysis of the permeates

MF stage	Isoflux	GP ¹	UTP ²	PVDF SW ³	SEM	R ²
1	0.19 ^c	0.37 ^a	0.30 ^b	0.05 ^d	0.007	>0.99
2	0.10 ^c	0.20 ^a	0.11 ^b	0.04 ^d	0.004	>0.99
3	0.06 ^b	0.12 ^a	0.06 ^b	0.03 ^c	0.007	0.98

^{a-d} Means in the same row not sharing a common superscript are different ($P < 0.05$).

¹ Data from J. Zulewska, unpublished data.

² Data ($n = 4$) from Hurt et al., 2010.

³ Data from Beckman et al., 2010.

Cumulative SP removal percentages of the Isoflux membranes (Table 2.10) were lower than those of the UTP and GP membrane systems examined by Hurt et al. (2010) and Zulewska (unpublished data), respectively, at each stage of processing ($P < 0.05$). Therefore, the Isoflux SP removal percentages were also lower than theoretical values. Conversely, no differences were

detected ($P > 0.05$) between the cumulative SP removal percentages of the Isoflux membranes and PVDF SW membranes reported by Beckman et al. (2010) at each stage.

Table 2.10. Mean ($n = 3$) cumulative serum protein (SP) removal percentage (% of original SP) after each stage of the 0.14 μm Isoflux ceramic, 0.10 μm graded permeability (GP) ceramic, 0.10 μm uniform transmembrane pressure (UTP) ceramic, and 0.30 μm polyvinylidene fluoride spiral-wound (PVDF SW) microfiltration (MF) processes as determined by Kjeldahl analysis of the permeates

MF stage	Isoflux	GP ¹	UTP ²	PVDF SW ³	SEM	R ²
1	39.5 ^c	56.0 ^b	64.8 ^a	38.6 ^c	1.33	>0.99
2	58.4 ^c	82.6 ^b	87.8 ^a	59.3 ^c	1.42	>0.99
3	70.2 ^b	96.5 ^a	98.3 ^a	70.3 ^b	2.15	>0.99

^{a-c} Means in the same row not sharing a common superscript are different ($P < 0.05$).

¹ Data from J. Zulewska, unpublished data.

² Data ($n = 4$) from Hurt et al., 2010.

³ Data from Beckman et al., 2010.

It was estimated that 7 MF stages would be necessary to remove at least 95% of the SP from skim milk using the present Isoflux MF process (Table 2.11). This is over twice the number of stages required by both the GP and UTP processes and equivalent to the number of stages needed by the PVDF SW process to achieve the same goal. Moreover, the Isoflux membranes would require approximately 2.4 times as much membrane surface area as the UTP system and 3.6 times as much surface area as the GP membranes to remove 95% of the SP from 1000 kg of skim milk in 12 h (Table 2.11). Though the PVDF SW membranes would require even more surface area than the Isoflux membranes to perform the same task (Table 2.11), the PVDF SW membranes are far less expensive than the Isoflux membranes. Cheryan (1998) reported that, in 1996, polymeric MF membranes and their associated hardware (pumps, controls, and fittings) cost between \$225 and \$350 (\$50 to \$100 membranes alone) per m^2 of membrane surface area. This was less than the estimated \$2200 to \$6000 (\$500 to \$3000 membranes alone) per m^2 for a

comparable ceramic MF system. This order-of-magnitude difference in cost still exists today. Despite their comparatively low capital costs, because polymeric membranes exhibit greater sensitivities to cleaning regimes and high temperatures, they are more difficult to clean and have shorter lifetimes than ceramic membranes. Polymeric membrane lifetimes are typically between 12 and 18 months, but ceramic membranes could last as long as 10 years (Cheryan, 1998).

Table 2.11. Number of stages and membrane surface area (m²) theoretically required to remove 95% of the serum proteins (SP) from 1000 kg of skim milk in 12 h using 0.14 µm Isoflux ceramic, 0.10 µm graded permeability (GP) ceramic, 0.10 µm uniform transmembrane pressure (UTP) ceramic, and 0.30 µm polyvinylidene fluoride spiral-wound (PVDF SW) microfiltration (MF) processes

	Isoflux	GP ¹	UTP ²	PVDF SW ³
Number of stages	7	3	3	7
Surface area	6.86	1.91	2.82	14.24

¹ Calculated based on data from J. Zulewska, unpublished data.

² Calculated based on data from Hurt et al., 2010.

³ Calculated based on data from Beckman et al., 2010.

Provided that good cleaning practices were maintained, it could benefit a processor who lacks the capital to invest in ceramic membranes to choose PVDF SW membranes over Isoflux membranes for skim milk SP removal. However, if a company's goal was to consistently produce a micellar CN concentrate with very low SP and lactose content for high heat applications, then, it would be advantageous to opt for the ceramic GP or UTP systems instead of the Isoflux or PVDF SW membranes. When considering ceramic Isoflux membranes, aside from the additional costs associated with purchasing more membranes to achieve the same outcome as the GP or UTP ceramics, it should be taken into account that the Isoflux process would generate over twice as much permeate as the GP and UTP processes. Not only would this increase a plant's water consumption and energy costs, but permeate from the latter stages would only

contain a marginal amount of dairy solids that could be recovered by more selective filtration processes (i.e., ultrafiltration or nanofiltration). If no such processes were implemented downstream of the producer's MF operation, and the permeates were sent down the drain without pretreatment, the lactose, SP, and NPN present in these streams would elevate the processor's wastewater biological oxygen demand (BOD). Depending on the municipality, this may cause the dairy plant to incur additional costs.

Possible Reasons for Differences in SP Removal with Various Ceramic Membranes.

There was a relatively low level of TP in the TAMI Isoflux membrane's first stage permeate (0.35%) when compared to those of the Membralox GP and UTP configurations (0.54% and 0.58%, respectively) (Hurt et al., 2010; J. Zulewska, unpublished data). Given that CN never exceeded 0.03% in any of these MF permeates, it follows that SP were rejected to a greater extent by the Isoflux ceramic membranes than by the GP and UTP ceramic membranes.

To understand why there was such a large difference in performance of these 3 systems, it may be useful to review the differences among these membrane processes and their operation. In cross-flow MF, the high rate of solvent passage through the membrane (i.e., flux) and the difference in flux between the inlet and outlet ends of the membrane promote fouling. In order to mitigate this problem, high cross-flow velocities can be used to limit concentration polarization, thereby reducing fouling in the membrane. The retentate cross-flow velocities were high and similar for the 3 ceramic membrane systems discussed: 6.4 m/s for the UTP (Hurt et al., 2010), 7.1 m/s for the GP (J. Zulewska, unpublished data), and 6.5 m/s for the Isoflux. Though operating at such high cross-flow velocities reduces the fouling problem overall, fouling at the inlet end of the membrane is increased due to the higher TMP and flux at this location. Unless something is done to provide resistance that will slow down flux at the inlet or provide a more

uniform flux from inlet to outlet despite the difference in applied pressure on the retentate side of the membrane, the benefits of high cross-flow velocities cannot be fully realized. To achieve this in the UTP system, the MF permeate is pumped in a recirculation loop at high speed in parallel to the flow of the retentate to create a parallel pressure decrease from the membrane inlet to outlet. This unique approach maintains a very low and uniform TMP ($\Delta\text{TMP} = 25 \pm 3$ kPa) and a relatively uniform flux from the inlet to the outlet end of the membrane. This approach has been shown to work very well and gives rates of SP removal from skim milk that are close to theoretical values (Hurt et al., 2010). The negative aspect of this approach is the additional energy cost required to recirculate the MF permeate. In an effort to eliminate the added cost of the permeate recirculation while maintaining similar process performance, the TAMI Isoflux (Grangeon et al., 2002) and Membralox GP (Garcera and Toujas, 2002) ceramic membranes were developed.

Both the Isoflux and GP membrane designs were engineered to achieve a decrease in hydraulic resistance along the length of the membrane from the inlet to the outlet to eliminate the need for a permeate recirculation pump. Both membrane designs attempt to create higher hydraulic resistance at the inlet end of the membrane, but they use very different approaches. One key difference between the 2 technologies is the location of the hydraulic resistance gradient within the ceramic membrane. In the Isoflux system, the selective membrane layer on the inside of the retentate flow channels is thicker at the inlet and gradually decreases in thickness from the inlet to outlet. This selective layer (nominal pore size $0.14\text{ }\mu\text{m}$) is bonded to a ceramic support structure that has a pore size of about $6\text{ }\mu\text{m}$. It is not clear if the effective pore size in the Isoflux system also varies from inlet to outlet, with $0.14\text{ }\mu\text{m}$ representing an average. The hydraulic resistance gradient in the Membralox GP membrane is applied as a layer on the external surface

of the 12 μm ceramic support structure, not the selective layer as is the case with the Isoflux design. Additionally, it should be noted that the 0.1 μm selective layer on the inside of the retentate flow channel is the same in the Membralox GP and UTP systems.

Why was the cumulative SP removal for the 3-stage, 3X Isoflux system so much lower than the GP and UTP systems when operated under similar linear flow conditions using the same pumps and piping in our laboratory? Because the GP membrane contains a modified support structure and the Isoflux membrane contains a modified selective layer, the GP design might have less impact on the membrane's selectivity than the Isoflux design. If the Isoflux membrane's selective layer has a much smaller effective pore size at the inlet than at the outlet due to overlapping of the selective material, then it may be rejecting SP at the inlet end of the membrane. Credence is given to this theory because the UTP and GP selective layers were identical and both of these systems removed equivalent ($P > 0.05$) and theoretical levels of SP after 3 stages of processing (Table 2.10) despite their other design differences. Another possibility arises from the fact that TMP_o was generally quite low (or even negative) compared to TMP_i in both the Isoflux and GP membranes. From this, it can be surmised that the bulk of the SP removal occurred at the inlet portion of each of these membranes. If the Isoflux selective layer was hindering SP passage at the inlet, where SP passage was most favorable from a TMP standpoint, the overall removal per unit of membrane area would have been reduced. Another key difference in the design of the membranes is the shape of the flow channels. The GP and UTP retentate flow channels are round, but the Isoflux "sunflower" flow channels are not (Figure 2.8). The goals of the "sunflower" flow channel design are to minimize headloss due to permeate mixing within the macroporous support and to achieve more membrane surface area in the same volume of membrane stick while maintaining the strength of the ceramic support structure

(Grangeon and Lescoche, 1999). However, this modification produces a change in flow dynamics that could lead to different fouling behavior from that of the GP membrane. In the Isoflux membrane, the area of the flow channel that comes to an angular point will have more permeate removal in relation to the retentate in that area of the flow channel. Therefore, there may be much more concentration polarization occurring in this zone versus the more open portion of the same flow channel. If at the same time, the linear flow velocity in the angular location is lower compared to the other side of the flow channel due to viscous drag, then it would promote more concentration polarization and fouling in this zone of each flow channel in the Isoflux.

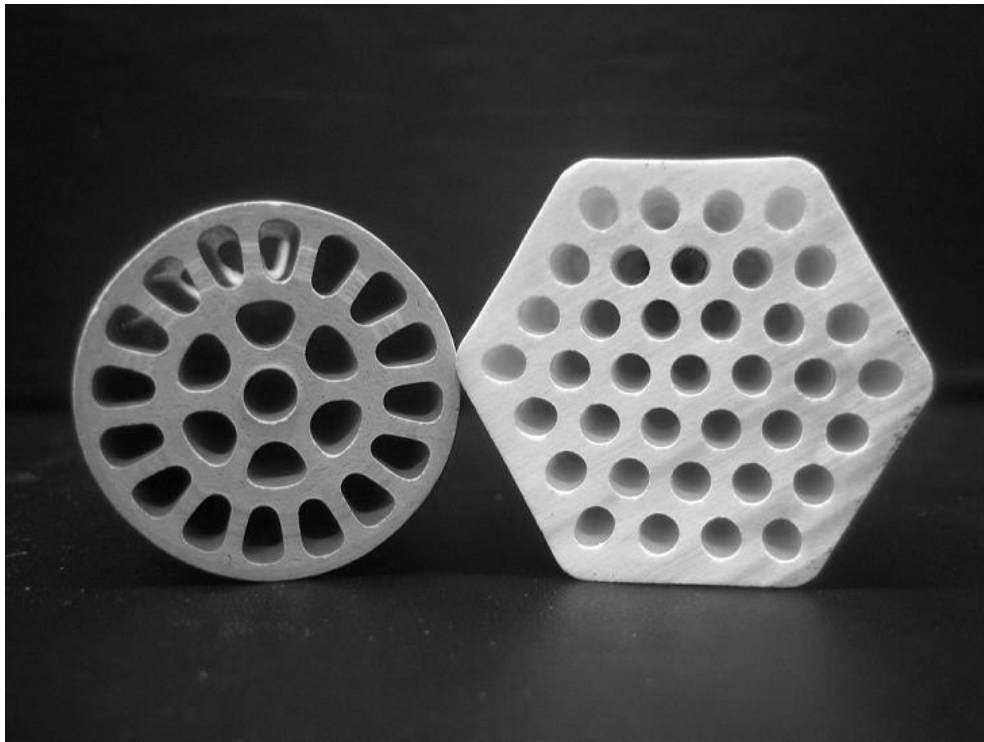


Figure 2.8. TAMI Isoflux (left) and Membralox GP (right) membrane cross sections.

Because the process' flux was maintained by adjusting the permeate removal valve, it should be anticipated that P_{p_i} would have decreased over processing time if membrane fouling had progressed. However, no decrease in P_{p_i} was detected ($P > 0.05$) over time during any of the processing stages (Figure 2.5). Still, it is likely that rapid, early fouling occurred during startup when the system was flushed with skim milk prior to stage 1 because P_{p_i} decreased over time at a constant flux (Figure 2.1). This indicated that a foulant layer was being deposited onto the surface of the membrane and impeding permeate and possibly even SP passage. Additional evidence supporting this theory was obtained by comparing fouling coefficients (FC) ($FC = 1 - (\text{fouled water flux/clean water flux})$) as proposed by Rao (2002) for the Isoflux, GP, and UTP membranes after 3X skim milk MF using the same MF system (Adams, unpublished data). The Isoflux membranes exhibited higher ($P < 0.05$) FC than both the GP and UTP systems, indicating greater resistance due to fouling (Figure 2.9).

It has been shown previously for PVDF SW membranes that a CN-based foulant layer becomes a highly selective layer that causes rejection of SP regardless of the characteristics of the membrane itself (Zulewska, in review). Daufin and Merin (1995) describe several instances where similar fouling layers have been ascribed to CN buildup during skim milk MF with ceramic membranes. It may be that this zone of the Isoflux membrane is fouled by a CN layer; and that layer is rejecting SP, producing a lower SP removal capacity than observed for the GP and UTP ceramic systems (Table 2.10). Further work is needed to understand which factor is the most critical in producing the difference in observed SP removal among these different membrane systems.

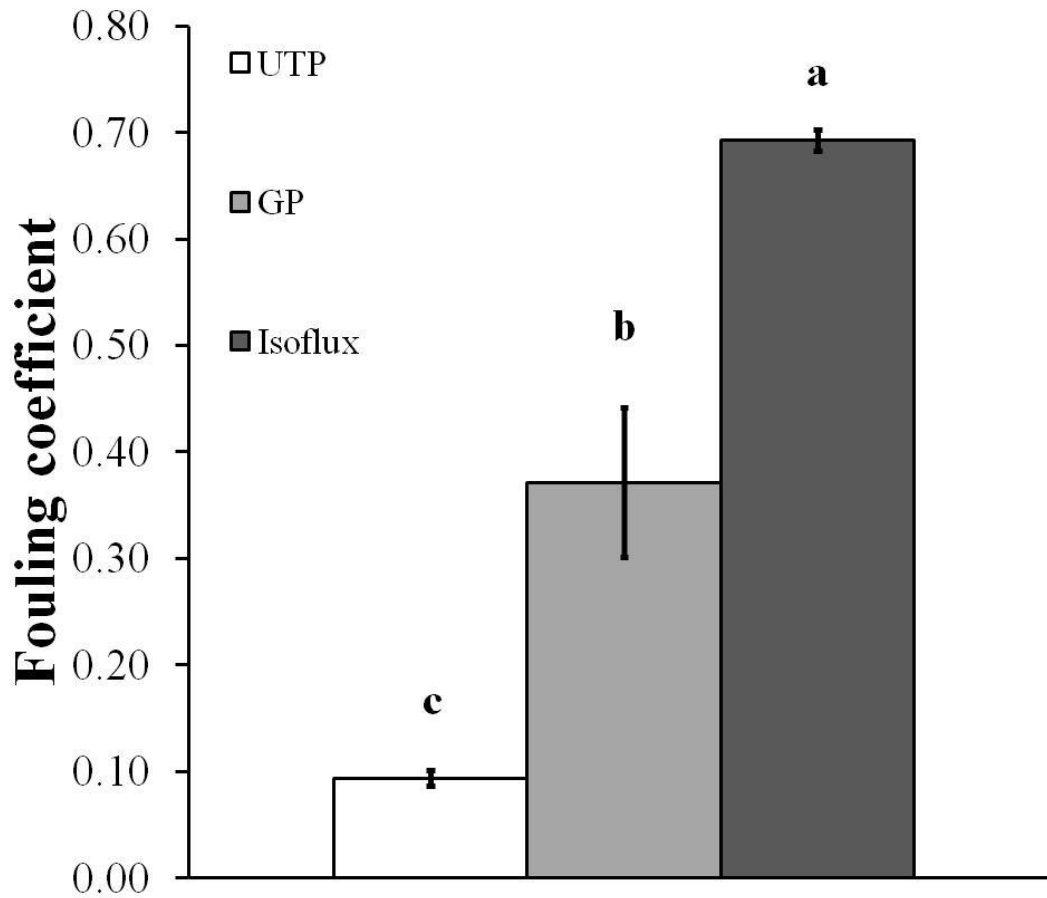


Figure 2.9. Mean ($n = 3$) fouling coefficients ($1 - (\text{fouled water flux} / \text{clean water flux})$) for ceramic $0.1 \mu\text{m}$ uniform transmembrane pressure (UTP), $0.1 \mu\text{m}$ graded permeability (GP), and $0.14 \mu\text{m}$ Isoflux membrane systems after 3X skim milk microfiltration. ^{a-c}Different letters indicate significant differences ($P < 0.05$) among membranes. Error bars represent standard deviations.

CONCLUSIONS

In contrast to 3X MF theoretical cumulative SP removal percentages of 68%, 90%, and 97% after 1, 2, and 3 stages of processing, respectively, the 3X Isoflux MF process only removed 39.5%, 58.4%, and 70.2% of skim milk SP after 1, 2 and 3 stages, respectively. These reductions were similar to those of the PVDF SW membranes ($P > 0.05$), but lower than GP and UTP ceramic membranes ($P < 0.05$). The SP removal rates for the Isoflux process were 0.19, 0.10, and 0.06 kg/m² h for the first, second, and third stages of processing, respectively. To remove 95% of the SP from 1000 kg of skim milk in 12 h it would take 7, 3, 3, and 7 stages, with 6.86, 1.91, 2.82, and 14.24 m² of membrane surface area for Isoflux, GP, UTP, and PVDF SW membranes, respectively. The MF systems requiring more stages would produce additional permeate at lower protein concentrations. The ceramic MF systems requiring more surface area would incur higher capital costs.

Possible reasons why the SP removal with the Isoflux membranes was lower than theoretical include: a range of membrane pore sizes existed (i.e., some pores were too small to pass SP), the selective layer modification and reverse flow conditions at the membrane outlet combined to reduce the effective membrane surface area, and the geometric shape of the Isoflux flow channels promoted early fouling of the membrane and rejection of SP.

ACKNOWLEDGMENTS

The authors thank the New York State Milk Promotion Board and Northeast Dairy Foods Research Center for partial funding of this research. The technical assistance of Steve Beckman, Michelle Bilotta, Maureen Chapman, Chassidy Coon, Emily Hurt, Jessica Mallozzi, and Mark Newbold from the Department of Food Science at Cornell University was greatly appreciated.

REFERENCES

- Association of Official Analytical Chemists. 2000. Official Methods of Analysis. 17th ed. AOAC, Gaithersburg, MD.
- Beckman, S.L., J. Zulewska, M. Newbold, and D.M. Barbano. 2010. Production efficiency of micellar casein concentrate using polymeric spiral-wound microfiltration membranes. *J. Dairy Sci.* 93: 4506-4517.
- Belfort, G., Davis, R.H. and A.L. Zydney. 1994. The behavior of suspensions and macromolecular solutions in crossflow microfiltration. *J. Membr. Sci.* 96:1-58.
- Cheryan, M. 1998. Ultrafiltration and Microfiltration Handbook. Page 68 in *Membrane Chemistry, Structure, and Function*. Technomic Publishing Company, Inc. Lancaster, PA.
- Daufin, G. and U. Merin. 1995. Fouling of inorganic membranes in filtration processes of dairy products. *Fouling and Cleaning in Pressure Driven Membrane Processes*. IDF, Brussels, Belgium.
- Evans, J., J. Zulewska, M. Newbold, M.A., Drake, D.M. Barbano. 2010. Comparison of composition and sensory properties of 80% whey protein and milk serum protein concentrations. *J. Dairy Sci.* 93:1824-1843.
- Garcera, R.M. and E. Toujas, inventors. 2002. Graded permeability macroporous support for crossflow filtration. Societe de Ceramiques Techniques, assignee. US Pat. No. 6,375,014 B1.
- Grangeon, A. and P. Lescoche, inventors. 1999. Inorganic tubular filter element including channels of non-circular section having optimized profile. *Technologies Avancees & Membranes Industrielles*, assignee. US Pat. No. 5,873,998.
- Grangeon, A., P. Lescoche, T. Fleischmann, and B. Ruschel, inventors. 2002. Cross-flow filter

- membrane and method for manufacturing it. Technologies Avancees & Membranes Industrielles, assignee. US Pat. No. 6,499,606 B1.
- Hurt, E. and D. M. Barbano. 2010. Processing factors that influence casein and serum protein separation by microfiltration. *J. Dairy Sci.* 93: 4928 - 4941.
- Hurt, E., J. Zulewska, M. Newbold, and D.M. Barbano. 2010. Micellar casein concentrate production with a 3X, 3-stage UTP ceramic membrane process at 50°C. *J. Dairy Sci.* 93: 5588-5600.
- Kaylegian, K.E., G.E. Houghton, J.M. Lynch, J.R. Fleming, and D.M. Barbano. 2006. Calibration of infrared milk analyzers: modified milk versus producer milk. *J. Dairy Sci.* 89:2817-2832.
- Lynch, J.M., D.M. Barbano, and J.R. Fleming. 1998. Indirect and direct determination of the casein content of milk by Kjeldahl nitrogen analysis: collaborative study. *JAOACI* 81:763-774.
- Quinones H. J., D. M. Barbano, and L.G. Philips. 1998. Influence of protein standardization by ultrafiltration on the viscosity, color, and sensory properties of 2 and 3.3% milks. *J. Dairy Sci.* 81:884-894.
- Rao, H. G. R. 2002. Mechanisms of flux decline during ultrafiltration of dairy products and influence of pH on flux rates of whey and buttermilk. *Desalination* 144:319–324.
- Singh, H. 1995. Heat-induced changes in casein, including interactions with whey proteins. *IDF/FIL Heat-induced changes in milk*. Pages 86-104. Brussels, Belgium.
- Verdi R.J., D.M. Barbano, M.E. Dellavalle, and G.F. Senyk. 1987. Variability in true protein, casein, nonprotein nitrogen, and proteolysis in high and low somatic cell count milks. *J. Dairy Sci.* 70:230-242.

- Walstra, P., J.T.M. Wouters, and T.J. Geurts. 2006. Dairy Science and Technology: Second Edition. Page 6 in Milk: Main Characteristics. Taylor & Francis Group. Boca Raton, FL.
- Zulewska, J., M. Newbold, and D. M. Barbano. 2011. Influence of casein on flux and passage of serum proteins during microfiltration using polymeric spiral-wound membranes at 50°C. J. Dairy Sci. (in review).

CHAPTER THREE

Effect of Annatto Addition and Bleaching on Ultrafiltration Flux During Production of 80% Whey Protein Concentrate and 80% Serum Protein Concentrate

ABSTRACT

The goals of this study were to determine if adding annatto color to milk or bleaching whey or microfiltration permeate influenced ultrafiltration (UF) flux, diafiltration (DF) flux, or membrane fouling during production of 80% whey protein concentrate (WPC80) or 80% serum protein concentrate (SPC80). Separated Cheddar cheese whey (18 vats using 900 kg of whole milk each) and microfiltration (MF) permeate of skim milk (18 processing runs using 800 kg of skim milk each) were produced to make WPC80 and SPC80, respectively. The 6 treatments, replicated 3 times each, that constituted the 18 processing runs within either whey or MF permeate UF were: 1) no annatto (NA), 2) NA + benzoyl peroxide (BPO), 3) NA + hydrogen peroxide (H_2O_2), 4) annatto (A), 5) A + BPO, and 6) A + H_2O_2 . Approximately 700 kg of whey or 530 kg of MF permeate from each treatment were heated to 50°C and processed in 2 stages (UF and DF) with the UF system in batch recirculation mode using a polyethersulfone spiral wound UF membrane with a molecular weight cutoff of 10,000 Da. Addition of annatto color had no effect on UF or DF flux. Bleaching whey or MF permeate with or without added color improved flux during processing. Bleaching with H_2O_2 usually produced higher flux than bleaching with BPO. Bleaching with BPO increased WPC80 flux to a greater extent than it did SPC80 flux. Though no differences in mean flux were observed for a common bleaching treatment between the WPC80 and SPC80 production processes during the UF stage, mean flux during WPC80 DF was higher than mean flux during SPC80 DF for each bleaching treatment. Water flux values before and after processing were used to calculate a fouling coefficient that

demonstrated differences in fouling which were consistent with flux differences among treatments. In both processes, bleaching with H₂O₂ led to the largest reduction in fouling. No effect of annatto on fouling was observed. The reasons for flux enhancement associated with bleaching are unclear.

INTRODUCTION

Flux decline and fouling during ultrafiltration (UF) of whey have been studied extensively (Tong et al., 1989; Heng and Glatz, 1991; Rao, 2002) because they limit processing efficiency. Sweet and acid wheys are usually treated prior to UF in order to remove or inactivate potential foulant material that may reduce process flux (Heng and Glatz, 1991; Pouliot, 1996). These pretreatments may involve upstream unit operations such as microfiltration (MF) or centrifugal separation to remove foulant, chemical adjustments such as pH modification, mineral chelation, or preheating to inactivate foulant, or a combination of the two (Pouliot, 1996). Because proteins, minerals, and lipids are generally considered the most prevalent foulants, pretreatments are usually intended to increase protein solubility, limit calcium phosphate precipitation and calcium bridging during UF, or remove lipids from the whey (Pouliot, 1996). As such, the chemistry and composition of the process feed stream is expected to influence UF fouling and flux decline. Though studies regarding flux decline during UF of MF permeate of skim milk have not been as common, data by Britten and Pouliot (1996) and Nelson and Barbano (2005) indicate that the composition and pH of MF permeate are more similar to those of sweet whey than acid whey.

Whey protein concentrates (WPC) and serum protein concentrates (SPC) are created by ultrafiltering cheese whey or 0.1 µm MF permeate of skim milk, respectively, to concentrate serum proteins (SP) and remove lactose and minerals (Nelson and Barbano, 2005). The UF

retentate can be concentrated by evaporation and spray dried to make a shelf-stable powder. Because SP in these ingredients are highly sought after, producers may further reduce the lactose and mineral contents of WPC and SPC below what a single UF step would accomplish by diafiltering (DF) the UF retentate before evaporation and drying. Diafiltration involves diluting the UF retentate with water, often back to its original mass, then repeating the UF process. This step washes out the nonprotein soluble milk solids that pass through the UF membrane and increases the protein content of the powder. Though SPC and 80% serum protein concentrate (SPC80) solutions have been shown to exhibit improved sensory characteristics under certain conditions and greater clarities than their WPC counterparts (Evans et al., 2009, 2010), they are not widely available in the dairy industry. Conversely, WPC and 80% whey protein concentrate (WPC80) are by-products of cheese manufacture that are widely available. Over 175 million kg of WPC were produced in the United States in 2008 (IDFA, 2009).

In the United States, the majority of WPC and WPC80 are produced from Cheddar and mozzarella whey. Cheddar is often colored using annatto, a yellow to orange food colorant derived from the *Bixa orellana* shrub (Kang, et al., 2010), to maintain cheese color consistency throughout the year. The principal color molecules in annatto are the carotenoids bixin and norbixin (Kang, et al., 2010). Unfortunately, not all of the bixin and norbixin remain in the cheese; some of these colorants pass into the Cheddar whey. Because whey products made from Cheddar cheese whey with added annatto color may contribute an undesirable yellow hue to a food product in which it is subsequently used, manufacturers of WPC and WPC80 often bleach the whey before spray drying to whiten the final protein concentrate. Currently, 2 bleaching agents, benzoyl peroxide (BPO) and hydrogen peroxide (H₂O₂), are approved and deemed generally recognized as safe (GRAS) for bleaching whey in the United States (US FDA 2011a,

b). Benzoyl peroxide completely degrades to benzoic acid during the bleaching process and this residue in whey products may not be allowed in some countries. When H_2O_2 is used for bleaching, residual H_2O_2 must be broken down into molecular oxygen and water with catalase enzyme.

When examining the functional properties of WPC80 that had been bleached with BPO or H_2O_2 , Jervis et al. (unpublished) noted that protein solubility increased after bleaching with H_2O_2 . Because increased protein solubility has been linked with a more sustainable UF flux (Heng and Glatz, 1991; de la Casa, 2007), it stands to reason that the bleaching treatments described above may improve membrane flux. Currently, BPO may only be added to whey for the purposes of bleaching and H_2O_2 may be used for bleaching or as an antimicrobial during electrodialysis (US FDA 2011a, b), but neither may be used exclusively for enhancing membrane flux. However, if a processor were to treat colored whey with BPO or H_2O_2 prior to UF with the intent of bleaching, any flux-enhancing benefits could also be realized. No study has quantified the effects of bleaching whey or MF permeate on UF flux. Moreover, even though annatto addition is not expected to impact UF flux, no study has verified this hypothesis. The objectives of this study were to measure the effects of bleaching and annatto coloring of whey and MF permeate on UF and DF flux during the production of WPC80 and SPC80 and to examine these treatments' effects on a polyethersulfone spiral wound (PES SW) membrane's tendency to foul during WPC80 and SPC80 processing.

MATERIALS AND METHODS

Experimental Design

For both WPC80 and SPC80 manufacture, a 3 X 2 full factorial design with 3 levels of bleaching (no bleach, 50 ppm BPO, and 500 ppm H_2O_2) and 2 levels of coloring (no annatto and

0.066 mL annatto/kg of milk) was employed. The experiments were replicated 3 times, resulting in 18 total processing runs for WPC80 manufacture and 18 total processing runs for SPC80 manufacture. Each individual processing run was conducted over 3 consecutive days in a week.

Whey Protein Concentrate Production

Cheddar Cheese Whey Manufacture. On the first day of processing, raw whole milk (about 900 kg) for Cheddar cheese production was pasteurized with a plate heat exchanger (Model 080-S, AGC Engineering, Manassas, VA) at 72°C for 16 s, cooled to 4°C, and held overnight. The following day, the pasteurized milk was manufactured into Cheddar cheese and Cheddar cheese whey as described by Evans et al. (2009). For the treatments with added annatto, the colorant (Annatto cheese color - 2X, P/N 70741, Chr Hansen, Inc., Milwaukee, WI) was added to the milk (0.066 mL/kg of milk) before ripening. The curds and whey were continuously stirred at 38°C until the target whey draining pH of 6.45 was attained. The whey was drained through a sieve to remove cheese fines and immediately pasteurized using a plate heat exchanger equipped with regeneration, heating, and cooling sections (Model 080-S, AGC Engineering, Manassas, VA) at 72°C for 16 s. The whey was cooled to 50°C at the exit of the pasteurizer and immediately processed with a cream separator (Model 619, DeLaval, Inc., Kansas, MO) to reduce the fat content. The fat contents of the whey before and after separation were 0.21% \pm 0.02 and 0.042% \pm 0.004, respectively. The whey was mixed and sampled directly before and after cream separation. After separation, if the whey was not going to be bleached, it was cooled to 4°C with a plate heat exchanger and held overnight at \leq 4°C.

Bleaching of Whey. If the whey was going to be bleached, it was recirculated through a plate heat exchanger in a large stainless steel tank to heat it to 66°C. Two different bleaches were used, BPO at 50 ppm (Oxylite Type XX Benzoyl Peroxide 32% by weight, Nelson Jameson,

Marshfield, WI) or H₂O₂ at 500 ppm (35% H₂O₂, FCC grade, Columbus Chemical Industries, Inc., Columbus, WI). When bleaching with BPO, the powdered bleach was mixed with about 30 kg of whey using a high shear mixer then added to the remainder of the whey. The whey was held for 30 min at 66°C with agitation then cooled with a plate heat exchanger and held overnight at 4°C. When bleaching with H₂O₂, the liquid bleach was added to about 30 kg of whey, mixed with the remainder of the separated whey, and agitated for 30 min at 66°C. The H₂O₂ concentration in the liquid bleach was diluted from 35% to 10% concentration. The 10% concentration was verified with a 10% H₂O₂ test strip (Indigo Instruments, Niagara Falls, NY). If the H₂O₂ concentration was lower than 10%, then the actual concentration was calculated and the amount of H₂O₂ was adjusted to achieve an added level of 500 ppm in the cheese whey. After 30 min at 66°C, the whey was cooled with a plate heat exchanger to 50°C, liquid catalase enzyme derived from *Aspergillus niger* (FoodPro CAT, PD 216626-2.0EN Danisco, Madison, WI) was added at 20 ppm, and the whey was mixed for 10 min. The whey was then cooled with a plate heat exchanger and held overnight at ≤ 4°C.

Ultrafiltration of Whey. The following day, approximately 700 kg of separated whey was weighed into a vat, heated to 50°C using a plate heat exchanger, and processed with a UF system in batch recirculation mode using a PES SW UF membrane (Model 3838, GEA NIRO Inc., Hudson, WI; nominal molecular weight cutoff: 10,000 Da, surface area: 13.6 m²). Before processing, the UF membrane was short cleaned using the procedure described by Evans et al. (2009). The membrane was then flushed with 50°C RO water to neutral pH and the clean water flux was determined by operating only the feed pump with an inlet pressure of 172 kPa. The following standard conditions were applied when determining UF water flux measurements: an inlet pressure of 172 kPa was applied using only the inlet pump, 50°C reverse osmosis (RO)

water was fed to the system, and water flux was measured by collecting permeate in a tared, 19 L bucket over 30 s, weighing it, and dividing the derived mass flow rate (kg/h) by the membrane surface area (m^2). A volumetric flux was derived from the mass flux, assuming 1 L of permeate = 1 kg at 50°C. The initial clean water flux was about 54 $\text{L}/\text{m}^2 \text{ h}$. During processing, the system was operated in a constant pressure mode with 276 kPa of retentate inlet pressure, 103 kPa of retentate outlet pressure, and no backpressure on the permeate side of the membrane. Whey was ultrafiltered for about 120 min. Every 15 min during processing, flux was measured and samples of the permeate and the retentate were taken for compositional analysis using an infrared spectrophotometer (IR) (Lactoscope FTIR, Delta Instruments, Drachten, The Netherlands) to monitor the process. The IR was calibrated using modified milk samples as described by Kaylegian et al. (2006). Ultrafiltration was continued until the protein content of the retentate was 41% protein as a percentage of lactose plus fat plus protein, as determined using IR. The corresponding CF was about 5X. After UF, the retentate was diluted with pasteurized RO water at 50°C to bring the weight back to the original weight of the starting whey for DF. The membrane was not cleaned before proceeding to the DF stage. The mixture was recirculated through the membrane for 5 min to ensure complete mixing, then the DF process was started. The diluted UF retentate was diafiltered for about 135 min. Diafiltration was continued until the protein content of the retentate measured by IR was 91.2 to 91.6% protein as a percentage of lactose plus fat plus protein in the retentate. The corresponding CF was about 11.3X. After producing the liquid WPC80, the UF system was cleaned using the procedure described by Evans et al. (2009). The fouled water flux before cleaning was, on average, 39% of the initial clean water flux (21 vs. 54 $\text{L}/\text{m}^2 \text{ h}$) and the clean water flux after cleaning was similar to the clean water flux prior to processing (about 51 $\text{L}/\text{m}^2 \text{ h}$.)

Serum Protein Concentrate Production

Pre-Microfiltration Processing. On the first day of processing, raw whole milk (about 1150 kg) was pasteurized with a plate heat exchanger (Model 080-S, AGC Engineering, Manassas, VA) at 72°C for 16 s, cooled to 50°C, and separated with a centrifugal cream separator (Model 619, DeLaval, Inc., Kansas, MO). After separation, the skim milk (about 1060 kg) was kept at 50°C and processed with a UF system in batch recirculation mode using a PES SW membrane (Model 3838, GEA NIRO Inc., Hudson, WI) with a molecular weight cutoff of 10,000 Da. This was a different membrane than the one used for both WPC80 and SPC80 productions. Before processing, the UF membrane was cleaned following the procedure described by Evans et al. (2009). The initial clean water flux was about 41 L/m² h. The skim milk was ultrafiltered for about 4 h to achieve a CF of approximately 2.2X. After UF, the retentate was diluted back to the original TP content of the skim milk as determined by IR. For the treatments with added annatto, the colorant (Annatto cheese color - 2X, P/N 70741, Chr Hansen, Inc., Milwaukee, WI) was added (0.066 mL/kg of milk) to the diluted UF retentate. The diluted UF retentate was then cooled using a plate heat exchanger and stored overnight at $\leq 4^{\circ}\text{C}$. The UF system was then cleaned as described by Evans et al. (2009). This UF step was conducted to reduce the lactose content of the MF feed so that the MF retentate produced in this study could be used in another study. In practice, SPC80 could be produced without ultrafiltering the skim milk prior to MF. In such a case, SPC80 UF and DF processing parameters (i.e., CF and IR targets) would be similar to those used during the production of WPC80 described above.

Microfiltration. The next day, the diluted UF retentate was microfiltered in a continuous feed-and-bleed 3X process using a pilot-scale system. The day before processing, the MF system was cleaned as described by Zulewska et al. (2009). The MF system (Tetra Alcross M7,

TetraPak Filtration Systems, Aarhus, Denmark) was equipped with ceramic Membralox graded permeability (GP) membranes (Pall Corporation, Cortland, NY, nominal pore diameter = 0.1 μm , surface area = 1.7 m^2). Seven tubular, 19-channel ceramic membranes were housed in the tubular stainless steel MF module. The MF system consisted of a feed pump (type LKH 10/110 SSS 1.75 kW) and a retentate recirculation pump (type LKH 20/125 SSS 6.3 kW), both from Alfa Laval, (Kansas City, MO). The retentate recirculation pump was equipped with a variable frequency drive (MC Series, Model M12100C, Lenze AC Tech, Uxbridge, MA) and a magnetic flow transmitter (I/A Series, IMT25, Foxboro, Foxboro, MA) so that the cross-flow velocity could be controlled and monitored, respectively. Variable area flow meters from GEMÜ Valves, Inc. (Atlanta, GA) were used to measure the volumetric removal rates of both the retentate (model 55/--/23) and permeate (model 57/--/23) streams. The membranes were mounted vertically in the MF system with retentate flow from the top to the bottom of the module. Because the membranes were mounted vertically, the inlet and outlet gauge pressures had to be corrected for differences due to the weight of the vertical column of liquid. Corrections were determined as follows: with 50°C RO water in the system, only the feed pump turned on, and the retentate and permeate outlet valves closed, the retentate inlet pressure (R_{p_i}), permeate inlet pressure (P_{p_i}), retentate outlet pressure (R_{p_o}), and permeate outlet pressure (P_{p_o}) were measured. Gauge pressure correction factors were calculated as follows: the R_{p_i} gauge pressure correction was P_{p_o} minus R_{p_i} , the R_{p_o} gauge pressure correction was P_{p_o} minus R_{p_o} , the P_{p_i} gauge pressure correction was P_{p_o} minus P_{p_i} , and the P_{p_o} gauge pressure correction was zero. These correction factors were determined at the beginning of each processing run. Next the retentate recirculation pump was turned on, the retentate removal rate was set to 60 L/h, and the permeate removal rate was set to 120 L/h. The elevation corrected inlet and outlet pressures were measured and the

TMP from the retentate to the permeate side of the membrane at the inlet (TMP_i) and the outlet (TMP_o) ends of the membrane were calculated.

The MF system was started on 50°C RO water and there was a transition from water to milk with both pumps running, the recirculation rate was approximately 712 L/min which corresponded to a cross-flow velocity of approximately 7.1 m/s. Approximately 150 kg of the diluted UF retentate was used to flush the 50°C water out of the system at the beginning of the process. About 46 kg of retentate and 92 kg of permeate were collected in standard 38 L milk cans, the weights were recorded using a high capacity scale (Champ, Ohaus Corporation, Florham Park, NJ), and both were discarded. While flushing the water out of the system, samples of retentate and permeate were collected every 5 to 15 min and analyzed for composition by IR to ensure that all of the water had been removed from the system. After flushing the water from the system, the remaining skim milk (about 800 kg) was added to the system and retentate and permeate were collected continuously. Retentate and permeate removal rates, as measured by the aforementioned variable area flow meters, were controlled using manual diaphragm valves and maintained at approximately 60 and 120 L/h, respectively. Typical retentate (R_{p_i}) and permeate (P_{p_i}) inlet pressures were 455 and 240 kPa, respectively, and typical retentate (R_{p_o}) and permeate (P_{p_o}) outlet pressures were 225 and 255 kPa, respectively. The flux was measured every 15 min and maintained at approximately 72 L/m² h. Samples of the permeate and retentate were also taken every 15 min for composition analysis using IR to monitor the process. The CF was monitored every 15 min by collecting retentate and permeate from the system in 2 tared, 19 L buckets over 2 min. After collection, the buckets' weights were determined using a balance (SB 32000, Mettler Toledo, Columbus, OH) and the CF was calculated as the sum of the retentate (about 2040 g) and permeate (about 4080 g) masses divided by the retentate mass. If the

measured CF fell outside of the range of 3.00 ± 0.05 , the removal rates were adjusted and the weighing process was repeated. At the end of the MF stage, the collected retentate and permeate were mixed separately and sampled. The masses of the permeate and retentate collected throughout the MF stage were totaled and used to calculate an overall stage CF. Average retentate and permeate masses collected during processing were 273 kg and 538 kg, respectively, resulting in an average CF of 2.97. After processing, the MF system was cleaned as described by Zulewska et al., (2009). The fouled water flux determined at 50°C before cleaning was typically about 235 L/ m² h and the clean water flux determined after cleaning at 50°C was similar to the initial clean water flux (about 400 L/m² h). If the permeate was not going to be bleached, it was cooled to 4°C with a plate heat exchanger and held overnight at $\leq 4^{\circ}\text{C}$.

Bleaching of MF Permeate. If the MF permeate was going to be bleached, it was subjected to the same bleaching treatments described above for whey, then cooled to 4°C with a plate heat exchanger and held overnight at $\leq 4^{\circ}\text{C}$.

Ultrafiltration of MF Permeate. The following day, approximately 530 kg of MF permeate was weighed into a vat, heated to 50°C using a plate heat exchanger, and processed using the same UF system used for WPC80 manufacture. Before processing, the UF membrane was short cleaned following the procedure described by Evans et al. (2009). The initial clean water flux was about 53 L/m² h. During processing, the system was operated in a constant pressure mode with 276 kPa of retentate inlet pressure, 103 kPa of retentate outlet pressure, and no backpressure on the permeate side of the membrane. The MF permeate was ultrafiltered for about 90 min. Every 15 min during processing, flux was measured and samples of the permeate and the retentate were taken for composition analysis using IR to monitor the process. Ultrafiltration was continued until the protein content of the retentate was 51% protein as a

percentage of lactose plus fat plus protein, as determined by IR. The corresponding CF was about 3.8X. After UF, the retentate was diluted with pasteurized RO water at 50°C to bring the weight back to the original total weight of the starting MF permeate for DF. The membrane was not cleaned before proceeding to the DF stage. The mixture was recirculated through the membrane for 5 min to ensure complete mixing, then the DF process was started. Diluted UF retentate was DF for about 120 min. Diafiltration was continued until the protein content of the retentate measured by IR was 92% protein as a percentage of lactose plus fat plus protein in the retentate. The corresponding CF was about 11.2X. After producing the liquid SPC80, the UF system was cleaned as described by Evans et al. (2009). The fouled water flux before cleaning was, on average, 36% of the initial clean water flux (19 vs. 53 L/m² h) and the clean water flux after cleaning was similar to the clean water flux prior to processing (about 53 L/m² h).

Fouling Coefficient Calculations

Water flux before and after manufacturing WPC80 and SPC80 were used to estimate membrane fouling after processing. A fouling coefficient (FC) as proposed by Rao (2002) was calculated for each processing run using the following equation: $FC = 1 - (\text{fouled water flux} / \text{clean water flux})$. Greater FC values indicated a greater loss of water permeability (i.e., more membrane fouling). Mean values were calculated from the 3 replicates of each treatment and reported. In one WPC80 run, a fouled water flux was not recorded. To account for this missing fouled water flux value, an average of the 2 remaining fouled water flux values for the treatment was used with the run's clean water flux value to calculate the run's FC.

Chemical Analyses

The MF permeate was analyzed for total solids (TS), fat, total nitrogen (TN), nonprotein nitrogen (NPN), and noncasein nitrogen (NCN) content using forced air oven drying (AOAC,

2000; method 990.20; 33.2.44), ether extraction (AOAC, 2000; method 989.05; 33.2.26), Kjeldahl (AOAC, 2000; method 991.20; 33.2.11), Kjeldahl (AOAC, 2000; method 991.21; 33.2.12), and Kjeldahl (AOAC, 2000; method 998.05; 33.2.64) methods, respectively. Crude protein (CP) was calculated by multiplying TN by 6.38, TP was calculated by subtracting NPN from TN and multiplying by 6.38, casein (CN) was calculated by subtracting NCN from TN and multiplying by 6.38, and SP content was calculated by subtracting NPN from NCN and multiplying by 6.38. The separated Cheddar cheese whey was measured for TS, fat, and CP using the same methods described above. The pH of the Cheddar whey and MF permeate were measured with a solid polymer electrode (HA405-DXK-S8/120, Mettler-Toledo, Bedford, MA) and an Accumet 915 pH meter (Fisher Scientific, Pittsburgh, PA) that was calibrated at 50°C using standard pH 4 and 7 buffer solutions (Fisher Scientific, Pittsburgh, PA).

Statistical Analysis

All data were analyzed by ANOVA using the Proc GLM (general linear model) procedure of SAS (SAS version 8.02, 1999-2001, SAS Institute Inc., Cary, NC). To determine if there were significant differences ($P < 0.05$) in composition or pH among color and bleaching treatments of the separated Cheddar cheese whey or MF permeate, the GLM was dependent variable = bleach + color + replicate + bleach*color + error. To determine if there were significant differences ($P < 0.05$) in TS, fat, CP, and pH between separated Cheddar cheese whey and MF permeate regardless of color or bleaching treatments, the GLM was dependent variable = feed type + replicate (feed type) + error. The ANOVA models comparing whey and MF permeate TS, fat, CP, and pH independent of the color and bleaching treatments were significant overall ($P < 0.05$); therefore the least square means of the whey and MF permeate were compared using the LSMEANS statement.

To determine if there were significant differences ($P < 0.05$) in UF or DF flux among bleaching or color treatments, a full split plot ANOVA model was constructed for each product (WPC80 or SPC80) during each processing stage (UF or DF) using the following main effects and all 2-way and 3-way interactions: bleach, color, replicate, and processing time. Additionally, due to the nonlinear decay of flux over time, predictors were constructed from the squared time term and all possible 2-way and 3-way interactions. Bleach, color, bleach x color, bleach x replicate, and color x replicate were treated as whole plot variables in the split plot ANOVA models. Consequently, the error term for the whole plot variables would be bleach x color x replicate if the bleach color and replicate terms were all included in the model. Time was treated as a continuous sub plot variable in the split plot ANOVA models. Distortion of the ANOVA by multicollinearity in the model was minimized by transforming the processing time (Glantz and Slinker, 2001). Time was transformed as follows: transformed time = processing time – [(last processing time – first processing time) / 2]. This transformation made the data set orthogonal with respect to time. Predictors within each model were examined for significance ($P < 0.05$) using the output from the Type III sums of squares table. A backward elimination procedure was used to remove nonsignificant terms ($P > 0.05$) from each model to create reduced models. Nonsignificant terms that took part in significant higher order interactions were allowed to remain in the reduced models. An F test was carried out on each reduced model to verify that its predictive ability was not significantly different ($P > 0.05$) from that of its respective full model (Ott and Longnecker, 2004). This criterion was satisfied for all 4 models. Because the effect of color was determined to be nonsignificant ($P > 0.05$), the whole plot error term for each final model was bleach x replicate. All reduced ANOVA models (Table 3.1, Table 3.2) were significant overall ($P < 0.05$), therefore the least square means for the bleaching treatments were

compared using the LSMEANS statement with a Tukey-Kramer adjustment for multiple comparisons. To emphasize differences in the average flux of a treatment as opposed to initial or final flux values, data were truncated prior to analysis by removing the first time point during UF (i.e., UF flux at 0 min) and the last time point during DF (i.e., DF flux at end of processing). Mean flux values (i.e., the average flux over the entire processing time less the initial and final measurements) for bleaching treatments among the WPC80 and SPC80 processes were also compared. The GLM for each processing stage (UF or DF) was $\text{flux} = \text{bleach} + \text{feed} + \text{bleach} * \text{feed} + \text{rep}(\text{feed}) + \text{error}$. Both processing stage ANOVA models were significant overall ($P < 0.05$), therefore the least square means for the bleach*feed interaction were compared using the LSMEANS statement with a Tukey-Kramer adjustment for multiple comparisons.

To determine if there were significant differences ($P < 0.05$) in membrane FC due to bleaching or color treatments, an ANOVA model was constructed for each product (WPC80 or SPC80) using the following main effects and all 2-way interactions: bleach, color, and replicate. After the previously described model-reduction procedure was applied, the final GLM for each product was $\text{FC} = \text{bleach} + \text{replicate} + \text{bleach} \times \text{replicate} + \text{error}$. All reduced ANOVA models were significant overall ($P < 0.05$), therefore the least square means for the bleaching treatments were compared using the LSMEANS statement with a Tukey-Kramer adjustment for multiple comparisons.

Table 3.1. ANOVA split-plot design with df, type III SS, and *P* values for predictive variables of ultrafiltration (after first 15 min of processing) and diafiltration (prior to last 15 min of processing) flux during the production of 80% whey protein concentrate

Predictive variable	Ultrafiltration			Diafiltration		
	df	SS	<i>P</i>	df	SS	<i>P</i>
Whole plot						
Bleach	2	846.55	0.0003	2	717.56	0.0005
Color	1	NS ¹	NS	1	NS	NS
Replicate	2	105.54	0.0138	2	41.56	0.0844
Bleach x color	2	NS	NS	2	NS	NS
Bleach x replicate ²	4	14.03	<.0001	4	17.02	<.0001
Color x replicate	2	NS	NS	2	NS	NS
Bleach x color x replicate	4	NS	NS	4	NS	NS
Sub plot						
Time	1	594.83	<.0001	1	77.52	<.0001
Time x bleach	2	20.64	<.0001	2	4.90	0.0030
Time x color	1	NS	NS	1	NS	NS
Time x replicate	2	4.28	0.0036	2	NS	NS
Time x bleach x color	2	NS	NS	2	NS	NS
Time x bleach x replicate	4	NS	NS	4	NS	NS
Time x color x replicate	2	NS	NS	2	NS	NS
Time x time	1	33.44	<.0001	1	14.66	<.0001
Time x time x bleach	2	NS	NS	2	NS	NS
Time x time x color	1	NS	NS	1	NS	NS
Time x time x replicate	2	NS	NS	2	NS	NS
Time x time x bleach x color	2	NS	NS	2	NS	NS
Time x time x bleach x replicate	4	NS	NS	4	NS	NS
Time x time x color x replicate	2	NS	NS	2	NS	NS
Reduced model df	14			12		
Reduced error df	142			158		
Total df	156			170		
R – squared	0.9680			0.9404		

¹ The predictive variable was not significant ($P > 0.05$) and not included in the reduced model.

² Used as whole plot error term for bleach and replicate in final model.

Table 3.2. ANOVA split-plot design with df, type III SS, and *P* values for predictive variables of ultrafiltration (after first 15 min of processing) and diafiltration (prior to last 15 min of processing) flux during the production of 80% serum protein concentrate

Predictive variable	Ultrafiltration			Diafiltration		
	df	SS	<i>P</i>	df	SS	<i>P</i>
Whole plot						
Bleach	2	156.90	0.0347	2	749.07	0.0005
Color	1	NS ¹	NS	1	NS	NS
Replicate	2	17.83	0.4468	2	16.53	0.2628
Bleach x color	2	NS	NS	2	NS	NS
Bleach x replicate ²	4	35.93	<.0001	4	17.39	<.0001
Color x replicate	2	NS	NS	2	NS	NS
Bleach x color x replicate	4	NS	NS	4	NS	NS
Sub plot						
Time	1	129.72	<.0001	1	22.58	<.0001
Time x bleach	2	NS	NS	2	4.78	0.0005
Time x color	1	NS	NS	1	NS	NS
Time x replicate	2	NS	NS	2	NS	NS
Time x bleach x color	2	NS	NS	2	NS	NS
Time x bleach x replicate	4	NS	NS	4	NS	NS
Time x color x replicate	2	NS	NS	2	NS	NS
Time x time	1	7.05	0.0071	1	NS	NS
Time x time x bleach	2	NS	NS	2	NS	NS
Time x time x color	1	NS	NS	1	NS	NS
Time x time x replicate	2	NS	NS	2	NS	NS
Time x time x bleach x color	2	NS	NS	2	NS	NS
Time x time x bleach x replicate	4	NS	NS	4	NS	NS
Time x time x color x replicate	2	NS	NS	2	NS	NS
Reduced model df	10			11		
Reduced error df	86			129		
Total df	96			140		
R - squared	0.8181			0.9594		

¹ The predictive variable was not significant (*P* > 0.05) and not included in the reduced model.

² Used as whole plot error term for bleach and replicate in final model.

RESULTS AND DISCUSSION

Ultrafiltration Stage Feed Compositions

No composition or pH differences were detected ($P > 0.05$) among bleaching or color treatments within a given UF feed material (i.e., separated Cheddar whey or MF permeate) (Table 3.3). Therefore, even though there were 18 different cheese manufactures and 18 different MF processing runs of skim milk, the composition of the separated wheys and MF permeates were very consistent from processing run to run. Separated Cheddar whey TS, fat, and CP concentrations were all higher ($P < 0.0001$) than those of the MF permeate (Table 3.3). Whey TS were higher because lactose, soluble minerals, and NPN were removed from the skim milk used to produce the MF permeate during the UF step prior to MF. The resulting UF retentate was subsequently diluted back to the skim milk's original mass with RO water, thereby further reducing the lactose, soluble mineral, and NPN concentrations in the serum phase. The whey also likely contained more solubilized colloidal calcium phosphate due to the mineral complex's migration from the CN micelles into the whey during the cheese making process' acidification step. Whey fat content was greater than that of the MF permeate because the 0.10 μm MF membrane used to produce the MF permeate retained the majority of the few fat globules present in the MF feed material (i.e., diluted UF retentate of skim milk). Whey CP concentration was higher than MF permeate CP because some NPN was washed out of the skim milk used to make the MF permeate in the UF and dilution steps prior to MF. Also, MF permeate lacked the proteolysis products created during the cheese making process (such as glycomacropeptide). Whey pH was lower ($P < 0.0001$) than MF permeate pH (Table 3.3) due to the fermentation of lactose to lactic acid during the cheese making process.

Table 3.3. Mean (n = 3) compositional¹ and pH² data for separated Cheddar cheese whey and 0.1 µm microfiltration (MF) permeate of skim milk used to feed the ultrafiltration unit during production of 80% whey protein concentrate and 80% serum protein concentrate, respectively

	Treatment ³						SEM	R - squared	\bar{x}
	NA - NB	NA - BPO	NA - H ₂ O ₂	A - NB	A - BPO	A - H ₂ O ₂			
Separated whey ^a									
TS	6.710	6.703	6.728	6.706	6.727	6.710	0.021	0.68	6.714
Fat	0.043	0.037	0.044	0.042	0.043	0.040	0.003	0.61	0.043
CP	0.909	0.896	0.916	0.918	0.917	0.912	0.015	0.66	0.911
pH	6.37	6.35	6.39	6.36	6.36	6.36	0.030	0.29	6.37
MF permeate ^a									
TS	3.266	3.170	3.223	3.245	3.309	3.328	0.084	0.71	3.257
Fat	0.001	0.004	0.003	0.004	0.005	0.007	0.003	0.48	0.004
CP	0.725	0.723	0.701	0.719	0.723	0.735	0.029	0.49	0.721
NPN	0.098	0.105	0.095	0.102	0.100	0.104	0.004	0.68	0.100
NCN	0.677	0.666	0.607	0.664	0.621	0.645	0.043	0.51	0.647
TP	0.627	0.618	0.606	0.618	0.623	0.632	0.027	0.45	0.621
CN	0.048	0.056	0.093	0.055	0.102	0.091	0.036	0.49	0.074
SP	0.579	0.562	0.513	0.563	0.521	0.541	0.041	0.50	0.546
pH	6.71	6.66	6.71	6.72	6.71	6.73	0.036	0.57	6.71

¹ TS = total solids; CP = crude protein = total nitrogen x 6.38; NPN = nonprotein nitrogen x 6.38; NCN = noncasein nitrogen x 6.38; TP = true protein = CP minus NPN; CN = casein = CP minus NCN; SP = serum proteins = NCN – NPN.

² pH determined at 50°C.

³ No annatto and no bleach (NA-NB), annatto and no bleach (A-NB), no annatto and 50 ppm benzoyl peroxide (NA-BPO), annatto and 50 ppm benzoyl peroxide (A-BPO), no annatto and 500 ppm hydrogen peroxide (NA-H₂O₂), and annatto and 500 ppm hydrogen peroxide (A-H₂O₂).

^a Means within the same row are not different among treatments ($P > 0.05$).

Flux During 80% Protein Concentrate Production

80% Whey Protein Concentrate. The addition of annatto did not affect ($P > 0.05$) UF or DF flux during the production of WPC80 (Table 3.1). However, bleaching treatments increased ($P < 0.05$) flux when compared to those without bleach (Tables 3.1 and 3.4). During whey UF (Figure 3.1), treatments without bleach exhibited lower flux than BPO treatments, which in turn exhibited lower flux than H_2O_2 treatments ($P < 0.05$). The same pattern occurred during whey DF (Figure 3.2); treatments without bleach exhibited lower flux than BPO treatments, which in turn exhibited lower flux than H_2O_2 treatments ($P < 0.05$).

Table 3.4. Mean ($n = 3$) ultrafiltration (UF) and diafiltration (DF) flux ($L/m^2 h$) at $50^\circ C$ during the production of 80% whey protein concentrate from separated Cheddar cheese whey treated with no annatto and no bleach (NA-NB), annatto and no bleach (A-NB), no annatto and 50 ppm benzoyl peroxide (NA-BPO), annatto and 50 ppm benzoyl peroxide (A-BPO), no annatto and 500 ppm hydrogen peroxide (NA- H_2O_2), and annatto and 500 ppm hydrogen peroxide (A- H_2O_2) before processing

	NA-NB	NA-BPO	NA- H_2O_2	A-NB	A-BPO	A- H_2O_2	SEM	R ²
UF	14.9 ^c	18.5 ^b	20.0 ^a	14.7 ^c	18.6 ^b	20.1 ^a	0.60	0.97
DF	16.8 ^c	20.0 ^b	21.6 ^a	16.0 ^c	19.6 ^b	22.1 ^a	0.64	0.94

^{a - c} Means in the same row not sharing a common superscript are different ($P < 0.05$).

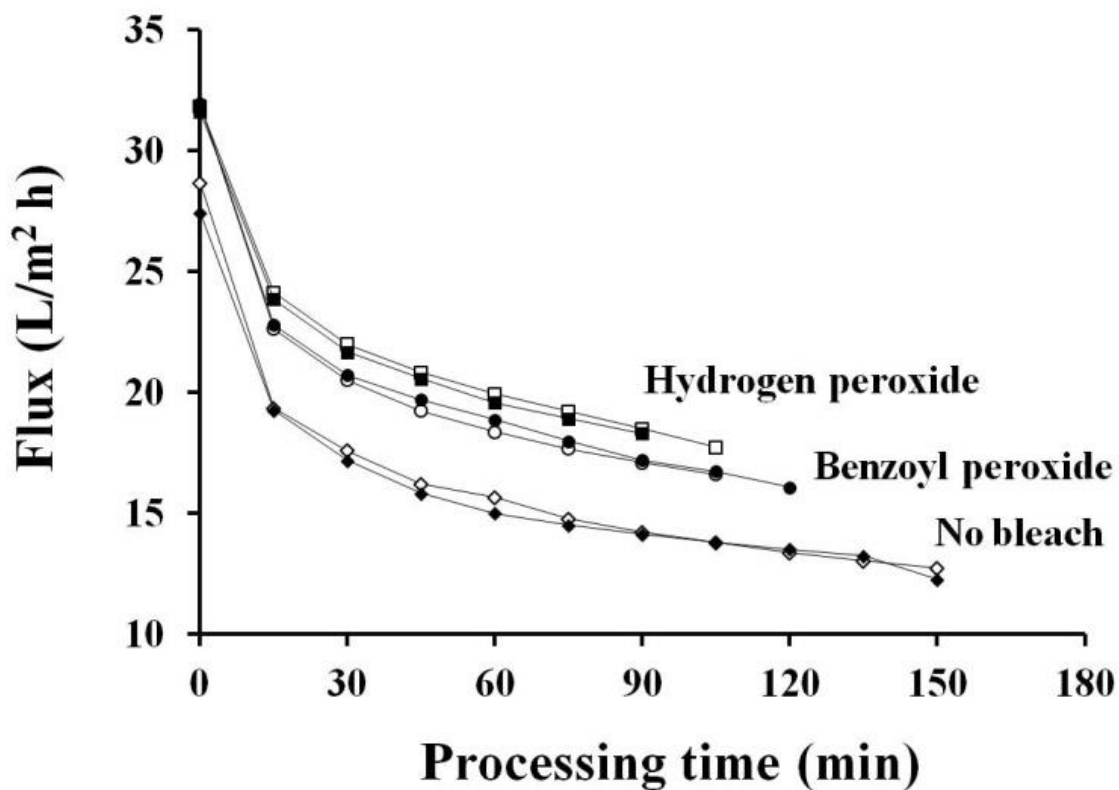


Figure 3.1. Mean ($n = 3$) flux at 50°C during the ultrafiltration of separated Cheddar cheese whey treated with no annatto and no bleach (◇), annatto and no bleach (◆), no annatto and 50 ppm benzoyl peroxide (○), annatto and 50 ppm benzoyl peroxide (●), no annatto and 500 ppm hydrogen peroxide (□), and annatto and 500 ppm hydrogen peroxide (■) before processing.

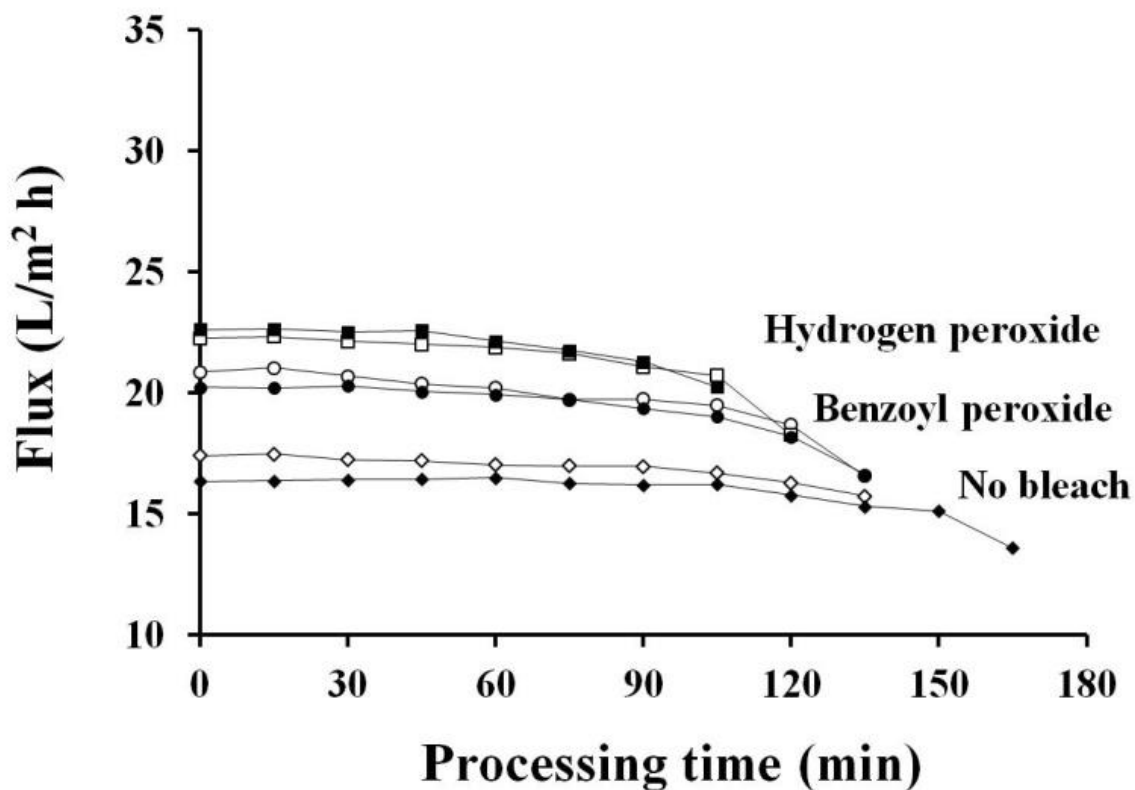


Figure 3.2. Mean ($n = 3$) flux at 50°C during the diafiltration of separated Cheddar cheese whey treated with no annatto and no bleach (◇), annatto and no bleach (◆), no annatto and 50 ppm benzoyl peroxide (○), annatto and 50 ppm benzoyl peroxide (●), no annatto and 500 ppm hydrogen peroxide (□), and annatto and 500 ppm hydrogen peroxide (■) before processing.

80% Serum Protein Concentrate. The addition of annatto did not affect ($P > 0.05$) UF or DF flux during the production of SPC80 (Table 3.2). However, bleaching increased ($P < 0.05$) flux in most instances (Tables 3.1 and 3.5). During MF permeate UF (Figure 3.3), H_2O_2 treatment flux was higher ($P < 0.05$) than flux in treatments without bleach. No differences ($P > 0.05$) in UF flux between treatments without bleach and treatments bleached with BPO or between the 2 bleaching treatments were detected. During MF permeate DF (Figure 3.4), treatments without bleach exhibited lower flux than BPO treatments, which in turn exhibited lower flux than the H_2O_2 treatments ($P < 0.05$).

Table 3.5. Mean ($n = 3$) ultrafiltration (UF) and diafiltration (DF) flux ($L/m^2 h$) at $50^\circ C$ during the production of 80% serum protein concentrate from $0.1 \mu m$ microfiltration permeate of skim milk treated with no annatto and no bleach (NA-NB), annatto and no bleach (A-NB), no annatto and 50 ppm benzoyl peroxide (NA-BPO), annatto and 50 ppm benzoyl peroxide (A-BPO), no annatto and 500 ppm hydrogen peroxide (NA- H_2O_2), and annatto and 500 ppm hydrogen peroxide (A- H_2O_2) before processing

	NA-NB	NA-BPO	NA- H_2O_2	A-NB	A-BPO	A- H_2O_2	SEM	R ²
UF	16.7 ^b	16.5 ^{ab}	19.5 ^a	15.9 ^b	17.4 ^{ab}	18.9 ^a	0.96	0.82
DF	14.3 ^c	15.6 ^b	19.9 ^a	13.9 ^c	16.2 ^b	20.0 ^a	0.54	0.96

^{a - c} Means in the same row not sharing a common superscript are different ($P < 0.05$).

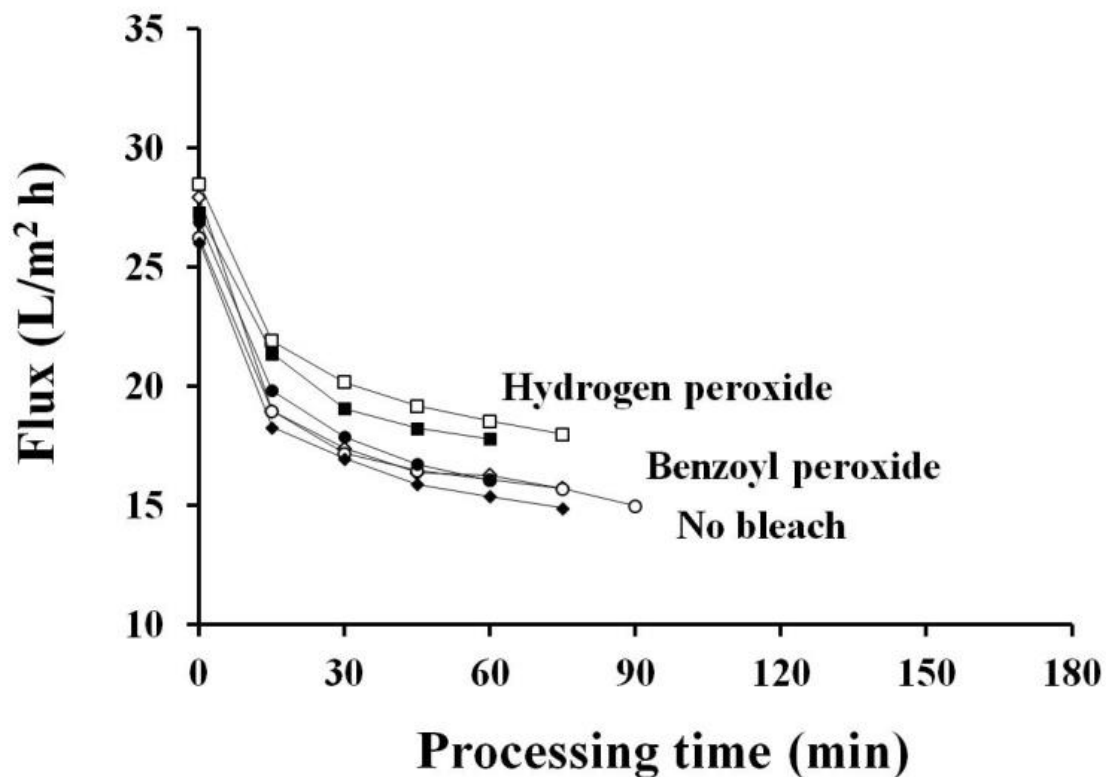


Figure 3.3. Mean ($n = 3$) flux at 50°C during the ultrafiltration of 0.1 μm microfiltration permeate of skim milk treated with no annatto and no bleach (\diamond), annatto and no bleach (\blacklozenge), no annatto and 50 ppm benzoyl peroxide (\circ), annatto and 50 ppm benzoyl peroxide (\bullet), no annatto and 500 ppm hydrogen peroxide (\square), and annatto and 500 ppm hydrogen peroxide (\blacksquare) before processing.

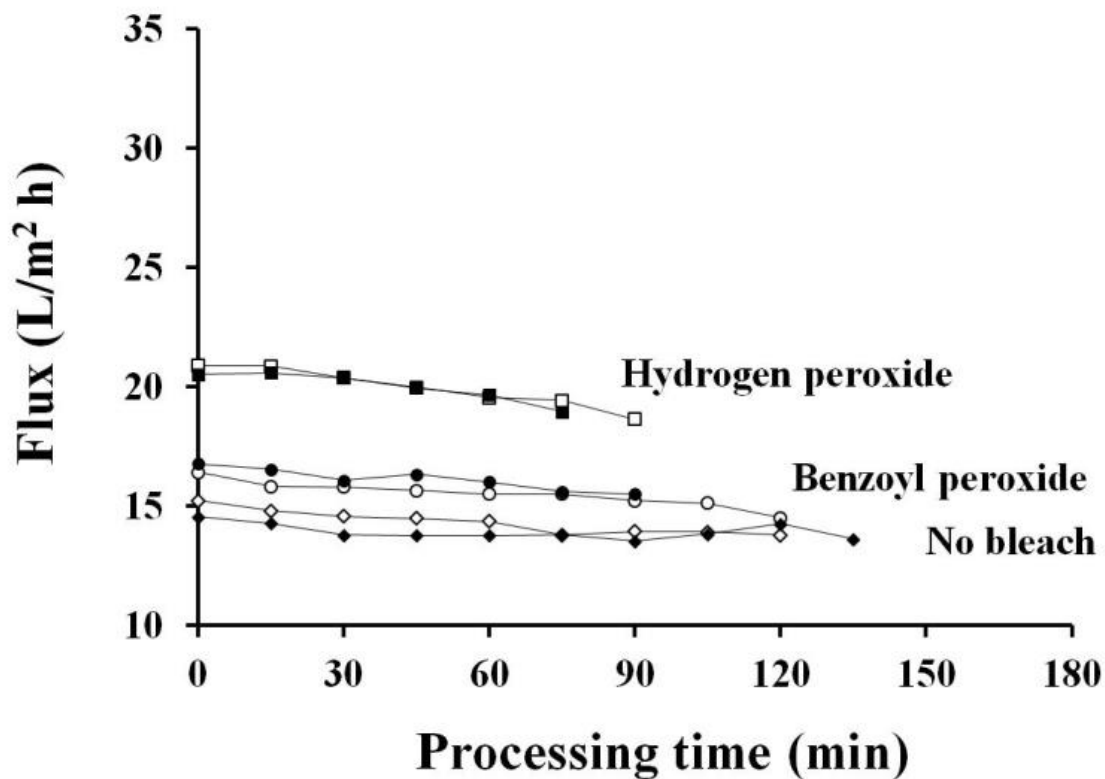


Figure 3.4. Mean ($n = 3$) flux at 50°C during the diafiltration of 0.1 μm microfiltration permeate of skim milk treated with no annatto and no bleach (\diamond), annatto and no bleach (\blacklozenge), no annatto and 50 ppm benzoyl peroxide (\circ), annatto and 50 ppm benzoyl peroxide (\bullet), no annatto and 500 ppm hydrogen peroxide (\square), and annatto and 500 ppm hydrogen peroxide (\blacksquare) before processing.

80% Whey Protein Concentrate, 80% Serum Protein Concentrate Comparison.

Because the addition of annatto was not found to influence flux in any of the above instances, mean flux values of the 3 bleaching treatments and 2 production processes (i.e., WPC80 and SPC80) were compared without considering the color treatment (Table 3.6). There were no differences ($P > 0.05$) in mean UF flux during WPC80 and SPC80 productions within any of the common bleaching treatments. However, SPC80 mean DF flux was lower ($P < 0.0001$) than the observed flux during WPC80 processing for each bleaching treatment. This difference was surprising given that the SPC80 feed material for the DF stage only contained about 65%, 9%, and 79% of the TS, fat, and CP, respectively, when compared to that of the WPC80 DF feed. The fact that the MF permeate pH was higher ($P < 0.0001$) than that of the separated whey may have caused the lower observed flux. Though the calcium content of the MF permeate was likely lower than that of the separated whey, the form of the calcium in the MF permeate could be a more aggressive foulant. A higher pH, which increased further as a result of the dilution prior to DF (about 6.63 for WPC80 DF feed and about 6.82 for SPC80 DF feed), would favor the formation of apatite calcium structures, which are known to promote fouling (Hayes et al., 1974; Hickey et al., 1980). This effect could be confirmed in a future study by lowering the pH of the MF permeate by using a diafiltration water with a small amount of acid added. The implication of this finding for a manufacturer is that processing milk solids with a SPC manufacturing process as opposed to a WPC one may ultimately result in slightly lower flux values during DF regardless of the bleaching treatment chosen.

Table 3.6. Mean ($n = 6$) ultrafiltration (UF) and diafiltration (DF) flux ($L/m^2 h$) at $50^\circ C$ during the production of 80% whey protein concentrates (WPC) and 80% serum protein concentrates (SPC) made from separated Cheddar cheese whey or $0.1 \mu m$ microfiltration permeate of skim milk, respectively, treated with no bleach (NB), 50 ppm benzoyl peroxide (BPO), or 500 ppm hydrogen peroxide (H_2O_2) before processing

	WPC- NB	WPC- BPO	WPC- H_2O_2	SPC- NB	SPC- BPO	SPC- H_2O_2	SEM	R^2
UF	14.8 ^d	18.6 ^{ab}	20.1 ^a	16.3 ^{cd}	17.0 ^{bc}	19.2 ^a	0.90	0.86
DF	16.4 ^c	19.8 ^b	21.8 ^a	14.1 ^d	15.9 ^c	20.0 ^b	0.73	0.95

^{a-d} Means in the same row not sharing a common superscript are different ($P < 0.05$).

Membrane Fouling During 80% Protein Concentrate Production

80% Whey Protein Concentrate. No differences in membrane fouling, as measured by FC (Figure 3.5), were observed during WPC80 processing due to annatto coloring of the whey ($P > 0.05$). Fouling coefficients were lower ($P < 0.01$) for WPC80 production when bleaching treatments were applied to whey (Figure 3.5). Furthermore, processes in which the wheys were bleached with BPO exhibited higher FC than processes in which wheys were bleached with H_2O_2 ($P < 0.01$). There was a strong negative correlation ($R^2 = 0.93$) between the average of the UF and DF flux values and fouling coefficient for each treatment (Figure 3.6), indicating that flux differences were associated with differences in membrane fouling.

80% Serum Protein Concentrate. No differences in membrane fouling, as measured by FC (Figure 3.7), were observed during SPC80 processing due to annatto coloring of the MF permeate ($P > 0.05$). Processes that did not include a bleaching step and processes in which the MF permeates were bleached with BPO resulted in higher FC ($P < 0.001$) (i.e., more fouling) than processes in which MF permeates were bleached with H_2O_2 (Figure 3.6). No differences in FC were detected between treatments without bleaching steps and those that included BPO bleaching steps ($P > 0.05$). There was a strong negative correlation ($R^2 = 0.82$) between the

average of the UF and DF flux values and fouling coefficient for each treatment (Figure 3.6), indicating that flux differences were associated with differences in membrane fouling.

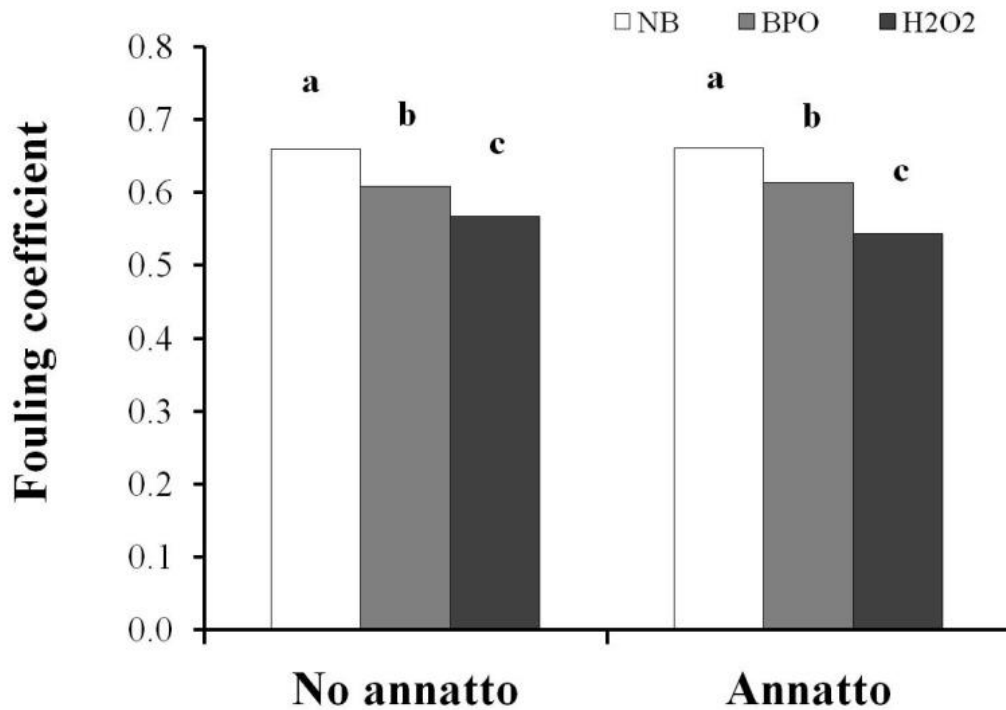


Figure 3.5. Effect of annatto colorant and bleaching treatments (NB = no bleach; BPO = 50 ppm benzoyl peroxide; H2O2 = 500 ppm hydrogen peroxide) of separated Cheddar cheese whey on fouling coefficients ($1 - (\text{fouled water flux} / \text{clean water flux})$) of polyethersulfone membranes after the production of 80% whey protein concentrate. Higher values indicate more fouling.^a °Different letters indicate significant differences ($P < 0.05$) among treatments; SE = 0.02; $R^2 = 0.91$.

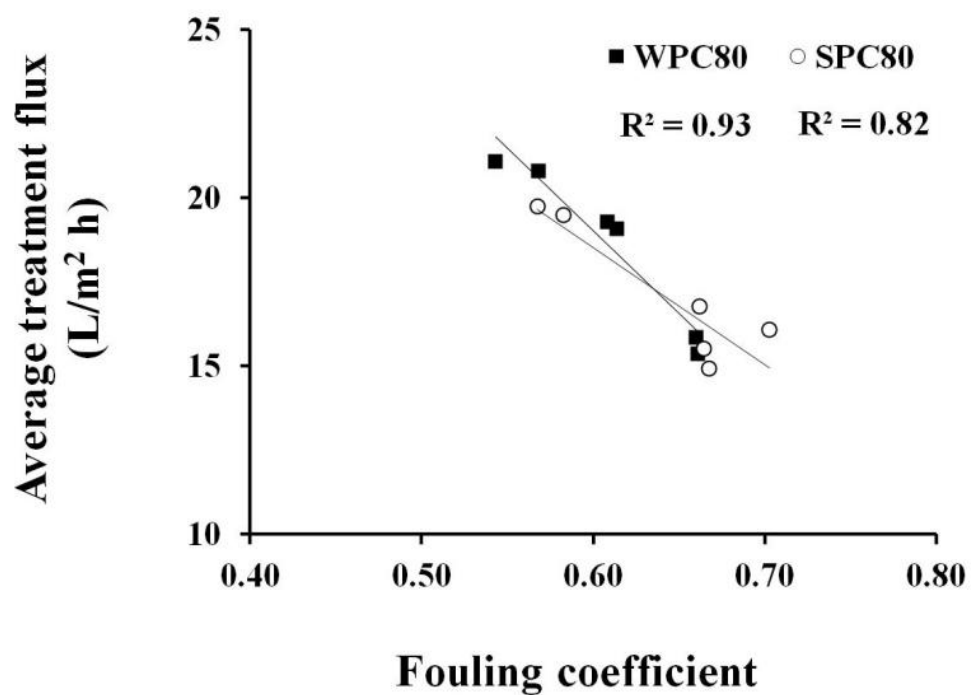


Figure 3.6. Linear correlations between average of ultrafiltration and diafiltration flux values and fouling coefficients ($1 - (\text{fouled water flux} / \text{clean water flux})$) from treatments within 80% whey protein concentrate (WPC80) (■) and 80% serum protein concentrate (SPC80) (○) ultrafiltration production processes.

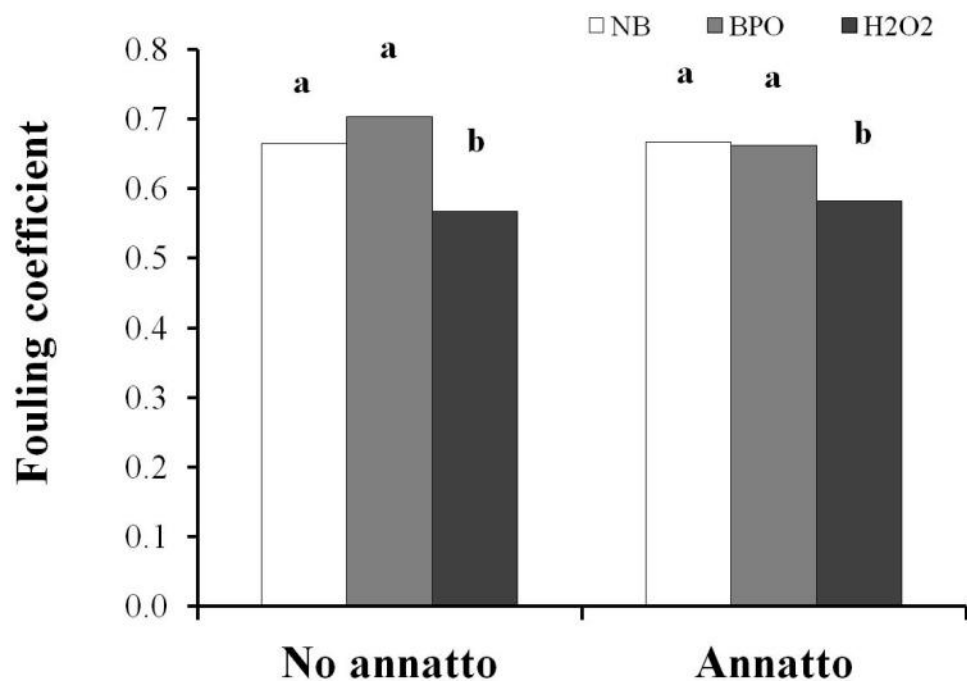


Figure 3.7. Effect of annatto colorant and bleaching treatments (NB = no bleach; BPO = 50 ppm benzoyl peroxide; H2O2 = 500 ppm hydrogen peroxide) of 0.1 μ m microfiltration permeate of skim milk on fouling coefficients ($1 - (\text{fouled water flux} / \text{clean water flux})$) of polyethersulfone membranes after the production of 80% serum protein concentrate. Higher values indicate more fouling. ^{a-b}Different letters indicate significant differences ($P < 0.05$) among treatments; SE = 0.03; $R^2 = 0.86$.

Possible Reasons for the Observed Effects of Bleaching

The fact that BPO and H₂O₂ affected flux values during the production of WPC80 and SPC80 to varying degrees suggests that these bleaching agents may reduce membrane fouling through different mechanisms. As noted above when describing the SPC80 UF step prior to MF, this study was originally designed to determine the impact of annatto and bleaching on the flavor and functionality of SPC80 and WPC80. Only after the UF processes were carried out did the patterns described above begin to emerge. In spite of this, while a more robust experimental design could have been conducted with the present goals in mind, the findings of these bleaching agents' effects on flux enhancement remain valid for our exploratory study. With this in mind, the authors would like to address several factors which may have contributed to our results.

First, the bleaching agents' chemical forms should be considered. Whereas H₂O₂ was a liquid, BPO was added as a powder. Approximately 68% of this powder was composed of cornstarch filler to facilitate the delivery of the BPO. This equated to a concentration of about 0.01% starch being incorporated into the feed material. Though sugars such as lactose are not generally regarded to be potential foulants (Rice et al., 2008), high molecular weight carbohydrates such as amylose (a component of cornstarch) have been shown to foul polymeric membranes during cross-flow UF at concentrations as low as 0.01 g/L (about 0.001%) (Susanto and Widiyasa, 2009). Consequently, the starch carrier in the BPO may have offset some of the bleaching agent's flux-enhancing effects by contributing to the fouling problem.

Second, the H₂O₂ treatment required the use of catalase enzyme and the BPO treatment did not. However, it is doubtful that this source of variation contributed to the H₂O₂ treatment's observed flux-enhancing properties. According to its specification sheet, the catalase enzyme preparation contained the following ingredients: "protein (enzymes), water, sodium chloride,

sodium citrate, and sodium biphosphate.” The only enzyme present in this product is catalase (Danisco Technical Services, personal communication), so the potential for proteolytic activity from contaminating enzymes can be ruled out. Sodium citrate and sodium biphosphate are excellent chelating agents. They are capable of binding calcium ions which would otherwise contribute to calcium bridging, thereby promoting membrane fouling. However, the maximum concentration of these salts combined would be less than 0.002% in the whey or MF permeate based on the 20 ppm catalase delivery rate. This concentration would be below the useful addition of sodium citrate (0.2%) quoted by Maubois (1980) for whey flux improvement and far below the approximate 0.4% which was found to be effective by Taddei et al., (1988).

Bleaching with H_2O_2 improved both WPC80 and SPC80 flux in all instances. Past studies that have examined the effects of H_2O_2 on SP in whey (Cooney and Morr, 1972) have used peroxide concentrations far in excess of that used in the present study (0.05% w/w). When treating dialyzed whey with H_2O_2 concentrations between 1 and 2%, Cooney and Morr (1972) observed considerable SP denaturation and aggregation. However, they noted that no SP denaturation or aggregation was observed in whey treated with 0.5% H_2O_2 at 25°C. Recent work done by Jervis et al. (unpublished) in conjunction with this study focused on the functional properties of the WPC80 produced by each treatment described in the present study. They observed that when heating 10% w/w solutions of treated WPC80 at 90°C at pH 7, only the concentrates bleached with H_2O_2 failed to gel after 10 min. Upon adjustment of the pH to 4.6 and subsequent heating, only the H_2O_2 treatments still exhibited some soluble protein (i.e., protein that did not gel). Because the solutions prepared from WPC80 that were bleached with BPO did gel under these conditions, it can be surmised that these bleaching treatments affected the SP differently. At present, no similar analyses have been carried out on the SPC80 samples to

confirm that the same pattern holds for these samples. The apparent increase in protein solubility with the H₂O₂-treated WPC80 samples observed by Jervis et al., (unpublished) was attributed to SP proteolysis incurred during the bleaching treatment. Because the 90°C heat treatment used by Jervis et al., (unpublished) was greater than the UF processing temperature (50°C) and the denaturation temperature of SP (about 70°C), it cannot be concluded that a similar advantage in protein solubility would be observed during UF processing. However, it is well established that protein solutions will exhibit flux minima during UF at the protein's isoelectric point because of maximum membrane adsorption due to minimum protein solubility (Swaminathan et al., 1981; Hanemaaijer et al., 1989; de la Casa et al., 2007). Heng and Glatz (1991) determined that flux during UF of acid whey was reduced when SP were precipitated (i.e., solubility was reduced) using carboxymethyl cellulose prior to processing. Therefore, if the H₂O₂ treatment proteolyzed the SP, thus creating more soluble peptide fractions, membrane flux would be expected to increase, as was observed. Consequently, the mechanism which improves membrane flux when bleaching with H₂O₂ may be protein-driven. It is possible that bleaching with BPO affected flux by altering the SP structure as well, but this may have occurred to a much lesser extent based on the functionality data presented by Jervis et al. (unpublished).

Tong et al., (1989) observed that the proteinaceous foulant responsible for flux decline during whey UF was composed of CN proteolysis products and α -LA. The former was only present when the cheese had been coagulated with calf rennet as opposed to a protease derived from *Mucor pusillus*. These proteolysis products were absent from the UF foulant when whey produced with calf rennet was treated with the *M. pusillus* protease prior to UF. Presumably, the microbial coagulant proteolyzed the CN peptides even further, causing roughly a 40% increase in UF flux. Because these CN proteolysis products were absent in the MF permeate used to produce

SPC80 in the present study, one would not expect to observe differences in flux or fouling between the SPC80 treatments without bleach and those with BPO if such differences during WPC80 production were due to the breakdown of CN proteolysis products by BPO. This was the case, as the BPO treatment flux during SPC80 production was not different ($P > 0.05$) from that of the no bleach treatment flux during SPC80 production (Table 3.6); nor was it different ($P > 0.05$) from that of the BPO treatment flux during WPC80 production (Table 3.6). The same logic could be applied if the BPO acted on the fat to cause changes in flux, as the fat content of the MF permeate was almost negligible at an order of magnitude lower than that of the separated Cheddar whey (0.004% vs. 0.04%) (Table 3.3). Consequently, the mechanism by which BPO enhances flux may be due to an effect on fat, protein (specifically, CN proteolysis products), or both.

CONCLUSIONS

Ultrafiltration and DF flux from WPC80 and SPC80 production processes were examined after each process' feed material had been subjected to annatto coloring and bleaching treatments. Addition of annatto color had no effect on UF or DF flux ($P > 0.05$). Bleaching whey or MF permeate with or without added color usually improved flux during processing. Bleaching with H_2O_2 produced a higher flux than bleaching with BPO. Bleaching with BPO increased WPC80 flux to a greater extent than it did SPC80 flux. Relative to the average UF and DF flux of unbleached whey (15.6 L/m² h), average UF and DF flux of whey bleached with BPO was greater ($P < 0.05$) by about 22% and average UF and DF flux of whey bleached with H_2O_2 was greater ($P < 0.05$) by about 32%. Relative to UF flux of unbleached MF permeate (16.3 L/m² h), UF flux of MF permeate treated with BPO was not different ($P > 0.05$) and UF flux of MF permeate treated with H_2O_2 was greater ($P < 0.05$) by about 16%. Relative to DF flux of

unbleached MF permeate (14.1 L/m² h), DF flux of MF permeate bleached with BPO was greater ($P < 0.05$) by about 13% and DF flux of MF permeate bleached with H₂O₂ was greater ($P < 0.05$) by about 42%. Though no differences ($P > 0.05$) in mean flux were observed for a common bleaching treatment between the WPC80 and SPC80 production processes during the UF stage, mean flux during WPC80 DF was higher ($P < 0.01$) than mean flux during SPC80 DF for each bleaching treatment. Water flux values before and after processing were used to calculate a FC that demonstrated differences in fouling which were consistent with flux differences resulting from the bleaching treatments. In both processes, bleaching with H₂O₂ led to the largest reduction in fouling ($P < 0.05$). No effect of annatto on fouling was observed ($P > 0.05$). The reasons for flux enhancement associated with bleaching are unclear.

ACKNOWLEDGMENTS

The authors thank the New York State Milk Promotion Board and Northeast Dairy Foods Research Center for partial funding of this research. The technical assistance of Irma Amelia, Tim Barnard, Steve Beckman, Michelle Bilotta, Maureen Chapman, Chassidy Coon, Aneela Hameed, Emily Hurt, and Mark Newbold from the Department of Food Science at Cornell University was greatly appreciated.

REFERENCES

- Association of Official Analytical Chemists. 2000. Official Methods of Analysis. 17th ed. AOAC, Gaithersburg, MD.
- Britten, M. and Y. Pouliot. 1996. Characterization of whey protein isolate obtained from milk microfiltration permeate. Lait 76:255-265.
- Cooney, C.M., and C.V. Morr. 1972. Hydrogen peroxide alteration of whey proteins in whey and concentrated whey systems. J. Dairy Sci. 55:567-573.

- de la Casa, E. J., A. Guadix, R. Ibanez, and E. M. Guadix. 2007. Influence of pH and salt concentration on the cross-flow microfiltration of BSA through a ceramic membrane. *Biochem. Eng. J.* 33:110-115.
- Evans, J.P., J. Zulewska, M. Newbold, M.A. Drake, and D.M. Barbano. 2009. Comparison of composition, sensory and volatile components of thirty-four percent whey protein and milk serum protein concentrates. *J. Dairy Sci.* 92:4773-4791.
- Evans, J.P., J. Zulewska, M. Newbold, M.A. Drake, and D.M. Barbano. 2010. Comparison of composition and sensory properties of 80% whey protein and milk serum protein concentrates. *J. Dairy Sci.* 93:1824-1843.
- Glantz, S. A., and B. K. Slinker. 2001. Multicollinearity and what to do about it. Pages 185-187 in *Primer of Applied Regression & Analysis of Variance*. 2nd edition. McGraw-Hill, Inc. New York, NY.
- International Dairy Foods Association. 2009. Dairy facts: 2009 edition. IDFA, Washington, D.C.
- Hanemaaijer, J. H., T. Robbertsen, T. van den Boomgaard, and J.W. Gunnink. 1989. Fouling of ultrafiltration membranes – the role of protein adsorption and salt precipitation. *J. Membr. Sci.* 40:199-217.
- Hayes, J.F., J.A. Dunkerley, and L.L. Muller. 1974. Studies on whey processing by ultrafiltration II: improving permeation rates by preventing fouling. *Aust. J. Dairy Technol.* 29:132-140.
- Heng, M.H. and C.E. Glatz. 1991. Chemical pretreatments and fouling in acid whey ultrafiltration. *J. Dairy Sci.* 74:11-19.

- Hickey, M.W., R.D. Hill, and B.R. Smith. 1980. Investigations into the ultrafiltration and reverse osmosis of wheys 1: the effects of certain pretreatments. *New. Zeal. J. Dairy Sci.* 15:109-121.
- Kang, E.J., R.E. Campbell, E. Bastian, and M.A. Drake. 2010. Invited review: annatto usage and bleaching in dairy foods. *J. Dairy Sci.* 93:3891-3901.
- Kaylegian, K.E., G.E. Houghton, J.M. Lynch, J.R. Fleming, and D.M. Barbano. 2006. Calibration of infrared milk analyzers: modified milk versus producer milk. *J. Dairy Sci.* 89:2817-2832.
- Maubois, J.L. 1980. Ultrafiltration of whey. *J. Soc. Dairy Tech.* 33:55-58.
- McDonough, F.E., R. E. Hargrove, and R. P. Tittsler. 1968. Decolorization of annatto in Cheddar cheese whey. *J. Dairy Sci.* 51:471-472.
- Nelson, B.K. and D.M. Barbano. 2005. A microfiltration process to maximum removal of serum proteins from skim milk before cheese making. *J. Dairy Sci.* 88:1891-1900.
- Ott, R.L. and M.T. Longnecker. 2004. A First Course in Statistical Methods. Page 619 in Multiple Regression. Brooks/ Cole – Thomson Learning. Belmont, CA.
- Pouliot, Y. 1996. "Pretreatments to minimize long-term fouling," in IDF Bulletin 311: Advances in Membrane Technology for Better Dairy Products. International Dairy Federation, Brussels.
- Rao, H. G. R. 2002. Mechanisms of flux decline during ultrafiltration of dairy products and influence of pH on flux rates of whey and buttermilk. *Desalination* 144:319–324.
- Rice, G., A. Barber, A. O'Conner, G. Stevens, and S. Kentish. 2009. Fouling of NF membranes by dairy ultrafiltration permeates. *J. Membr. Sci.* 330:117-126.
- Susanto, H. and I.N. Widiassa. 2009. Ultrafiltration fouling of amylose solution: behavior,

- characterization and mechanism. *J. Food Eng.* 95:423-431.
- Swaminathan, T., M. Chaudhuri, and K.K. Sirkar. 1981. Effect of pH on solvent flux during stirred ultrafiltration of proteins. *Biotechnol. Bioeng.* 23:1873-1880.
- Taddei, C., P. Aimar, G. Daufin, and V. Sanchez. 1988. Factors affecting fouling of an inorganic membrane during sweet whey ultrafiltration. *Lait.* 68:157-176.
- Tong, P.S., D.M. Barbano, and W.K. Jordan. 1989. Characterization of proteinaceous membrane foulants from whey ultrafiltration. *J. Dairy Sci.* 72:1435-1442.
- US FDA. 2011a. 21 CFR 184.1157: Benzoyl peroxide. <http://www.accessdata.fda.gov/scripts/cdrh/cfdocs/cfcfr/CFRSearch.cfm?fr=184.1157> Accessed Sept. 3, 2011.
- US FDA. 2011b. 21 CFR 184.1366: Hydrogen peroxide. <http://www.Accessdata.fda.gov/scripts/cdrh/cfdocs/cfcfr/CFRSearch.cfm?fr=184.1366> Accessed Sept. 3, 2011.
- Zulewska, J., M. Newbold, and D.M. Barbano. 2009. Efficiency of serum protein removal from skim milk with ceramic and polymeric membranes at 50°C. *J. Dairy Sci.* 92:1361-1377

CHAPTER FOUR

Conclusions and Future Work

Fouling limits the productivity of membrane processes by reducing the flux and changing the rejection characteristics of the membrane. These drawbacks are the results of concentration polarization, adsorption of foulant to the membrane's surface, and in some cases, membrane compaction. While fouling cannot be eliminated completely, processors may limit its progression by choosing membrane materials or designs which adsorb less foulant, optimizing processing conditions such as cross-flow velocity, temperature, and TMP, or pretreating system feeds to reduce their propensities to foul.

The first study presented in this thesis determined that in contrast to 3X MF theoretical cumulative SP removal percentages of 68%, 90%, and 97% after 1, 2, and 3 stages of processing, respectively, the 3X Isoflux MF process only removed 39.5%, 58.4%, and 70.2% of skim milk SP after 1, 2 and 3 stages, respectively. These reductions were similar to those of the PVDF SW membranes ($P > 0.05$), but lower than GP and UTP ceramic membranes ($P < 0.05$). Possible reasons why the SP removal with the Isoflux membranes was lower than theoretical include: a range of membrane pore sizes existed (i.e., some pores were too small to pass SP), the selective layer modification and reverse flow conditions at the membrane outlet combined to reduce the effective membrane surface area, and the geometric shape of the Isoflux flow channels promoted early fouling of the membrane and rejection of SP.

Given the differences in SP removal efficiency observed in the 4 MF systems, further work could be directed to assess the capacity of other membrane designs of industrial interest to remove skim milk SP. Because the effects of channel shape and the Isoflux selective layer gradient were not decoupled in the present study, it is not currently possible to determine the

exact cause of the Isoflux membrane's poor SP removal performance. Future work could focus on evaluating these characteristics in an iterative manner using tailor-made membranes. Another approach may be to operate the current MF system with the Isoflux membranes inverted in the housing (so that the thicker layer of selective material is oriented toward the outlet) to determine whether or not the multiple layers of selective material likely impeded SP passage at the inlet. Microscopic imaging methods of the membranes before and after processing could also help to determine the cause of the Isoflux design's inefficiency.

In the second study described in this thesis, UF and DF flux from WPC80 and SPC80 production processes were examined after each process' feed material had been subjected to annatto coloring and bleaching treatments. Addition of annatto color had no effect on UF or DF flux ($P > 0.05$). Bleaching whey or MF permeate with or without added color usually improved flux during processing. Bleaching with H_2O_2 produced a higher flux than bleaching with BPO. Bleaching with BPO increased WPC80 flux to a greater extent than it did SPC80 flux. Though no differences ($P > 0.05$) in mean flux were observed for a common bleaching treatment between the WPC80 and SPC80 production processes during the UF stage, mean flux during WPC80 DF was higher ($P < 0.01$) than mean flux during SPC80 DF for each bleaching treatment. Water flux values before and after processing were used to calculate a FC that demonstrated differences in fouling which were consistent with flux differences resulting from the bleaching treatments. In both processes, bleaching with H_2O_2 led to the largest reduction in fouling ($P < 0.05$). No effect of annatto on fouling was observed ($P > 0.05$). The reasons for flux enhancement associated with bleaching are unclear.

Due to the ad hoc nature of the second study, a more controlled experiment could be designed and carried out on a smaller scale (i.e., using a stirred cell UF apparatus) to determine

the cause of the observed increase in flux after bleaching. In these studies, factors which are known to influence fouling such as fat content and calcium form (modified by adjusting the pH or the addition of calcium sequestering agents) could be examined systematically. Solubility of the powders produced from the present study's processes could also be studied more thoroughly, as increased protein solubility is presently hypothesized to be a cause of the observed flux enhancement.